Royal Netherlands
Meteorological Institute
Ministry of Infrastructure and the Environment

Deltares
Enabling Delta Life

Implications of the KNMI'14 climate scenarios for the discharge of the Rhine and Meuse

comparison with earlier scenario studies

Deltares

Implications of the KNMI'14 climate scenarios for the discharge of the Rhine and Meuse

comparison with earlier scenario studies

Frederiek Sperna Weiland
Mark Hegnauer
Laurene Bouaziz
Jules Beersma

1220042-000

Deltares

Title
Implications of the KNMI'14 climate scenarios for the discharge of the Rhine and Meuse

Client	Project	Reference	Pages
Rijkswaterstaat, WVL	1220042-000	1220042-000-ZWS-0004	73

Keywords

Rhine, Meuse, CMIP5 climate projections, KNMI'14 scenarios, climate impact assessment

Summary

In this assessment we investigate potential changes in discharge for the rivers Meuse and Rhine due to climate change using:

1) The KNMI'14 scenarios for the Rhine and Meuse basins
2) A selection of 183 simulations from the recently developed Coupled Model Inter-comparison Project (CMIP5) datasets, that are based on the IPCC representative concentration pathways of the 5th IPCC assessment report.

To simulate discharge for the gauging stations (amongst others) Borgharen and Lobith and to simulate the flow into the main river, the hydrological rainfall - runoff models (HBV) for the Rhine and Meuse were used. Hereto the KNMI'14 and CMIP5 climate scenario sets were down-scaled to the sub-catchments of the hydrological model. For the calculation of the distribution of (extreme) high discharges for Rhine (Lobith) and Meuse (Borgharen) rivers, the Generator of Rainfall and Discharge Extremes (GRADE) was used. For these calculations, the historical time-series for precipitation and temperature were resampled to synthetic time-series of 50.000 years using the KNMI weather generators for the Rhine and Meuse basins.

For the Rhine the hydraulic SOBEK model was run to simulate the propagation of the flood wave and to include the effect of flooding on the simulated flow at Lobith. Additionally the most extreme high flows are post-processed to include flooding occurring at very extreme discharges in the dike rings upstream of the Netherlands, between Wesel and Lobith. Finally, changes in both high and low flow statistics have been calculated.

The resulting discharge projections were compared with existing discharge projections i.e. those based on KNMI'06 and the results from the international AMICE (Meuse) and RheinBlick2050 (Rhine) projects. The comparison focussed on the annual cycle of the mean discharge, the mean annual minimum 7-day flow, the mean annual maximum flow and extreme flows with long return periods. It should be noted that the comparison with earlier results is also influenced by changes in the data handling as well as in the model set up since 2006. These changes include improvements of down-scaling methods, extension of the historical time-series, improvements of the method to account for the climate induced change in potential evaporation, improved representation of the Swiss lakes (for the Rhine basin) and, finally, the recalibration of the hydrological models used.

The results show that the implications of the KNMI'14 scenarios on both rivers are a general tendency towards increasing discharges in winter and spring and decreasing discharges in (late) summer. For the Rhine and Meuse the mean winter and mean annual maximum discharge are projected to increase whereas the mean summer and mean annual minimum 7-day discharge are projected to decrease. According to most scenarios, mean annual discharge shows a clear increase as well.

Deltares

Title
Implications of the KNMI'14 climate scenarios on the future discharge of the Rhine and the Meuse

Client	Project	Reference	Pages
Rijkswaterstaat, WVL	1220042-000	1220042-000-ZWS-0004	73

The range of the change in (extremely) high discharges for all KNMI'14 scenarios is relatively small for 2050 (for the 1250-year event between 4250 and 4450 m^3/s for the Meuse and between 15,210 and 15,950 m^3/s for the Rhine when flooding is taken into account) and increases in 2085 (for the 1250-year event between 4110 to 4760 m^3/s for the Meuse and between 14,950 and 17,100 m^3/s for the Rhine when flooding is taken into account). These ranges of the change in discharge are consistent with the ranges of the change in extreme multi-day precipitation in the KNMI'14 scenarios. Yet, the width of the ranges in the CMIP5 projections for the winter months seems slightly larger than for the KNMI'14 scenarios. This indicates that the range of change in extreme discharges projected for 2050 may be somewhat underestimated in KNMI'14.

The effect of upstream flooding is taken into account for the Rhine. This includes the effect of the potential flood areas between Wesel and Lobith, which are taken into account by correcting the discharges calculated by Sobek above 16,000 m^3/s (start of flooding around Emmerich) for the potential flooding volumes and considering the maximum flow over the dikes between Wesel and Lobith . The correction of the Sobek results was needed, because the Sobek model does not incorporate correctly the flooding between Wesel and Lobith. The result is that for very long return periods (above ~1000 years) the differences between the scenarios become small, largely due to the limited discharge capacity of the Rhine between Wesel and Lobith. The maximum discharge at Lobith will be between 17,500 and 18,000 m^3/s.

Comparison of the new, KNMI'14 based, discharge projections with the existing discharge projections results in the following conclusions:

- Generally the trends in discharge envisaged by the KNMI'14 scenarios for the Rhine and Meuse are comparable with those envisaged in most of the existing scenarios (AMICE WET, KNMI'06 and RheinBlick2050). There are (a) larger differences between the dry and wet seasons and (b) more water in the wet (winter and spring) period and less in the dry (late) summer, autumn period (so both increase and decrease of precipitation).
- Specifically, the KNMI'14 scenarios for the Rhine result in higher extreme discharges compared to the KNMI'06 scenarios. For both 2050 and 2085 the KNMI'14 scenarios give for the 1250-year event at most 600 m^3/s larger discharges (respectively for G_L and for W_H) than the earlier KNMI'06 W+ scenario. For the Rhine the W+ scenario roughly lies between the KNMI'14 G_H and W_L scenarios in 2050.
- For the Meuse the KNMI'14 W_H scenario gives comparable results to the KNMI'06 W+ scenario. For 2050 KNMI'14 scenarios give for the 1250-year event at most 200 m^3/s larger discharges (G_L) than the earlier KNMI'06 W+ scenario. For 2085 the difference becomes smaller, the 1250-year discharge for W_H is 100 m^3/s higher than the KNMI'06 W+ scenario.

Deltares

Title
Implications of the KNMI'14 climate scenarios for the discharge of the Rhine and Meuse

Client	Project	Reference	Pages
Rijkswaterstaat, WVL	1220042-000	1220042-000-ZWS-0004	73

Version	Date	Author	Initials	Review	Initials	Approval	Initials
1.0	oct. 2015	Frederiek Sperna Weiland		Jaap Kwadijk		Gerard Blom	
		Jules Beersma					
		Mark Hegnauer					
		Laurene Bouaziz					

State
Final - amended paragraph 3.2.1

Contents

Appendices

1 Introduction

1.1 Background

Rijkswaterstaat (RWS) requested Deltares and the Royal Netherlands Meteorological Institute (KNMI) to assess changes in discharge for the Rhine and Meuse resulting from the newly available KNMI'14 climate scenarios and the climate model projections of the Coupled Model Inter-comparison Project (CMIP5) that are part of the IPCC 5th assessment report. Subsequently a comparison of these new discharge projections for the Rhine and Meuse had to be made with existing discharge projections from earlier scenario sets. The existing discharge projections are those used in: (a) the Delta programme (these are based on the KNMI'06 climate scenarios); (b) the international AMICE project for the Meuse and (c) the international RheinBlick2050 project for the Rhine. Climate change impact studies, in general, and river discharge impact studies are on-going. Emission projections and thus climate change projections change over time and methods to transform climate change scenarios into discharge scenarios/projection become more sophisticated. Thus, the comparison between the new and existing discharge projections also shows the effects of the different approaches and improvements as a result of scientific progress of the past 10 years.

KNMI'14 scenarios
In 2014 KNMI has published a new set of four climate scenarios for the Netherlands – KNMI'14 - the follow up of the KNMI'06 scenarios. In the beginning of 2015 these scenarios were complemented with the corresponding KNMI'14 scenarios specifically designed for the Rhine and the Meuse basins. This is an improvement with respect to the KNMI'06 scenarios for which there were no specific scenarios for the Rhine and Meuse basins (and, in practise, the KNMI'06 scenarios for the Netherlands were also applied in the Rhine and Meuse basins). Because of the large spatial extend of these river basins it was ensured that the changes in e.g. precipitation and temperature in the KNMI'14 scenarios vary spatially over the basins. The changes projected in the basins are, however still consistent with the KNMI'14 climate scenarios for the Netherlands. For the construction of the KNMI'14 scenarios for the Rhine and Meuse basins the same set of simulations with the regional climate model RACMO2, forced by the global climate model EC-Earth (together EC-Earth-RACMO2), and subsequent post processing were used. The method is discussed in detail in Lenderink et al. (2014). It ensures the consistency between the KNMI'14 scenarios for the Netherlands and the KNMI'14 scenarios for the Rhine and Meuse basins. For the latter, however, the initial set of four scenarios is extended with a fifth scenario. It turned out that the scenario with the driest conditions in summer (i.e. with the largest precipitation decreases in summer), W_H, was not dry enough for the Rhine and Meuse basin in comparison with the range provided by the CMIP5 projections. Therefore an additional scenario denoted as $W_{H,dry}$ was constructed (for details see Lenderink and Beersma, 2015). This additional 5th scenario is in particular relevant to determine the ranges of change in seasonal mean discharge and in low discharges at Lobith and Borgharen, the latter of which typically occur in (late) summer. For the range of change in (extremely) high discharges at Lobith and Borgharen, which typically occur during the (late) winter, this scenario is less relevant, and the four original scenarios will determine the ranges of change in high discharge.

Climate datasets used for the IPCC 5th assessment report
In 2013 the IPCC 5th assessment report was published (IPCC, 2013) and new climate model datasets (CMIP5) became available. For many of these datasets a new, and improved,

generation of climate models was used and the emission scenario philosophy changed from emission scenarios to pre-scribed radiation pathways. KNMI developed an efficient method to down-scale these datasets to the Meuse and Rhine sub-catchments (Van Pelt et al., 2012; Kraaijenbrink et al., 2013). This enabled Deltares to perform a large number of hydrological simulations based on an ensemble of climate datasets from the IPCC 5th assessment report in order to assess changes in discharge extremes and their uncertainties for both the Rhine and Meuse rivers.

1.2 Existing climate discharge projections for the Rhine and Meuse

RheinBlick2050
Over the period 2008-2010 an international climate impact assessment was made for the Rhine river basin within the project RheinBlick2050 (Görgen et al., 2010). The project was initiated by the international Commission for the Hydrology of the Rhine Basin (CHR) and project partners came from research institutes and governmental organizations from Rhine countries. A thorough assessment was made based on climate model projections from the EU FP6 ENSEMBLES database which contains projections of global climate models from the IPCC 4th assessment report (IPCC, 2007), down-scaled with various regional climate models. The climate projections were transferred into discharge projections for the River Rhine. In the uncertainty analysis of the projected climate changes the aim was to fully assess uncertainties in climate models, scenarios, down-scaling / bias-correction techniques and hydrological models.

AMICE
Over the period 2009-2012 an international climate impact assessment was made for the Meuse river basin. This assessment was executed by research institutes and water managers from all Meuse countries and was part of the INTERREG-IVB project AMICE - ***A****daptation of the* ***M****euse to the* ***I****mpacts of* ***C****limate* ***E****volution*. RWS was one of the project partners and Deltares conducted the hydrological analysis for RWS (Drogue et al., 2010).
Similar to the RheinBlick2050 project, the AMICE project strengthened the relation and the international co-operation between the Meuse countries and resulted in a number of scientific reports as well as successful pilot climate adaptation projects. Yet, due to time and budget limitations some simplifications have been made in the climate analysis and the implications for the hydrology of the River Meuse. In AMICE essentially two climate scenarios were derived, a ‘wet’- and a ‘dry’ scenario using a delta-change approach. Both scenarios were derived by averaging national climate scenarios used in national impact assessments.

1.3 Objectives

The objectives of this study are:

(1) To assess the hydrological effects of climate change on the Rhine and Meuse rivers based on the KNMI’14 scenarios and the CMIP5 climate model projections for the river basins.
(2) To compare the resulting hydrological changes with those from the KNMI’06 based hydrological projections, the RheinBlick2050 project (for the Rhine) and the AMICE project (for the Meuse).

2 Existing climate discharge projections for Meuse and Rhine

2.1 General: KNMI'06 scenarios

The KNMI'06 scenarios consist of four distinct climate change scenarios for 2050 and 2100. The scenarios were designed for The Netherlands and include seasonal and monthly changes in temperature and precipitation. The scenarios have been constructed using information and statistics derived from GCM simulations that are part of the IPCC 4th assessment report (AR4), see for more information Hurk et al. (2006). The KNMI'06 time series transformation tools for precipitation and temperature were used to transform the historical 35-yr (1961-1995) climate time-series for the Rhine[1] and the Meuse[2] sub-basins (Homan et al., 2011; Bakker and Bessembinder, 2012). These series were used as input for the hydrological HBV models for the river Rhine and Meuse to simulate the implications of the climate scenarios for the discharges of both rivers.

KNMI'06 provides 4 scenarios for both 2050 and 2100:

Table 2.1: Overview of main meteorological feature of the KNMI'06 scenarios

Scenario	Global temperature increases in 2050 (2100)	Change of atmospheric circulation
G	+1 (2) ºC	weak
G+	+1 (2) ºC	strong
W	+2 (4) ºC	weak
W+	+2 (4) ºC	strong

The relevant results of the KNMI'06 scenarios are presented in Chapter 4 together with the corresponding results for KNMI'14, CMIP5 and the RheinBlick2050 / AMICE climate datasets.

2.2 Rhine: RheinBlick2050

The Rheinblick2050 project is extensively described by Görgen et al. (2010). A brief description of the methods is given below. The project used the results of the HadCM3 and ECHAM5 global climate models. These climate models were forced with an increase in atmospheric greenhouse gas concentrations according to the A1B emission scenario (IPCC, 2007). The results of the global models were bias corrected and downscaled for the Rhine basin using 20 different regional climate models (RCM's). This resulted in an ensemble of 20 regional climate projections. This ensemble was used as input for the HBV model of the Rhine (see section 3.3.2 for more information about the HBV model of the Rhine). The HBV model was calibrated and validated using observed series for the period 1961-1995 (the CHR-OBS data set; Görgen et al., 2010). This resulted in an ensemble of 20 discharge series at a daily time-step for all Rhine sub-catchments.

For the assessment of changes in extreme high flows the rainfall generator methodology of KNMI was used to generate 3000-year time series from the 30-year RCM time slices

[1] *For the Rhine these time series comprise time series of daily precipitation and temperature for the 134 HBV-Rhine sub-basins, i.e. the so called CHR-OBS data, see Görgen (2010).*

[2] *For the Meuse these time series comprise time series of daily precipitation and temperature for the 15 HBV-Meuse sub-basins, and described in Leander et al. (2005).*

(Leander and Buishand, 2007; Leander et al., 2008). For this high flow assessment, an ensemble of 7 bias-corrected RCM model projections was used.

From the overall ensemble of hydrological model simulations, changes in mean discharge, high and low flows have been assessed both for the near (2021-2050) and far (2071-2100) future. For details on the methods applied see Görgen et al. (2010), sections 2.4 and 3.2.

2.3 Meuse: AMICE

Within the AMICE project existing national climate scenarios, based on climate datasets from meteorological institutes and national and EU research projects, were used. All national scenarios were derived from climate models used for the IPCC 4th assessment report. For the construction of future climate change scenarios the Delta Change method was used. Based on their national scenarios all countries provided a 'wet' and a 'dry' climate scenario that consisted of basin average delta changes in precipitation and temperature per season for 2050 and 2100.

The methods used to construct these 'wet' and 'dry' scenarios for the Meuse basin differed considerably from country to country, and included statistical- down-scaling, downscaling using regional climate model and bias-correction methods. Due to the large heterogeneity between the projections available for the different countries it was decided to derive transnational basin-wide seasonal scenarios. The precipitation and temperature changes for these transnational basin wide scenarios were derived by a simple weighted averaging of the changes in the national basin wide scenarios. The weight for each national scenario was taken as the (relative) area of the Meuse basin located in each country (for more information see Drogue et al., 2010).

For the future discharge projections each AMICE-partner used his own hydrological model. For the historical situation the gridded precipitation and temperature observations of the E-OBS 0.25 dataset (Haylock et al., 2008) was commonly used as input for the hydrological models. Future time series of precipitation and temperature were obtained by transforming this historical dataset according to the trans-national climate scenarios using a classical delta method. Based on the hydrological simulations the impacts of climate change on high- and low-flow discharges for the 21st century (focussing on 2050 and 2100) were assessed. Each country focused on selected national gauges only.

For the Netherlands the Dutch HBV-Meuse model, calibrated by Van Deursen (2004), was used to assess the changes for Sint Pieter. Unfortunately, the performance of this HBV model in representing the observed discharges, using the historical E-OBS dataset as input, was not satisfactory. This might be due to the fact that the E-OBS dataset is based on fewer weather stations than the dataset the HBV-Meuse model was calibrated with. Alternatively the historical dataset of daily precipitation and temperature for the 15 HBV-Meuse sub-basins for the period 1961-1998 constructed by KNMI was used (Leander et al., 2005). The same dataset had also been used for the calibration of the HBV model (Leander et al., 2005; Keizer and Kwadijk, 2009; Van Deursen et al., 2004).

3 Methods: Generation of discharge projections for the Rhine and Meuse for CMIP5 projections and KNMI'14 scenarios

3.1 CMIP5

In 2013 the 5th IPCC assessment report has been published (IPCC, 2013). The climate simulations that form the back bone of this report have been conducted with climate models that were part of the fifth phase of the Coupled Model Intercomparison Project (CMIP5). Compared to the scenarios of the 4th assessment report, the definition of the climate forcing is new (Van Vuuren et al., 2010; IIASA, 2013). Previously, the climate models were forced with greenhouse gas concentrations which were prescribed by the IPCC SRES emission scenarios. Within the 5th assessment report, four Representative Concentration Pathways (RCPs) are prescribed that are used as climate model forcing. These RCPs each follow a pre-defined path of radiative forcing (W/m^2) that belongs to certain emission scenarios:

- RCP 2.6: In this pathway the radiative forcing peaks around 2050 after which there is a modest decline towards 2100 due to a declining use of oil and an overall decrease in energy use;
- RCP 4.5: In this pathway the radiative forcing stabilizes before 2100 due to the introduction of technologies and strategies that reduce greenhouse gas emissions;
- RCP 6.0: Here a stabilization, due to the introduction of technologies for greenhouse gas emissions, is reached after 2100;
- RCP 8.5: In this pathway there is a continuously increasing radiative forcing.

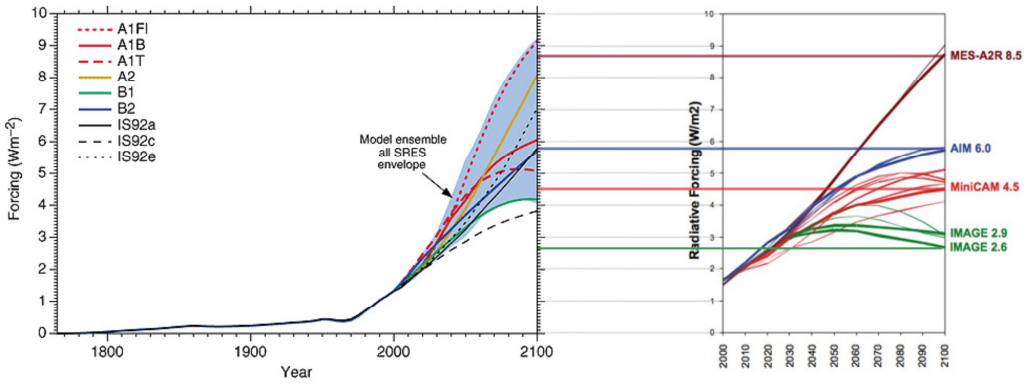

Figure 3.1 Comparison between radiative forcing according to the earlier IPCC scenarios IS92 and AR4 (left) and the new RCPs (right) after (IPCC, 2001; Moss et al., 2008; Taylor et al., 2012; Vecchi, 2012)

The lowest emission scenario, RCP 2.6, which assumes a relatively strong reduction in greenhouse gas emissions, was not used to develop the KNMI'14 scenarios. Yet, the G_L and G_H scenarios are fairly close to the average global temperature rise for RCP 2.6. Only the lower limit global temperature rise for RCP 2.6 is not covered by KNMI'14. To describe the effects of this lower limit on climate change in the Netherlands, as well as in the Rhine and Meuse basins, an additional scenario would be necessary. However the discharge projections based on CMIP5 in the subsequent sections do consider the RCP 2.6 scenario, i.e. of the overall 183 discharge projections, 45 represent RCP 2.6 (see Chapter 4). The results in Chapter 4 show that the discharge projections for the Rhine and the Meuse based on the KNMI'14 scenarios fit the range spanned by the full set of CMIP5 based discharge projections.

3.1.1 Meteorological and climate model datasets used

Historical data
For the **Meuse** basin the historical precipitation and temperature data from French and Belgium meteorological stations were interpolated to the 15 HBV-Meuse sub-basins (Buishand and Leander, 2011; Leander, 2009). The resulting historical meteorological dataset covers the period 1967-2007 and serves as the reference dataset for the application of the ADC method for the Meuse basin.

For precipitation in the **Rhine** basin version 2 of the HYRAS dataset prepared by the German Weather Service (DWD) is used (Rauthe et al., 2013). HYRAS is a gridded daily dataset with a spatial resolution of 1 km^2, which covers the period 1951 to 2006. It has been obtained by linear regression and inverse distance weighting based on 6200 precipitation stations (Rauthe et al., 2013). The gridded time-series have been aggregated to 134 HBV-Rhine sub-basins based on Thiessen's method.

The daily temperature time-series for the 134 HBV-Rhine sub-basins have been obtained by spatial aggregation (Thiessen's method) of the European gridded E-OBS 0.25 gridded dataset (Haylock et al., 2008). The temperature grids have been obtained by spatial interpolation of station data of approximately 2316 stations. The exact number varies over time and the station density is relatively high in Switzerland and the Netherlands (Haylock et al., 2008).

Climate model data
From the available CMIP5 runs (IIASA, 2013) the 183 runs with both daily precipitation and temperature data for the time-slices 1961-1995, 2021-2050 and 2071-2100 have been selected. Table 3.1 lists these GCMs runs together with the number of model runs per GCM (= runs with different initial conditions that represent natural climate variability) and the number of runs per RCP. The runs with FGOALS climate model have been excluded because they were officially withdrawn from the CMIP5 database. The EC-EARTH runs in the table are officially not in the CMIP5 database but are used as the basis for the KNMI'14 scenarios.

Table 3.1 Overview of GCMs used in this study together with the number of available runs and the number of specific RCPs available for those runs (Kraaijenbrink, 2013) – FGOALS-s2 (withdrawn from CMIP5 database) and EC-EARTH-v2.3 (used for construction of KNMI'14 scenarios) are not included in the CMIP5 results described in Section 3.1

Model	Model runs	RCP 2.6	RCP 4.5	RCP 6.0	RCP 8.5	Total
ACCESS1-0	1		1		1	2
ACCESS1-3	1		1		1	2
bcc-csm1-1	1	1	1	1	1	4
bcc-csm1-1-m	1	1	1	1	1	4
BNU-ESM	1	1	1		1	3
CanESM2	5	5	5		5	15
CCSM4	3	3	3	3	3	12
CMCC-CESM	1				1	1
CMCC-CM	1		1		1	2
CMCC-CMS	1		1		1	2
CNRM-CM5	1	1	1		1	3
CSIRO-Mk3-6-0	10	10	10	10	10	40
FGOALS-s2	3	1	3	1	3	8
GFDL-CM3	1	1		1	1	3
GFDL-ESM2G	1	1	1	1	1	4
GFDL-ESM2M	1	1	1	1	1	4
GISS-E2-R	1		1			1
HadGEM2-CC	3		1		3	4
HadGEM2-ES	4	4	4	4	4	16
inmc m4	1		1		1	2
IPSL-CM5A-LR	4	4	4	1	4	13
IPSL-CM5A-MR	1	1	1	1	1	4
IPSL-CM5B-LR	1		1		1	2
MIROC-ESM	1	1	1	1	1	4
MIROC-ESM-CHEM	1	1	1	1	1	4
MIROC5	3	3	3	1	3	10
MPI-ESM-LR	3	3	3		3	9
MPI-ESM-MR	3	1	3		1	5
MRI-CGCM3	1	1	1	1	1	4
NorESM1-M	1	1	1		1	4
EC-EARTH-v2.3	8				8	8
Total	69	46	57	30	66	199

3.1.2 The Advanced Delta Change method

KNMI has developed an Advanced Delta Change (ADC) method (Van Pelt et al., 2012) where the climate responses of global climate models are used to modify historical observed precipitation and temperature time series. In contrary to the standard Delta change method, the ADC method allows that the (relative) changes in the extreme precipitation differ from those in the mean precipitation. This improves the analysis of the effects of changes in future precipitation extremes. In this report the method is used to modify historical precipitation and temperature time-series for the HBV-catchments of the Meuse and Rhine for each of the 183 CMIP5 climate projections (and for each of the KNMI'14 climate scenarios for the Rhine and the Meuse basins, see section 3.2).

The ADC method (for details see van Pelt et al., 2012) and the software developed at KNMI to apply this method to CMIP5 climate model projections (see Ruiter,2012; Kraaijenbrink, 2013) are briefly described below. Figure 3.2 schematically summarizes the ADC method.

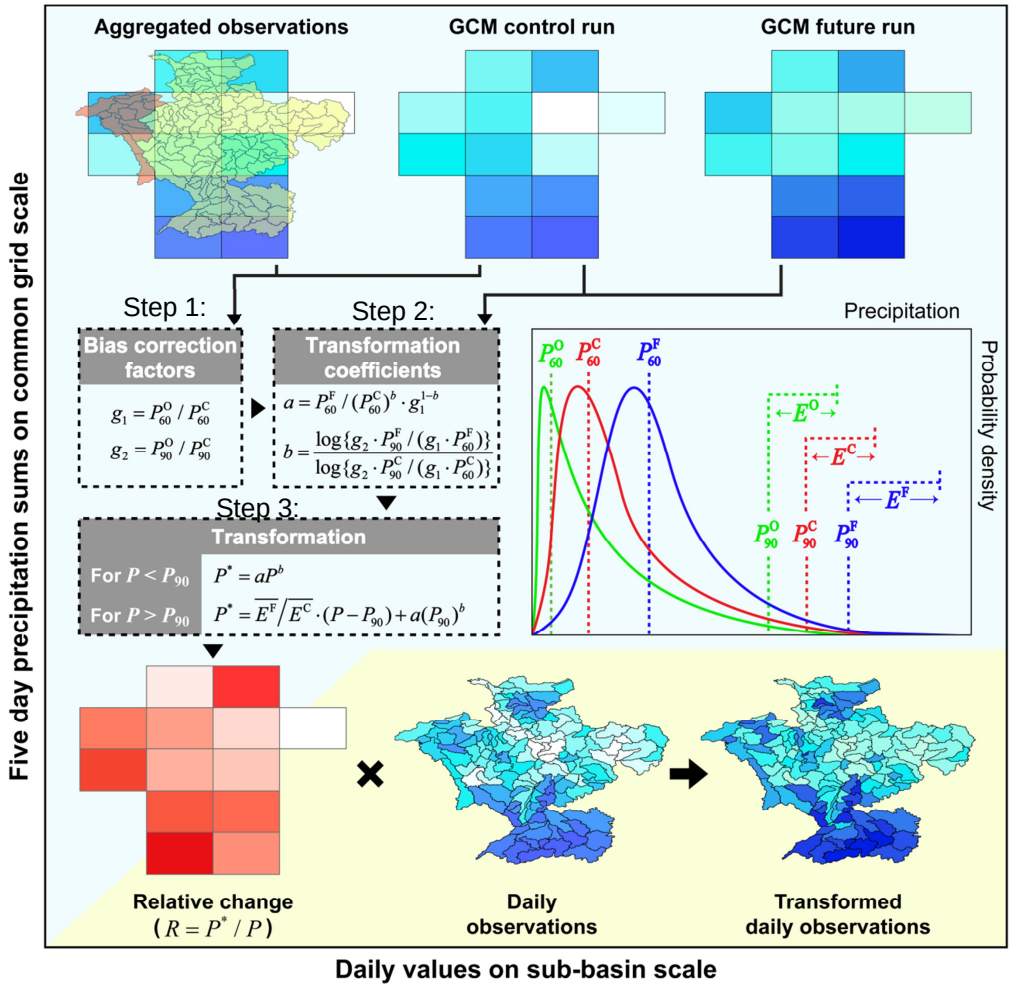

Figure 3.2 Schematic overview of the Advanced Delta-Change method (source: Kraaijenbrink, 2013; after Van Pelt et al., 2012)

Spatial aggregation
In the first step of the ADC method all global climate model (GCM) datasets are interpolated to a common grid with a resolution of 1.25 degrees latitude and 2.0 degrees longitude (top row Figure 3.). For each grid cell within the Rhine / Meuse basin, the cell specific values are smoothed by averaging the cell's value with the values of its eight-neighboring cells of the larger European grid and assigning the average value to the center cell.

Temporal aggregation
Extreme discharge events in the Rhine and Meuse basin are a result of extreme rainfall lasting for several days. Therefore the transformation method should also be based on a period of several days. A period of 5-days has been selected as a representative precipitation event period and the daily time-series are aggregated to time-series of 5-day sums. The transformation steps exist of 1) calculation of bias correction factors, 2) calculation of transformation coefficients and 3) transformation of the (historical) 5-day precipitation amounts, and finally 4) (not shown in Figure 3.) disaggregation of the transformed 5-day sums to daily sums, by applying the relative change of the 5-day sum to the individual days. For a detailed description of all steps see Kraaijenbrink (2013) and Van Pelt et al. (2012).

3.2 Construction of the KNMI'14 scenarios for Rhine and Meuse

The KNMI'14 scenarios for the Netherlands are based on an ensemble of EC-Earth-RACMO2 climate model simulations. RACMO2 is a high-resolution regional climate model that is used to project global climate model results to relatively small areas such as the Netherlands and the basins of the river Rhine and Meuse. How the four KNMI'14 scenarios are constructed from the EC-Earth-RACMO2 ensemble is described in Lenderink et al. (2014). Relevant to know is that the spread in seasonal temperature and precipitation changes in the CMIP5 climate model projections served as a reference for the spread in the KNMI'14 scenarios. The four KNMI'14 scenarios *for the Netherlands* represent 50–80% of the CMIP5 spread for summer and winter changes in seasonal mean precipitation and temperature as well as a limited number of monthly statistics (warm, cold, wet and dry months) (Lenderink et al., 2014). The aim for the (complementary) set of KNMI'14 scenarios *for the Rhine and Meuse basins* was that it represents a similar percentage of the CMIP5 spread in seasonal changes in precipitation and temperature in the Rhine and Meuse basins.

Exactly the same EC-Earth-RACMO2 ensemble and construction procedure as used for the KNMI'14 scenarios *for the Netherlands* is also used for the KNMI'14 scenarios *for the Rhine and Meuse basins*. As for the CMIP5 climate model projections (in the previous section) the ADC method is used to modify historical precipitation and temperature time-series for the HBV-catchments of the Meuse and Rhine for each of the KNMI'14 climate scenarios for the Rhine and the Meuse basins . Each of the four KNMI'14 scenarios is represented by different EC-Earth-RACMO2 samples (see Lenderink et al. 2014). The transformation coefficients used in the ADC method are first calculated for each of the EC-Earth-RACMO2 samples individually. Subsequently, the transformation coefficients for the ADC method are averaged over these samples, resulting in one set of ADC transformation coefficients for each of the four KNMI'14 scenarios. The only difference between applying the ADC method to the CMIP5 climate model projections and applying it to the KNMI'14 scenarios is that the spatial resolution of the underlying EC-Earth-RACMO2 simulations (which in the end is a high-resolution regional climate model) differs from that of the CMIP5 climate model projections (which are low-resolution global climate models), and that in the case of the KNMI'14 scenario's for the Rhine and Meuse basins the transformation coefficients are averaged (over the underlying EC-Earth-RACMO2 samples). Note that the ADC method automatically

accounts for the difference in spatial resolution. In both cases the ADC transformation is applied to the same historical data (which has a spatial resolution corresponding to the sub-basins in the HBV model, see Section 3.3.2).

3.2.1 The need for a fifth scenario

The most extreme KNMI'14 scenario in terms of summer drying is the W_H scenario. The mean change in precipitation over the Netherland is -23 % in that scenario (Figure 3.3, right panel), which is between the 25th (-21 %) and 17th percentile (-26%) out of CMIP5 (Figure 3.3, left panel). For the Rhine basin (upstream of Lobith) the CMIP5 change is a decrease of about 30 % (left panel), while the set of EC-Earth-RACMO2 samples used for the W_H scenario (for the Netherlands) projects a decrease only halve as large (right panel).

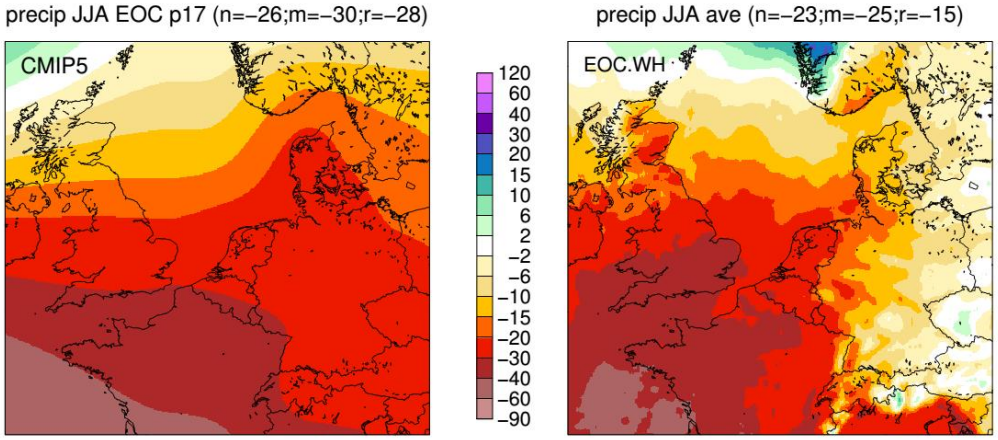

Figure 3.3 Response in mean summer precipitation compared to present-day climate (in % changes) in CMIP5 (left) and the W_H scenario (right). For CMIP5 the 17th percentile (i.e. the median or 50th percentile minus 1 standard deviation, assuming normality) of the distribution of changes derived from the CMIP5 model ensemble driven by emission scenarios RCP4.5, RCP6 and RCP8.5, all with equal weight) (data from climexp.knmi.nl/atlas). Changes averaged over the Netherlands (n), the Meuse catchment (upstream of Maastricht) (m) and the Rhine catchment (upstream of Lobith) (r) are given in the panel titles. "EOC" refers to the 30-yr End Of Century period and is equivalent to 2085.

Therefore an alternative scenario that is tailored to represent the potential of a relatively strong drying in summer over the Rhine basin as indicated by the range spanned by the CMIP5 model runs is introduced (Lenderink and Beersma, 2015) which is based on a different (CMIP5) global climate model, i.e. HadGEM2-ES. Two members of HadGEM2-ES are downscaled, again with the RACMO2 regional climate model. And again the ADC method is used to each of these 2 HadGEM2-ES-RACMO2 simulations to produce scenarios specifically for the Rhine and Meuse basins. This leads to an additional, i.e. 5th, KNMI'14 scenario for the Rhine and the Meuse basins. This fifth scenario is denoted as $W_{H,dry}$. $W_{H,dry}$ should be regarded as a twin scenario of W_H. W_H represents the scenario with the largest precipitation increase in winter combined with a relatively large (but not the largest) precipitation decrease in summer while $W_{H,dry}$ is complementary in the sense that it represents the scenario with the largest precipitation decrease in summer combined with a relative large (but not the largest) increase in winter. W_H is therefore the relevant scenario when precipitation increases in winter are important while $W_{H,dry}$ is the relevant one when

summer drying is at stake. Further details about the motivation for and construction of $W_{H,dry}$ can be found in Lenderink and Beersma (2015).

3.3 Estimating future extreme discharges

To translate the future changes in precipitation and temperature of the KNMI'14 scenarios into projections of future extreme discharges, use is made of the GRADE instrument (Hegnauer et al., 2014). GRADE, short for Generator of Rainfall And Discharge Extremes, was first developed and used to calculate the distribution of extreme discharges for the Rhine (at Lobith) and Meuse (at Borgharen) for use in the safety assessment project for the Dutch dikes (Hegnauer et al., 2014). GRADE consists of three components. A short description of each of the GRADE components is given below and a schematic overview of the components is given in Figure 3.4.

Component 1: Stochastic weather generator
The stochastic weather generators used for the Meuse and Rhine basins are based on nearest-neighbour resampling and produce very long rainfall and temperature series that preserve the statistical properties of the original (much shorter) series.

Component 2: HBV model
The HBV rainfall-runoff model calculates the runoff from the synthetic precipitation and temperature series. Temperature is needed to account for temporal snow storage as well as evapotranspiration losses. HBV is a conceptual hydrological model of interconnected linear and non-linear storage elements. It is widely used internationally under various climatic conditions and it forms also the basis for the flood forecasting system in the Netherlands of the rivers Rhine and Meuse.

Component 3: Hydrologic and hydrodynamic routing
This component of GRADE routes the runoff generated by HBV through the river stretches. For both the rivers Meuse and Rhine, a simplified hydrologic routing module is used in HBV, but this does not simulate well the physical processes such as retention and flooding. Therefore a hydrodynamic routing component is added. For this purpose, the Sobek hydrodynamic model is used for the Meuse starting from the station of Chooz on the French/Belgian border and for the Rhine from Maxau on the main river. However, only the largest flood waves (i.e. the by HBV calculated discharge is larger than 10.000 m3/s) are simulated with the Sobek model. These flood waves are selected from the results of the built-in routing in the hydrological model. This is done, because a full hydrodynamic simulation of the synthetic series is computationally not feasible.

3.3.1 Generating long rainfall and temperature records with the rainfall generator

The rainfall generators for the Rhine and Meuse basins are based on nearest-neighbour resampling. Nearest-neighbour resampling was originally proposed by Young (1994) to simulate daily minimum and maximum temperatures and precipitation. Lall and Sharma (1996) used a nearest-neighbour bootstrap to generate hydrological time series. Rajagopalan and Lall (1999) presented an application to daily precipitation and five other weather variables. Basically the same method is used for the rainfall generators for the Rhine and the Meuse basins. Especially for such multi-site applications summary statistics are needed to avoid problems with the large dimensionality of the data (Buishand and Brandsma, 2001).

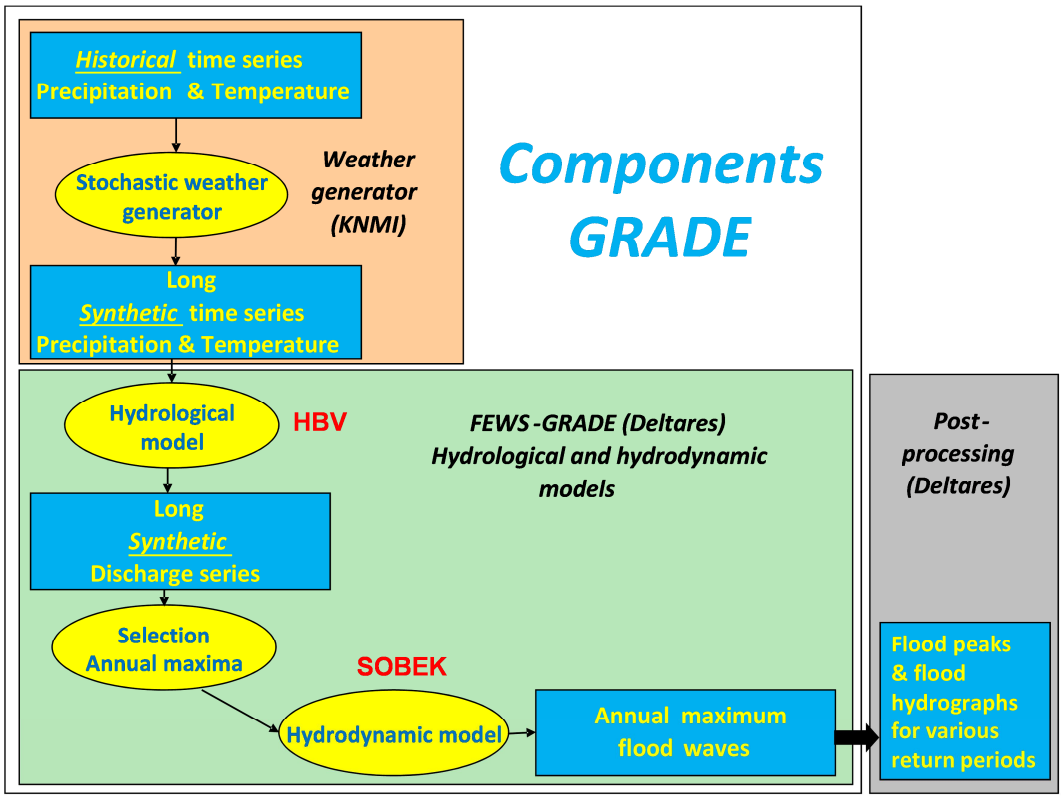

Figure 3.4 Components of GRADE.

In the nearest-neighbour method weather variables like precipitation and temperature are sampled simultaneously with replacement from the historical data. To incorporate autocorrelation (i.e the persistence of the weather), resampling depends on the simulated values for the previous day. Therefore, one first searches the days in the historical record that have the similar characteristics as those of the previously simulated day. One of these nearest neighbours is selected randomly and the observed values for the day subsequent to that nearest neighbour are adopted as the simulated values for the next day *t*. A feature vector (or state vector) is used to find the nearest neighbours in the historical record. The feature vector is formed out of a small number (3) summary statistics of (standardized) weather variables simulated for day *t-1*. The nearest-neighbours are ordered using a weighted Euclidean distance. Only the *k* nearest ones are selected. Subsequently a discrete probability distribution (or kernel) is required to select one of the k nearest neighbours. The decreasing kernel of Lall and Sharma (1996), which gives a higher weight to the closer neighbours, is used. Apart from constructing a feature vector the number *k* of nearest neighbours and the weights used in the Euclidean distance have to be determined. For the rainfall generators for the Rhine and Meuse, the weights are taken inversely proportional to the variance of the feature vector elements and *k* is set to 10. For the Rhine a 3-dimensional feature vector is used consisting of the daily mean temperature in the basin, the daily mean precipitation in the basin, and the daily fraction of locations with precipitation larger than 0.1 mm. The latter helps to distinguish between large-scale and convective precipitation. For the Meuse, the fraction of locations with precipitation is replaced by a term which enhances the day-to-day persistence of precipitation. For further details see Schmeits et al. (2014a and 2014b).

Both for the Rhine and Meuse basins 50.000-year (50K-yr) simulations of daily precipitation and temperature were performed respectively with the Rainfall generator for the Rhine basin and with the Rainfall generator for the Meuse basin. The 50K-yr simulation for the Rhine basin uses the historical period 1951 – 2006 as the base period while the 50K-yr simulation for the Meuse basin uses 1930 – 2008. Both these 50K-yr simulations are considered the reference simulations for GRADE (Hegnauer et al., 2014) and the details of these simulations are described in respectively Schmeits et al. (2014b) and Schmeits et al. (2014a). For the KNMI'14 climate scenarios these 50K-yr series also serve as the reference series for the current climate, and again the ADC method (described in section 3.1.2) is used to transform these 50K-yr series for the current climate into 50K-yr series for the future climate according to the KNMI'14 climate scenarios.

3.3.2 Hydrological simulations with HBV

For both the Rhine and Meuse historic and future river discharges have been simulated with the conceptual, semi-distributed rainfall runoff model HBV. The HBV model structure is shown in Figure 3.5.
The model structure can be divided into a number of routines. In the "snow routine" accumulation of snow and snow melt are determined according to the temperature. The "soil routine" controls which part of the rainfall and melt water forms excess water and how much is evaporated or stored in the soil. The "runoff generation routine" consists of an upper, non-linear reservoir representing fast runoff components and a lower, linear reservoir representing base flow. Flow routing processes are simulated with a simplified Muskingum approach.

Rhine
The HBV model for the Rhine is a semi-distributed hydrological model that consists of 148 sub-basins, covering the complete Rhine basin upstream of Lobith. The model is an extended version of the model that is used in the operational forecasting system of the Netherlands. This initial model contains 134 sub-basins (Eberle et al., 2005).

The lakes in Switzerland have a considerable effect on the discharges. Therefore, four of the initial 134 sub-basins have been further subdivided to include four large lakes in Switzerland in the HBV setup. This led to the 148 sub-basins (Hegnauer and Van Verseveld, 2013). The four lakes that are now included in the HBV-setup are:

- Lake Constance (German: Bodensee).
- Lake Neuchâtel (French : Lac de Neuchâtel, German : Neuenburgersee).
- Lake Lucerne (German: Vierwaldstättersee).
- Lake Zürich (German: Zürichsee).

The model has been re-calibrated following the GLUE methodology (Winsemius et al., 2013) with the focus on high discharges, resulting in a parameter set that represents best the high flows. This parameter set corresponds to the 50^{th} quantile parameter set in Hegnauer et al. (2014). The hydrological runs for the RheinBlick2050 and KNM'06 datasets for the Rhine have been run with older versions of the HBV model. The model used for these discharge projections did not include the lakes in Switzerland and was calibrated differently compared to the model used to calculate the discharges for the KNMI'14 scenarios. Furthermore, in the version used for the KNMI'14 scenarios, the method to estimate potential evaporation has been improved. This has resulted in small deviations in discharge simulations which can be seen for the reference situation in Table D.3 (Section D1.1) for the long-term average February and September discharges. A description of the potential evaporation method used for the different scenario datasets is given in Appendix A.

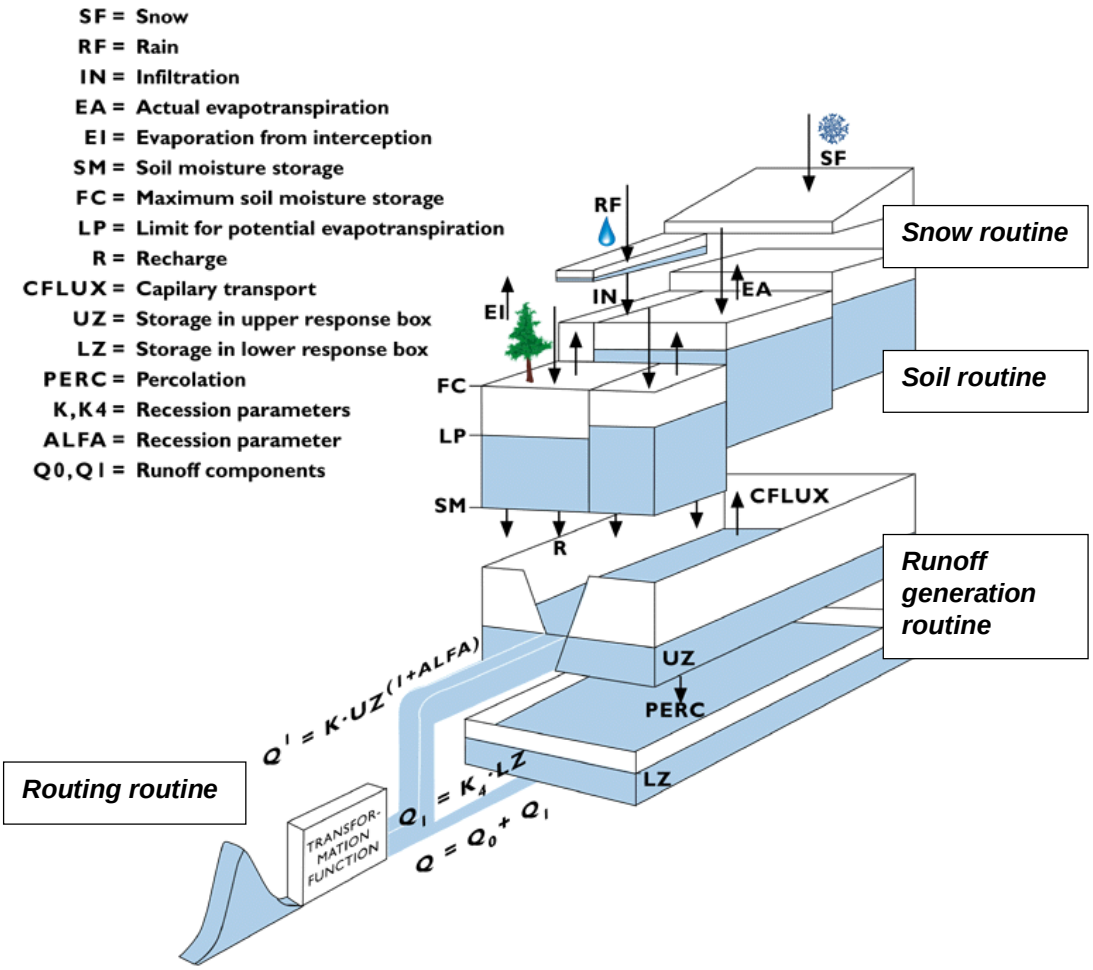

Figure 3.5 Schematic overview of the HBV rainfall-runoff model.

Meuse

The HBV model for the Meuse consists of 15 sub-basins. These sub-basins cover the whole Meuse basin upstream of Borgharen, which has an area of about 21,000 km^2 The HBV model runs with a daily time step. The model input consists of daily average precipitation, temperature and potential evapotranspiration for each sub-basin. The model has been calibrated using the GLUE (Generalized Likelihood Uncertainty Estimation) method with emphasis on the reproduction of high flows. The model for the Meuse is described in more detail in Hegnauer (2013).

The hydrological runs for the AMICE, KNMI'06 and CMIP5 datasets for the Meuse have been run with older versions of the HBV model, which used a different method for calculating potential evaporation. In Appendix A, a description of the potential evaporation method used for the different scenario datasets is given.

3.3.3 Modelling the flood wave propagation in the River Rhine

GRADE uses a 1D SOBEK-RE model to hydrodynamically calculate the propagation of the flood waves through the main stem of the Rhine. The use of the hydrodynamic model also enables to calculate flood damping because of upstream flooding of the Rhine in Germany.
To do so, in the hydrodynamic model of the Rhine the so called retention option in Sobek-RE is used. With the retention option flooding is simulated by assuming the flood areas (behind the dikes) as a series of retention basins that are filled once the water in the river exceeds a certain level.

The location and the volume of the flooded areas (the retention basins) are pre-defined based on more detailed 2D calculations using Delft-FLS and WAQUA models This retention option enables SOBEK to calculate 2D flooding using a 1D approach. More details can be found in Hegnauer and Becker (2014).

3.4 Flooding between Wesel and Lobith

In extremely rare cases, the magnitude of the discharge may be that large that we can assume that the water levels will exceed the top level of the embankments along the most downstream section of the River Rhine in Germany between Wesel and Lobith. In these cases the schematization of the SOBEK model currently used is insufficient to simulate flood wave propagation including the effect of flooding accurately. The potential flooded areas along the last stretch of the Rhine are not schematized sufficiently. The result is that the model overestimates the discharge at Lobith. This results in very limited flood damping along this stretch of the river, whereas based on the actual height of the dikes along this stretch it can be assumed that significant peak damping could occur.

In several studies, a hydraulic maximum discharge of the Rhine at Lobith is estimated between 17,500-18,000 m^3/s (e.g. Silva, 2003 and Paarlberg, 2014). Most of these studies refer to the results of the so called Niederrhein study by Lammersen (2004). The estimates are based on propagation of flood waves having a magnitude of maximum 17,822 m3/s at the Andernach gauging station which is located in the upstream section of the Niederrhein). In a more recent study by Paarlberg (2014) similar results are obtained. In this study a 2D waqua model was used to simulate the water levels in the Rhine. The calculated water levels were compared to the actual level of the dikes, see Figure 3.. From this figure it can be found that the hydraulic maximum discharge is indeed around 18,000 m^3/s. For some smaller stretches, the discharge capacity seems to be a bit smaller. One of these locations is Emmerich, where it is known that stretch of the dike is lower.

Therefore, for discharges beyond 18,000 m^3/s along the downstream section of the Niederrhein, in this study it is assumed that water is spilled over the embankments.
Since this spilling is not reliably represented in the SOBEK model the discharges simulated by the SOBEK model will be adjusted (see Section 3.4.3). Based on the above mentioned studies we assume that the maximum volume of water that can pass this section without exceeding the top of the embankments is indeed 18,000 m^3/s.

It is also assumed that the overflowing of the dikes along this stretch will start already when the discharge at Lobith exceeds 16,000 m^3/s, because then some locations, among which the lower parts of the dike at Emmerich, will start overflowing.

To get an idea how realistic this great amount of overflow is in the river stretch between Wesel and Lobith two additional checks have been performed:

1) Can the flood volume be stored within the flooded areas behind the dikes?
2) Is the overflow capacity of the dikes large enough to get rid of all the water?

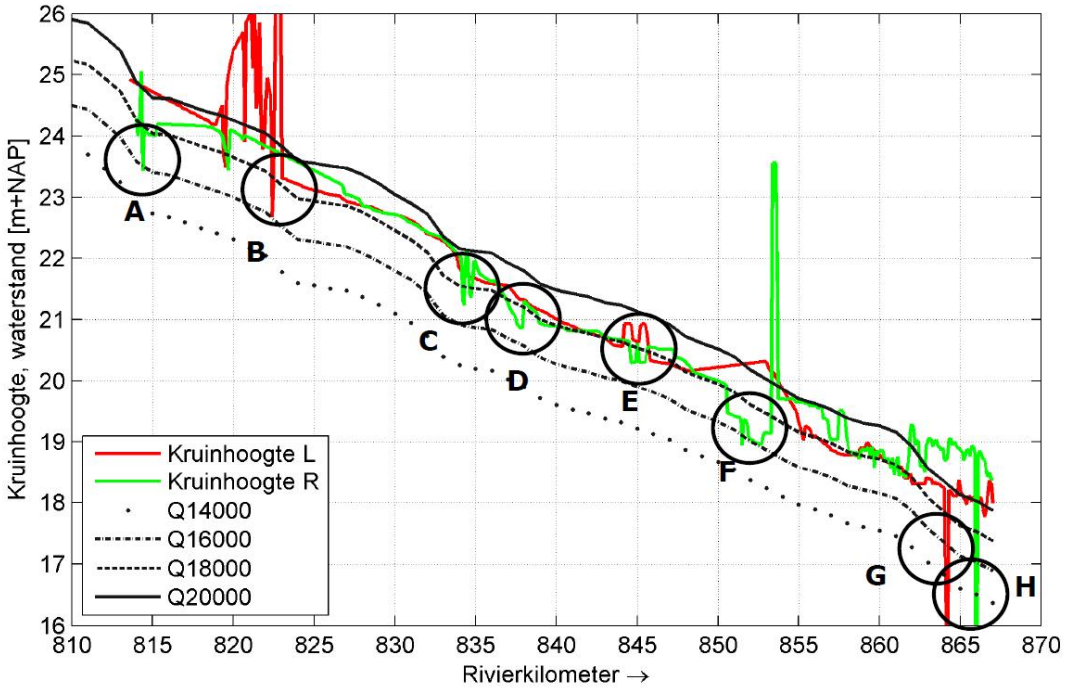

Figure 3.6 Overview of the calculated water levels for 4 different discharge levels, compared to the actual height of the dikes (left en right side). The spikes in the figure are most likely errors in the underlying data and should be checked in more detail. The letters correspond to locations with the lowest embankments. It should be checked in more detail whether it is likely that overtopping of these dike segment would also result in dike breaching (source: Paarlberg, 2014)

3.4.1 Limitation of the total flood volume

The maximum discharge capacity of 18,000 m^3/s is based purely on the hydraulic properties of the riverbed and the height of the dikes. Additionally we checked whether the amount of water overflowing the dikes can be maintained in the flood areas behind the dikes (dike rings 42 and 48, see Figure 3.7). If this would not be true, i.e. if the volume of the flood wave above 18,000 m^3/s is larger than the storage volume in the dike rings, the maximum discharge at Lobith could become higher since water would start to flow back into the main channel.

In a previous study by Vis et al. (2001), it was found that water within dike ring 48 will flow towards the IJssel (in the north of dike ring 48) and when water levels rise, water will overflow the IJssel dikes and flow into the IJssel valley. Indication for this behaviour is also found when analysing the Digital Elevation Model (see Figure 3.8). Here one can clearly see the slope of dike ring 48 is in north-western direction. Water that flows from the River Rhine into dike ring 48 most likely will follow the flow path of the old IJssel towards the area around Doesburg.

The maximum volume that can be contained within dike ring 48 is limited by the height of the dikes along the IJssel. As soon as the water level within dike ring 48 will reach the level of the top of the dikes, water will start spilling into the IJssel valley. The corresponding water level (i.e. the maximum water level within the dike ring) however, will not have any effect on the amount of water that can enter the dike ring upstream. The reason for that is that the surface level in the upstream area of the dike ring is higher than the level of the dikes along the IJssel. This means that the water levels close to the possible breach locations in Germany will most likely remain low and will have no limiting effect (backwater effects) on the flow capacity into the dike ring. A schematic overview of this is given in Figure 3.9.

The result of this is that there will be no limit on the volume that can be diverted from the main river during a flood event along the trajectory Wesel-Lobith. Therefore, based on this, there is no reason not to use the 18,000 m^3/s as a hydraulic maximum discharge. However, it should be noted that this is mainly based on dated research and simple reasoning. We strongly recommend an in-depth analysis In the near future that uses a sufficient and state-of-the-art 2D hydraulic model.

The effect of flooding in dike ring 48 has a limiting effect on the discharge at Lobith. However, events where water flows through dike ring 48 into the IJssel valley will lead to substantial flood damage on locations along the (old) IJssel, since the local protection levels do not take this into account. Further downstream in the IJssel this additional discharge will very likely lead to serious problems as during such events the water levels in the IJssel will be very close to their design levels.

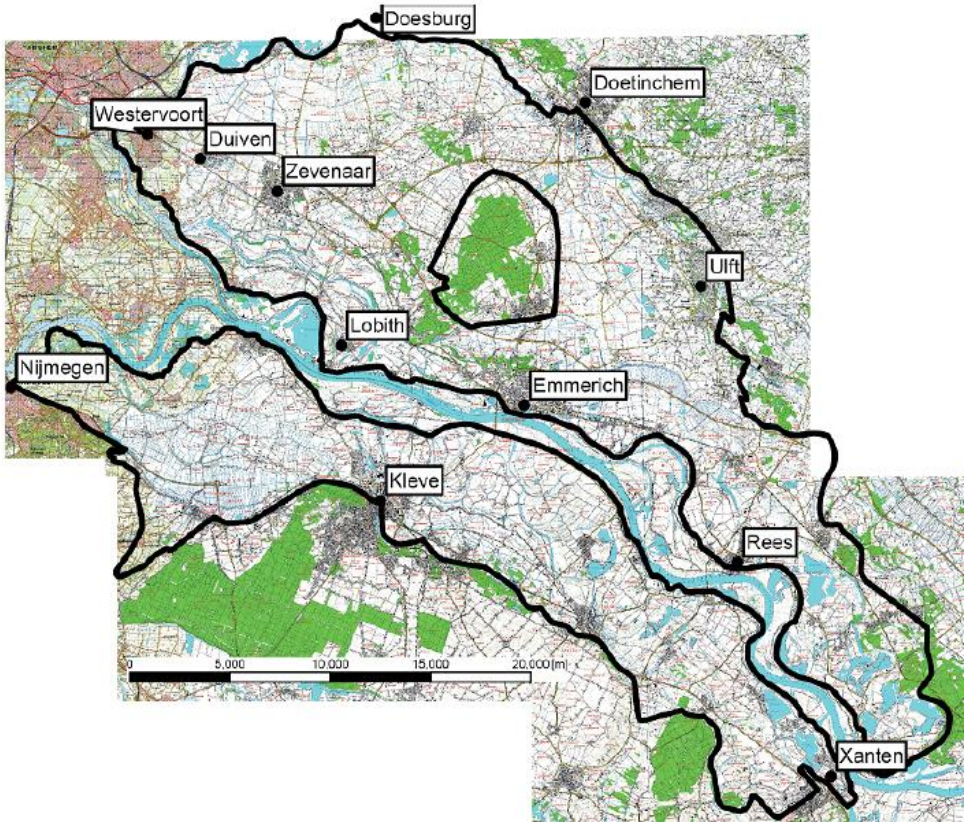

Figure 3.7 Topographic overview of dike rings 42 (left bank of the Rhine) and 48 (right bank of the Rhine). (source: Duits-Nederlandse werkgroep Hoogwater (2006a))

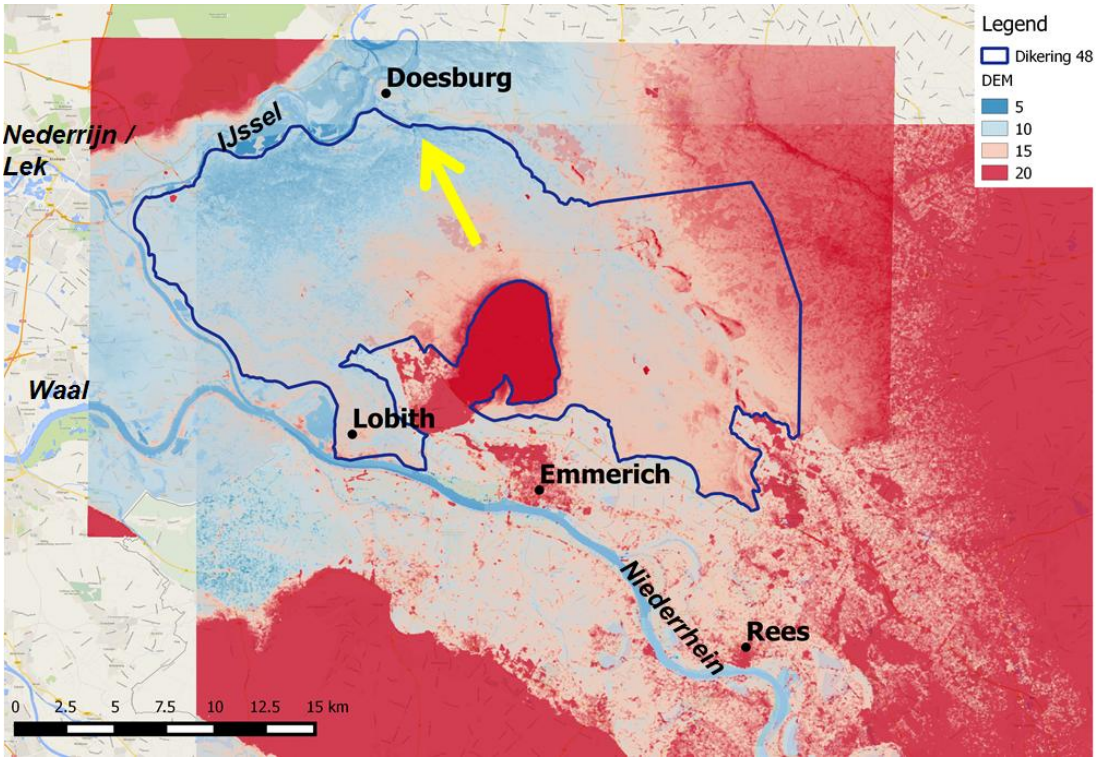

Figure 3.8 Elevation of the land within dike ring 48 indicating the slope of the land surface in north-west direction. The yellow arrow indicates the critical location where the elevation of the land is lowest and water would probably first start overflowing into the (old) IJssel valley

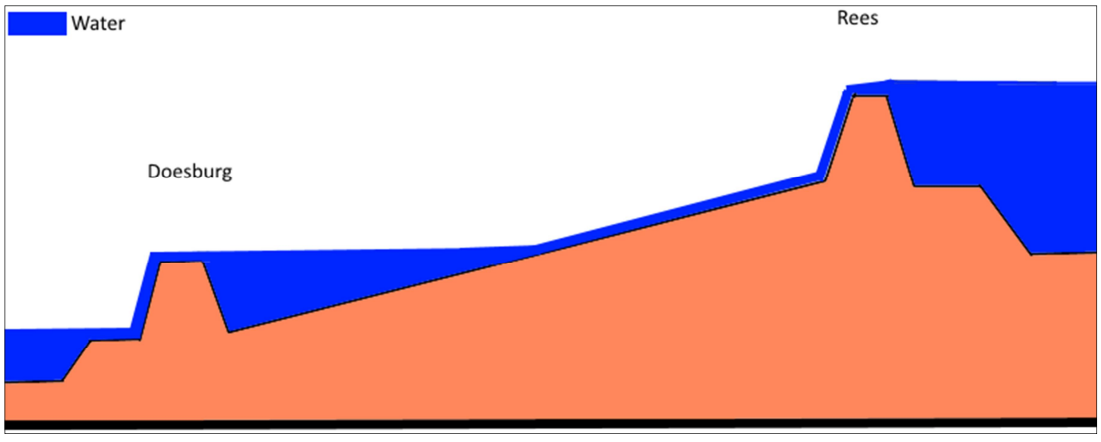

Figure 3.9 Schematic cross-section of dike ring 48 for the trajectory Rees-Doesburg (IJssel) in the situation of flooding at Rees. Note that the horizontal and vertical scales are exaggerated

3.4.2 Limitation of the dike overtopping capacity

Secondly a check is done if the overflow capacity of the dikes is large enough to get rid of all the water. From Figure 3.6 the total length of the dikes that will we be overtopped during an event of 18,000 m^3/s (or higher) can be obtained. The total length of the dikes at the left bank (red line) that will overflow at a discharge of 18,000 m^3/s is approximately 18 km. The length of the dikes at the right bank (green line) that will overflow is around 19 km, which makes it a total of approximately 37 km.

In studies about dike stability (e.g. RWS WVL, 2013, especially figure 10) it was found that for dikes in good condition a critical overflow discharge would be between 50-100 $l \cdot s^{-1} \cdot m^{-1}$. This means that the maximum discharge that could be lost due to overtopping of the dike without dike failure would be between 1850 and 3700 m^3/s. When higher overtop discharges occur, it becomes very likely that the dikes will fail.

In reality there will be no limit in the overflow discharge. When the discharge in the Rhine increases, the water level will rise accordingly, resulting in higher overflow discharges. The question rises whether the dikes will fail or not.

When a dike breaches, the discharge through a breach could increase rapidly. In the report by the German-Dutch working group (Duits-Nederlandse Werkgroep Hoogwater, 2006b,c) discharges up to 3000 m^3/s were calculated for dike breach locations along the Rhine. In Paarlberg (2014) four locations were identified where the level of the top of the dike is lower than the water level corresponding to the 18,000 m^3/s discharge (locations C-F in Figure 3.6). These locations might be at risk of breaking. However, these locations have not yet been studied in more detail. If at these locations (or any other location) indeed the dikes fail, an extra amount of water will be lost to flooding, reducing the discharge at Lobith significantly.

The conclusion is that much water can be lost just due to overtopping. For the most extreme discharges (>21,000 m^3/s) however, it is very likely that dikes will fail due to the extreme overflow discharges. Where, when and how many dikes will fail should be analysed in more detail, using high detail 2D hydrodynamic computations and methods that analyse the dike stability. Also the effect of dike failure on the discharge at Lobith should be analysed in more detail. Finally the effect of water flowing into the (old) IJssel needs further study.

3.4.3 Method for correction of the calculated discharge at Lobith

To correct for the overestimation of the discharge at Lobith, the discharge at Lobith calculated by Sobek is corrected. This correction procedure makes use of two basic choices.

The first choice involves the selection of the discharge value Q_0 for which it can be assumed that - discharges at Lobith below Q_0, are satisfactorily predicted by Sobek, while for discharges larger than Q_0 the model tends to overestimate the discharge at Lobith. This Q_0 should be as large as possible, and within the range where upstream flooding is significantly affecting the flow. In other words, Q_0 should be near the limit where the effects of flooding are still well represented by Sobek. This Q_0 will be in the order of 16,000 m^3/s, the moment that the first dikes along the stretch between Wesel and Lobith start to flood.

The second choice involves the selection of the maximum conveyance capacity Q_L that is expected to hold for the maximum discharge capacity. For the river Rhine this capacity is in the order of 18,000 m^3/s.

On the basis of Q_0 and Q_L the discharge (maximum) computed by Sobek is 'corrected' according to some function $f(\cdot)$. This function is a continuous, smooth, and monotonously increasing function such that $Q_c = f(\mathrm{Q}) = \mathrm{Q}$ (i.e. no correction) for $Q < Q_0$. For $Q > Q_0$ the function must also be increasing but such that for $Q \to \infty$ it gradually saturates to the prescribed limit value Q_L. For reason of smoothness at the 'breakpoint' Q_0, $f(\mathrm{Q})$ should be continuous and differentiable in $Q = Q_0$.

For such a function a large number of candidates are available. All these functions have the same behaviour of gradually increasing from Q_0 at $= Q_0$ to Q_L for $Q \to \infty$.

The difference is the speed of saturation. This is shown in *Figure 3.* for a selection of such functions (with Q_0=16,000 m^3/s and Q_L = 18,000 m^3/s). To correct the discharges at Lobith calculated with Sobek larger than 16,000 m^3/s the 'linear' correction formula (Eq. 3.4.1, corresponding to the black line in *Figure 3.*), has been adopted.

$$f_{Lin}(Q) = Q_0 + (Q_L - Q_0) \cdot \left(1 - \frac{1}{1 + \dfrac{Q - Q_0}{Q_L - Q_0}} \right) \qquad \text{Eq. 3.4.1}$$

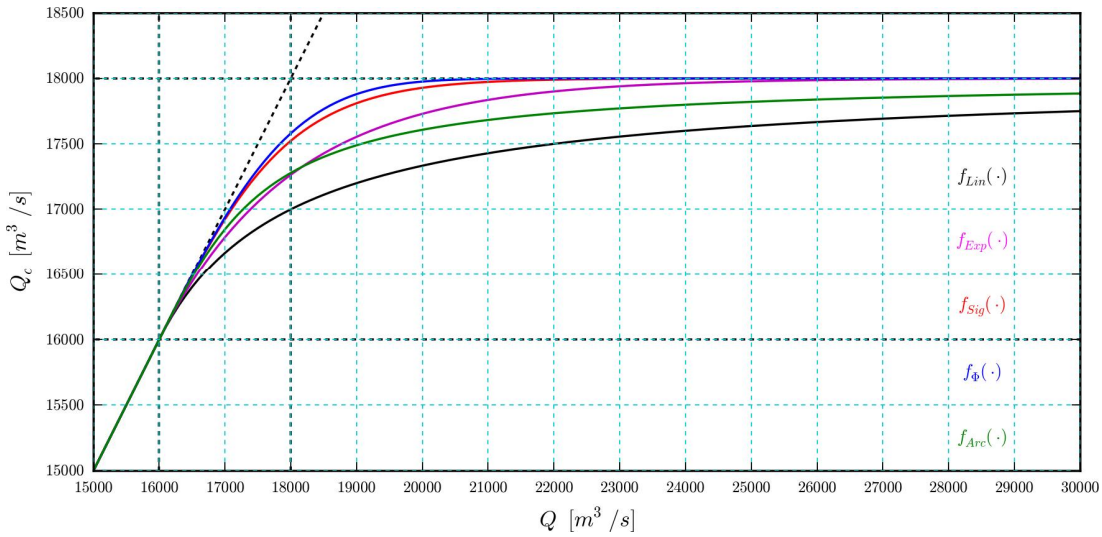

Figure 3.10 *Alternatives for the correction function, all based on Q_0 =16,000 and Q_L = 18000 m^3/s*

4 KNMI'14 discharge projections compared with earlier projections

4.1 KNMI'14 based changes in the discharge of the Rhine and Meuse

In the previous chapters we discussed the new climate scenarios that have been developed by the KNMI, the methods that have been applied to translate the climate changes into discharges of the River Rhine and Meuse and we provided brief overviews of international research projects that focussed on the effects of climate change in the Rhine and Meuse basins. In this chapter we will provide the effects of climate change on the discharge of the Rivers Rhine and Meuse according to the new KNMI'14 scenarios. We will also compare the changes with those that have been estimated in other projects and provide brief explanations of the hydrological responses. The setup of the chapter is as follows:

In section 4.1 we will provide the changes in discharge of the Rivers Rhine and Meuse. We will describe the changes in terms of changes in average annual and seasonal discharges, changes in low and changes high flows. Extended attention will be paid to the estimates of very extreme high flow events as these are of specific interest for the Netherlands flood management. We will analyse and explain the changes that result from the climate projections by considering the basin characteristics.

In section 4.2 we will compare the KNMI'14 projections for the river discharges with previous assessments of the effects of climate change. We also will compare the KNMI projections with projections where the full range of the CMIP5 climate change ensemble is transferred into changes of river discharge. The latter is to illustrate the range that the 4 KNMI'14 scenarios cover in respect to the full range of available climate projections

In section 4.3 we will discuss some of the differences in results compared with previous assessments that result from changes in the methods that have been applied since the previous studies.

In this analysis we focus on the changes at the gauging stations Borgharen (river Meuse) and Lobith (river Rhine). We provide a series of statistics to describe the changes. The analysis is based on the so-called hydrological year (November-October). The following statistics have been collected:

- Average monthly discharge and annual hydrographs
- Long term mean annual discharge (MQ)
- Long term mean annual lowest seven day flow (NM7Q)
- Annual maximum discharges (MHQ)
- Magnitude of extreme flood events with long return periods

4.1.1 KNMI'14 projections for the Meuse

Changes in the monthly discharge regime

According to the KNMI'14 scenarios climate change will result in increased discharge during the winter period and lower flows in the late summer period, changes are smallest for the G_L scenario.

The spread in projected discharge change is especially large for late summer, ranging from zero change for the G_L scenarios to a decrease of 100 m^3/s to a discharge of 40 m^3/s for 2085 projected by the $W_{H,dry}$ scenario (fig 4.1). For stations upstream in the Meuse basin (See Appendix B) we see a similar pattern of change.

We analysed the cause of the large reduction in late summer discharge for the $W_{H,dry}$ scenario by analysing the change in meteorological input data for one of the major sub-basins of the Meuse - the Ourthe basin. The reduction in precipitation for the summer months are large in the $W_{H,dry}$ scenario, especially for august when precipitation is approximately halved. At the same time we observe large increases in temperature and consequently evaporation.

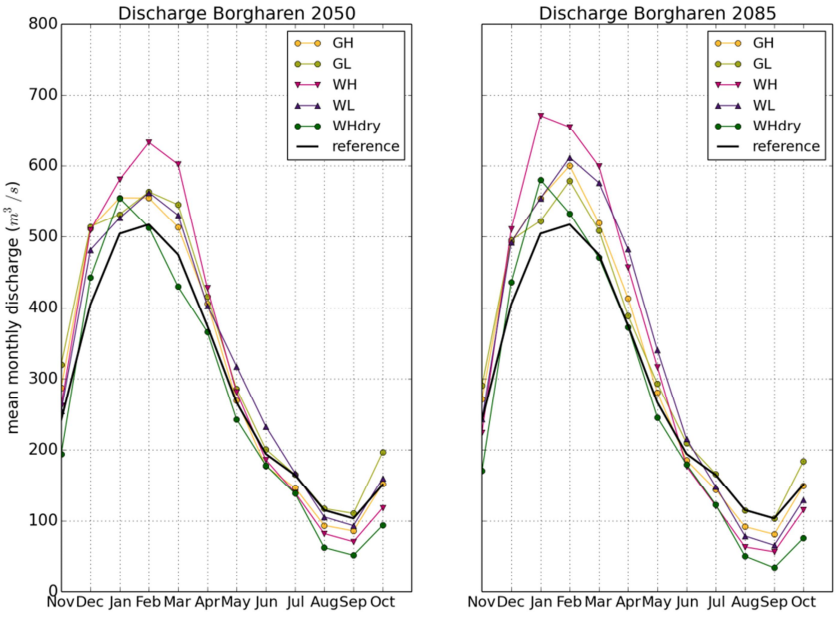

Figure 4.1 Average monthly discharge cycle for Borgharen for the five KNMI'14 scenarios

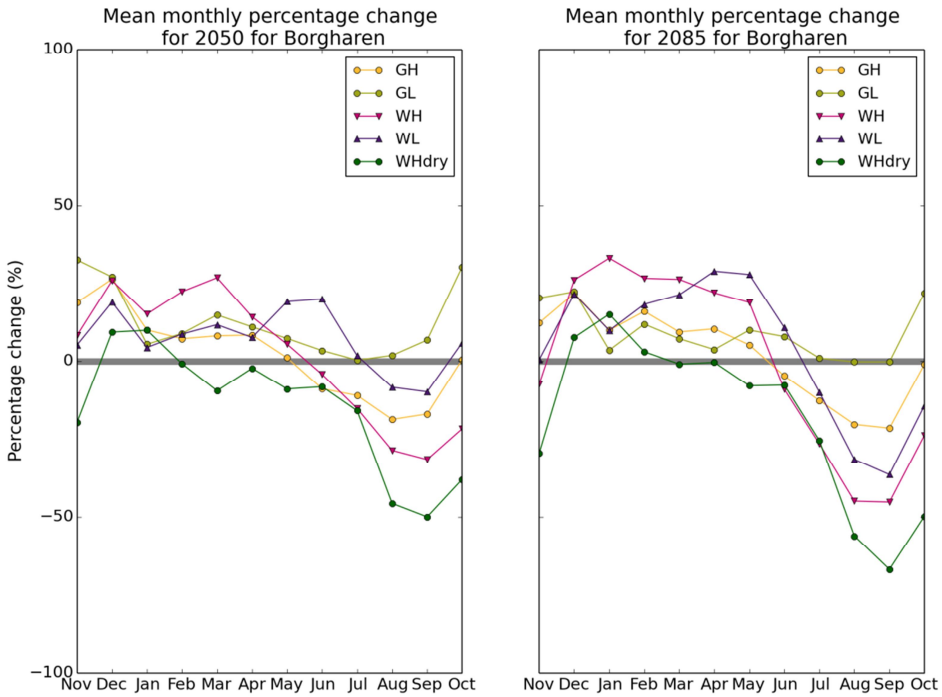

Figure 4.2 Percentage change in average monthly discharge cycle for Borgharen for the five KNMI'14 scenarios

Changes in annual mean, minimum and maximum discharges

Table 4.1 presents the current and the projected annual mean (MQ), average annual 7-day low flow (NM7Q), and average annual maximum discharges (MHQ).

Table 4.1 Current and projected annual mean, mean annual 7 day low flow and mean annual maximum discharge for Borgharen (m^3/s)

	Reference	2050					2085				
		G_L	G_H	W_L	W_H	$W_{H,dry}$	G_L	G_H	W_L	W_H	$W_{H,dry}$
MQ	290	330	310	320	320	270	320	315	325	330	270
NM7Q	45	45	40	40	35	25	45	40	35	30	20
MHQ	1635	1835	1800	1775	1890	1650	1790	1810	1900	1990	1770

The annual mean discharge in the Meuse basin will slightly increase for all KNMI'14 scenarios except the KNMI14 $W_{H,dry}$ scenario. Summer discharge decreases compensate for winter discharge increases (*Figure 4.2*) leading to little change in annual mean discharge. For the annual mean there is little difference between the 2050 and the 2085 conditions.

For the average annual 7-day low *flow*, the changes are small and there is a tendency towards discharge increases. Yet, large decreases are projected by the $W_{H,dry}$ scenario as a result of the summer precipitation decreases and evaporation increases.

All KNMI'14 scenarios project increases in mean annual maximum discharge, increases are largest towards the end of the century. The largest MHQ's are found for the KNMI'14 W_L - and especially the KNMI'14 W_H scenario, which have the largest precipitation increases in winter.

Changes in the months with the lowest and highest average discharge
September is the month with on average the lowest discharges for Borgharen for all scenarios. Therefore the long-term average discharges are quantified in Table 4.2. A range of changes including both in- and decreases is projected. Yet, it can be concluded that decreases are more likely – since only the G_L scenario for 2050 projects an increase.

February is for Borgharen for most KNMI'14 scenarios the month with the highest discharge. Exceptions are the $W_{H,dry}$ scenarios and the W_H scenario for 2085 where the highest average discharge occurs in January – see also figure 4.2. According to all scenarios February discharge is likely to increase.

Table 4.2 Change in the average September and February discharge at Borgharen (%) with respect to the reference discharge (m^3/s)

Average Discharge (m^3/s)	Reference	2050					2085				
		G_L	G_H	W_L	W_H	$W_{H,dry}$	G_L	G_H	W_L	W_H	$W_{H,dry}$
September	103	+7%	-17%	-10%	-32%	-50%	0%	-21%	-32%	-45%	-67%
February	514	+10%	+8%	+9%	+23%	0%	+13%	+17%	+16%	+27%	+4%

Changes in extreme discharges
In Figure 4.3 for 2050 the distribution of the annual discharge maxima at Borgharen are presented in the right panel. In the left panel, the corresponding basin average annual maximum 10-day precipitation for the winter half year is presented. Both extreme discharges and extreme 10-day precipitation increase in all scenarios compared to the reference period (i.e. the current climate). For return periods larger than about 100 years the increase in the discharges is around 10%.

The spread between the scenarios is relatively small for 2050. For return periods larger than 100 years only the G_L scenario stands out. In Table 4.3 the discharges for all scenarios are given for specific return periods.

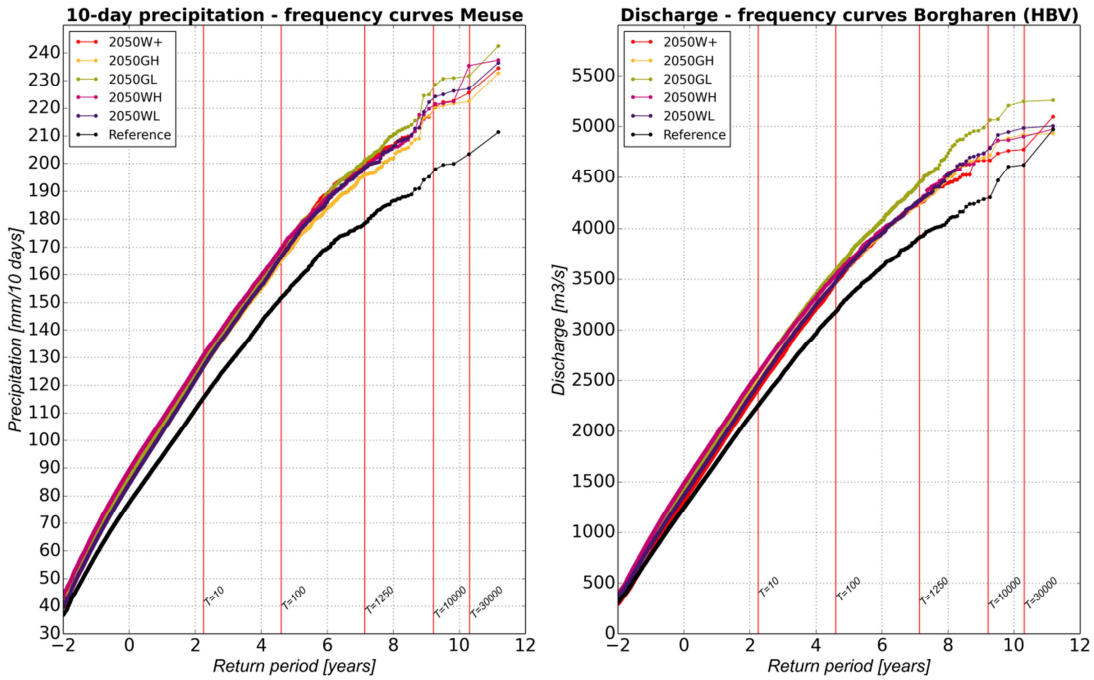

Figure 4.3 Cumulative (probability) distributions of the maximum precipitation in the Meuse basin in the winter half year (left) and of the annual discharge maxima at Borgharen (right) for the KNMI'14 scenarios for 2050 based on the hydrological model results (HBV). The black curve represents the reference situation (i.e. the current climate)

The reason for the small spread in the extreme discharge at Borgharen (Figure 4.3, right panel) is found in the relatively small spread in the extreme 10-day precipitation in the KNMI'14 climate scenarios (Figure 4.3, left panel). In 2050 the spread between the four scenarios (i.e. the difference between the scenarios with the largest and the smallest changes) in winter is about 1.5 °C for the change in mean temperature and about 13% for the change in mean precipitation (Lenderink and Beersma, 2014). Apparently the spread in the change of the extreme 10-day precipitation events in the winter half year in the four scenarios is considerably smaller, only about 5%, than the spread in the change in mean precipitation. This could be related to the fact that each of the four scenarios has a season in which the precipitation increase is 'above average' which may lead to similar increases of the extreme 10-day precipitation in the winter half year.

Why the G_L scenario gives the highest discharges in 2050 is not entirely clear. One indication is that the precipitation change in the G_L scenario for 2050 is relatively large in autumn compared to the other three scenarios and the winter season. This has two potential effects that likely contribute:

- Enhanced (soil) wetness in the catchment in general at the start of the wet season in the G_L scenario leads to a larger sensitivity for extreme precipitation events.
- Due to the relatively large precipitation change in autumn in the G_L scenario, many of the extreme precipitation events in autumn may become larger than those in the other seasons, thereby also dominating the annual maxima of the 10-day precipitation in the basin and of the discharge at Borgharen.

In Figure 4.4 is the equivalent of Figure 4.3 for 2085. In 2085 the difference between the four scenarios is clearly larger than for 2050 and the four scenarios are more distinct (both for the 10-day precipitation and the discharge at Borgharen. The scenario with the largest increases is W_H and the one with the smallest increases is G_H. For W_H the change in 10-day precipitation for return periods larger than about 100 years is in the order of 15%. The increase in the discharges at those return periods is in the order of 20%. The difference between the relative increase in precipitation and discharge might be caused by the non-linear behaviour of the soil. Apparently the soil gets fully saturated at some point during the winter, caused by the large increase in precipitation in the W-scenarios (on average +13% for W_L and +25% for W_H). This will result in more direct runoff and therefore higher peaks. In Table 4.3 the results for the Meuse are summarized and presented for specific return periods.

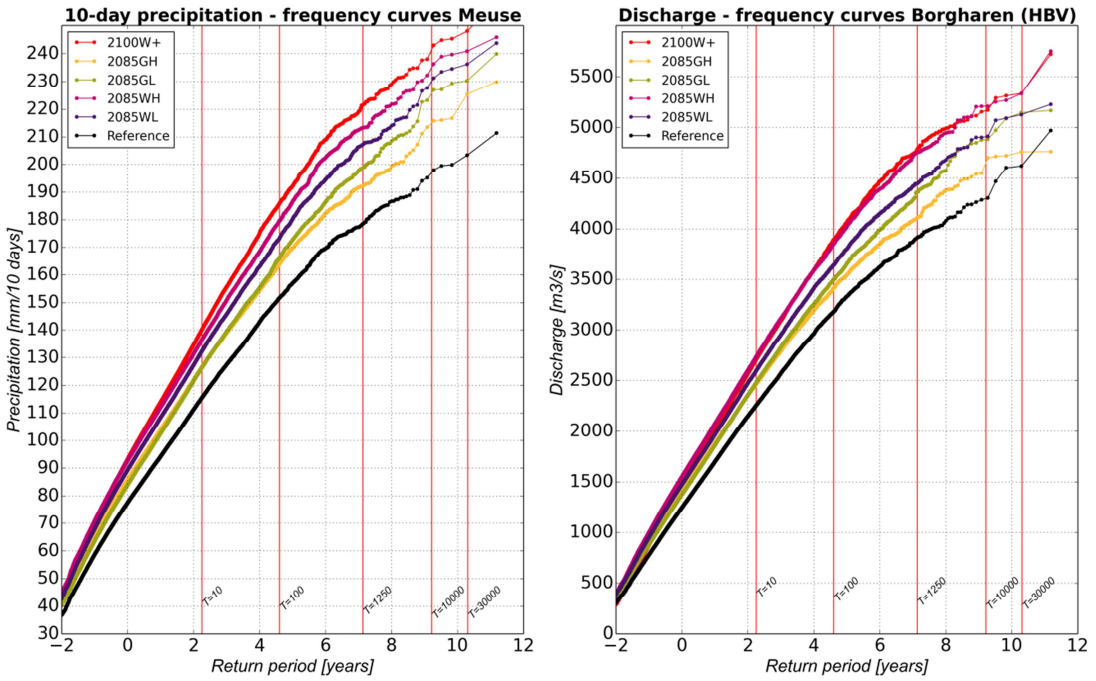

Figure 4.4 Cumulative (probability) distributions of the maximum precipitation in the Meuse basin in the winter half year (left) and of the annual discharge maxima at Borgharen (right) for the KNMI'14 scenarios for 2085 based on the hydrological model results (HBV). The black curve represents the reference situation (i.e. the current climate)

Table 4.3 Discharges at Borgharen (Meuse) for specific return periods for the 4 KNMI'14 climate scenarios in 2050 and 2085, and for the current climate (i.e. the reference situation)

Return period	Reference	2050G_L	2050G_H	2050W_L	2050W_H	2085G_L	2085G_H	2085W_L	2085W_H
[years]	*[m^3/s]*	*[m^3/s]*	*[m^3/s]*	*[m^3/s]*	*[m^3/s]*	*[m^3/s]*	*[m^3/s]*	*[m^3/s]*	*[m^3/s]*
10	2260	2570	2490	2470	2570	2480	2470	2600	2740
30	2740	3090	3000	3000	3080	3000	2960	3140	3300
100	3180	3590	3470	3480	3550	3500	3420	3640	3850
300	3540	3980	3870	3890	3900	3890	3770	4060	4300
1000	3860	4360	4200	4210	4210	4260	4060	4390	4680
3000	4080	4740	4500	4520	4540	4580	4390	4680	4950
10000	4350	5010	4720	4770	4730	4900	4580	4920	5210
30000	4590	5180	4870	4940	4910	5060	4760	5090	5370

The difference between the 2050 situation and the 2085 situation is presented in Figure 4.5 for all scenarios. It can be observed that the difference between the 2050 and 2085 situations is small for both G-scenarios. For the G-scenarios, in 2050 even higher discharges are projected than in 2085.

The reason for this "unexpected" behaviour essentially lies in the nature of the KNMI'14 scenario's and more specifically in the change in precipitation in autumn (see Table 4.4). For the Meuse basin for both G scenarios the increase in precipitation in the autumn in 2050 is larger than in 2085[3] (see Table 4.4). If, in addition, the autumn change is also larger than the winter change (as for the G_L scenario) the change in autumn precipitation may dominate the change in the discharge extremes and thus result in larger discharge extremes for 2050 compared to 2085.

For the W-scenarios, the difference between the 2050 and 2085 changes is larger, especially in winter, see Table 4.4.

Table 4.4 Relative change in season average precipitation for the autumn (September, October, November) and winter (December, January, February) for the Meuse basin

	Autumn		Winter	
	2050	**2085**	**2050**	**2085**
G_L	+9%	+7%	+3%	+5%
G_H	+6%	+5%	+6%	+10%
W_L	+2%	+3%	+6%	+13%
W_H	+5%	+5%	+16%	+25%

[3] *Due to the construction nature of the KNMI'14 climate scenarios the scenario changes contain a small part that is due to natural variability. In the G scenarios the difference in global mean temperature between 2050 and 2085 is only 0.5 ºC. For some changes, such as e.g. the change in mean precipitation in autumn, the effect of this additional 0.5 ºC in global mean temperature may be smaller than the natural variability contribution, effectively resulting in a larger change for 2050 than for 2085. Note that for the W scenarios the difference in global mean temperature between 2050and 2085 is three times as large (1.5 ºC). Its effect always dominates that of the natural variability contribution (which is the same for all scenarios).*

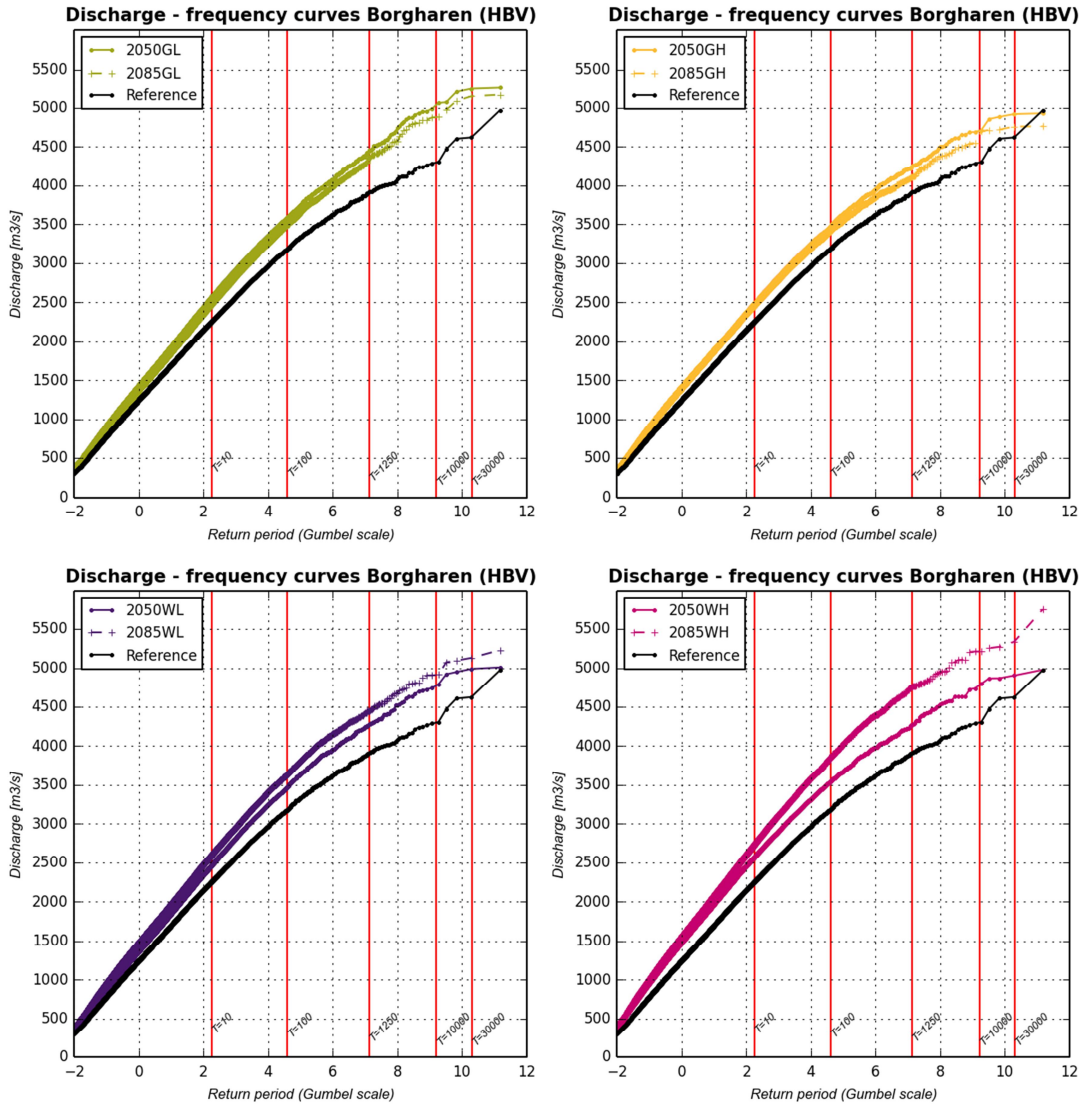

Figure 4.5 Discharge – frequency curves for the Meuse at Borgharen for all scenarios and years

4.1.2 KNMI'14 projections for the Rhine

The changes and future discharges described here focus on those at the gauging station Lobith. However, also changes at the gauging stations Maxau (representing the Alpine region) and Trier (representing the river Mosel) are briefly discussed as these partly explain the projected changes for Lobith. The extreme discharge analysis is presented in Section *changes in extreme discharges.*

Changes in the monthly discharge regime

The KNMI'14 scenarios envisage an increase in winter discharge and a decrease in late summer / autumn discharge for Lobith increasing the inter-annual variability compared to the reference climate. This change becomes more pronounced when approaching the end of the century but can already be observed in 2050.

Along the course of the Rhine different discharge changes are projected. Maxau is located upstream of Lobith and the river regime is strongly determined by snowfall and melt in the upstream Alpine sub-basins. Here the influence of temperature increases may be relatively large. More precipitation will fall as rain instead of snow, resulting in more fast runoff and less snow accumulation. At Trier, located along the Mosel, the flow is dominantly influenced by rain. At Lobith the graph shows a combined regime, the discharge changes of all upstream locations are aggregated and in the regime plot both changes from the area dominated by a rainfall regime (illustrated by Trier) and an are dominated by a snowmelt regime (illustrated by Maxau) can be seen. This explains why the summer discharge decreases at Lobith are smaller than at Trier.

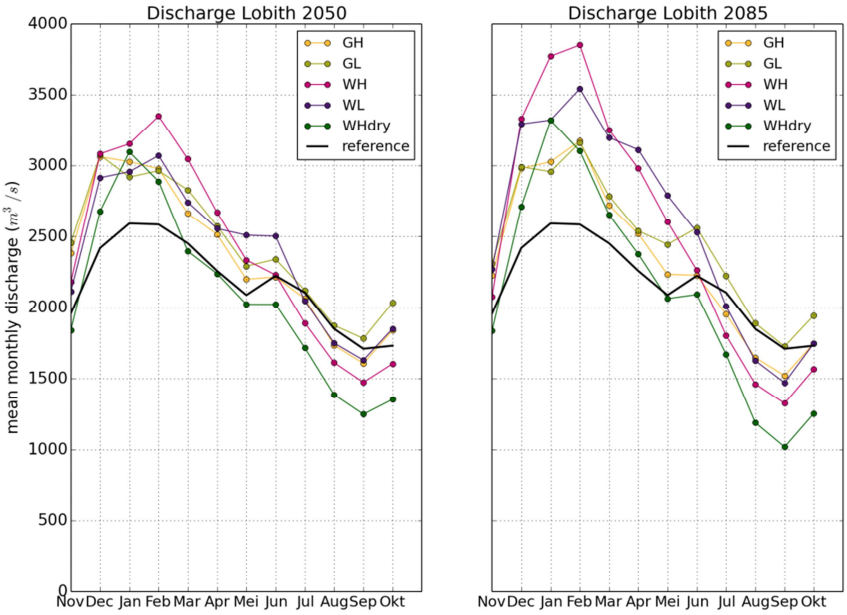

Figure 4.6 Average monthly discharge regime for Lobith for the five KNMI'14 scenarios in comparison to the reference situation

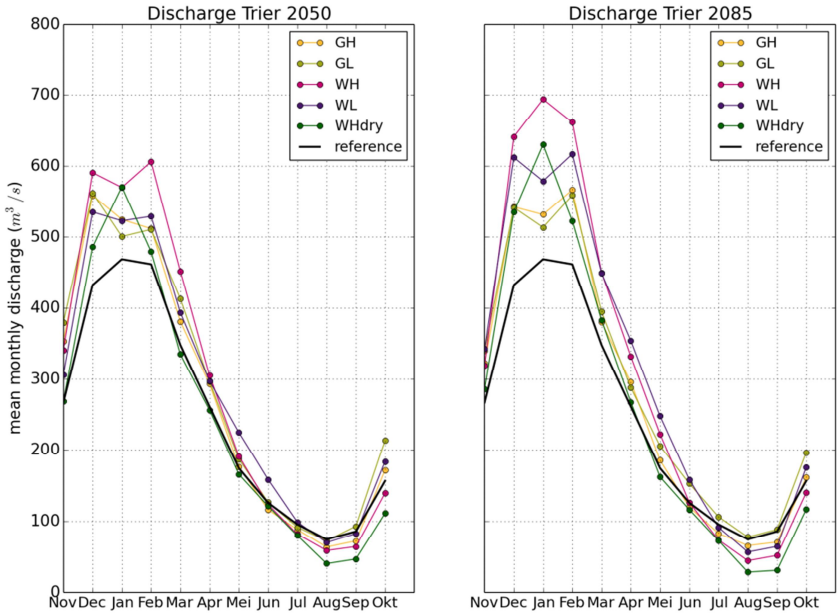

Figure 4.7 Average monthly discharge regime for Trier for the five KNMI'14 scenario in comparison to the reference situation

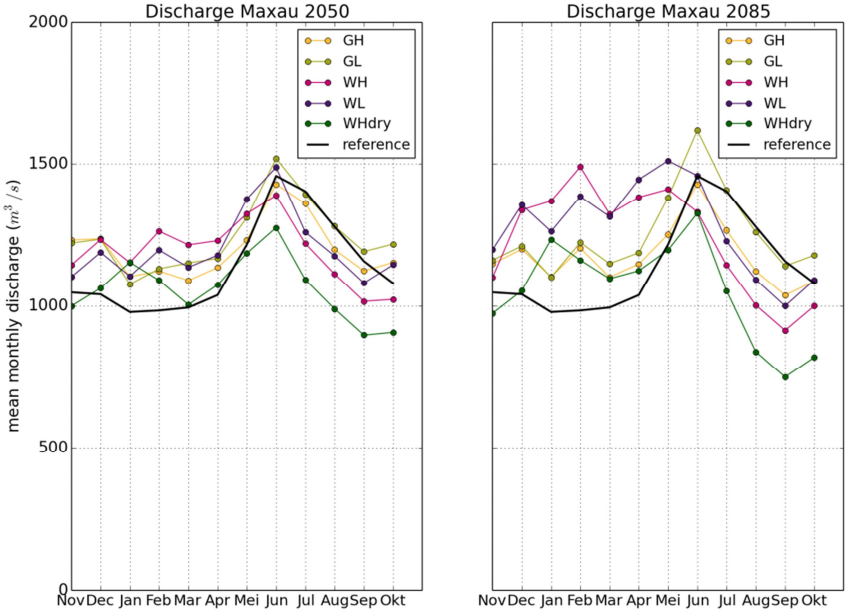

Figure 4.8 Average monthly discharge regime for Maxau for the five KNMI'14 scenarios in comparison to the reference situation

Changes in annual mean, minimum and maximum discharges
Table 4.5 presents the current and projected future *long term mean annual lowest seven day flow (NM7Q)*, annual mean (MQ) and annual maximum (MHQ) discharges.

Table 4.5 Changes in 7 day low flow, mean and maximum discharge for Lobith (m^3/s)

		2050					2085				
	Reference *(1951-2006)*	**G_L**	**G_H**	**W_L**	**W_H**	**$W_{H,dry}$**	**G_L**	**G_H**	**W_L**	**W_H**	**$W_{H,dry}$**
MQ	2160	2440	2350	2385	2380	2070	2460	2330	2570	2515	2100
NM7Q	1010	1095	1030	1020	960	825	1085	990	995	915	735
MHQ	7060	8365	8085	8260	8540	7450	8345	8100	9275	9710	8240

Mean discharge (MQ) at Lobith is projected to increase according to all KNMI'14 scenarios except the W_{Hdry} scenario for both 2050 and 2085. Increases range up to 400 m^3/s for the 2100 W_L scenario. For the G_L and G_H scenario there is little difference in discharges simulated for 2050 and 2100.

For *long term mean annual lowest seven day flow* (NM7Q) at 2050 the signal is mixed the G and W_L scenarios project small increases whereas W_H and especially $W_{H,dry}$ projects decreases. Towards the end of the century four out of five scenarios project decreases as a result of increased evaporation and decreased precipitation. The G_L scenario is the only scenario projecting a possible increase.

Mean annual maximum discharge (MHQ) is likely to increase according to all scenarios for both time horizons. For the G scenarios the difference between 2050 and 2085 is small – this directly results from the non-linearity in temperature increase over time. For both W_H and W_L maximum discharge increases towards the end of the century are large – ranging even up to 2000 m^3/s.

Changes in mean discharge in the on average driest and wettest months
In this paragraph we present changes in the on average wettest and driest months of the year, statistics of relevance for Dutch water resources management derived from the short historical records and short future projections.

September is the month with the lowest average discharge at Lobith for all KNMI14 scenarios. In Table 4.6 the average September discharges are shown. The projected range of changes includes mainly decreases. For 2085 only a tiny increase of 1% (G_L) is projected all other scenarios project decreases ranging up to 40% ($W_{H.dry}$).

February is the month with the highest average discharge at Lobith. Exceptions are the relatively dry and warm $W_{H,dry}$ scenarios, where the highest average discharges occurs in January for both 2050 and 2085, and the G_H and G_L scenarios for 2050 where highest average discharge occurs in December (see figure 4.6). This indicates a shift in time towards earlier months may occur as well. This could be a result of decreased snow accumulation in the Alps. The average February discharge is likely to increase according to all scenarios. Increases are largest towards the end of the century.

Table 4.6 Change in September discharge at Lobith

		2050					2085				
	Reference *(1951-2006)*	G_L	G_H	W_L	W_H	$W_{H,dry}$	G_L	G_H	W_L	W_H	$W_{H,dry}$
September	1710 (m^3/s)	+4%	-6%	-5%	-14%	-27%	+1%	-11%	-12%	-23%	-40%
February	2585 (m^3/s)	+15%	+15%	+19%	+30%	+12%	+22%	+23%	+32%	+49%	+20%

Change in the frequency of low flows

When the discharge at Lobith decreases below 1000 m^3/s the limited water depth can affect navigation (Ter Maat et al., 2013). At the same time chloride concentrations may increase above 250 mg/l which is a critical level for water intake for drinking water. We therefore present the average number of days per year with discharges at Lobith below 1000 m^3/s in Table 4.7. From the set of KNMI'14 scenarios only the W_H and $W_{H,dry}$ scenarios project increases in the number of days with discharges at Lobith of less than 1000 m^3/s. At the end of the century these low flow days could occur on average 61 days a year according to the $W_{H,dry}$ scenario. Yet, the remainder of scenarios indicate that a small improvement in the low flow situation may occur.

Table 4.7 Average number of days per year with a discharge at Lobith of less than 1000 m^3/s

		2050					**2085**				
	Reference *(1951-2006)*	**G_L**	**G_H**	**W_L**	**W_H**	**$W_{H,dry}$**	**G_L**	**G_H**	**W_L**	**W_H**	**$W_{H,dry}$**
# of days (Q_{LOB}<1000 m^3/s)	23	14	18	19	23	46	15	22	19	27	61

Change in extreme discharges

In Figure 4.9 the distributions of annual discharge maxima for the KNMI14 'scenarios for 2050 based on the hydrological model (HBV) are presented in the right panel. These results do not yet include the effect of upstream flooding, this is taken into account in the hydraulic model (Sobek), for which the results are presented later in this Chapter.

In the left panel of Figure 4.9, the annual maximum 10-day precipitation in the winter half year is plotted for all scenarios in 2050. It can be seen that both the extreme discharges and extreme 10-day precipitation increase with respect to the reference period (black lines). For the higher return periods (e.g. above 100 years), the increase in the discharge is around 10-15%. The same can be observed in the 10-day precipitation – frequency curves.

The spread in the scenarios is, similar to the Meuse, small for 2050. For higher return periods (above 100 years) only the G_L scenario stands out. The reason for the small spread is found in the climate scenarios. In 2050 the spread between the four scenarios (i.e. the difference between the scenarios with the largest and the smallest changes) in winter is about 13% for the change in mean precipitation (Lenderink and Beersma, 2014). Apparently the spread in the change of the extreme 10-day precipitation events in the winter half year in the four scenarios is considerably smaller, only about 5%, than the spread in the change in mean precipitation. This could be related to the fact that each of the four scenarios has a season in

which the precipitation increase is 'above average' which may lead to similar increases of the extreme 10-day precipitation in the winter half year.

The fact that G_L gives the highest discharges in 2050 can be explained by:

- The fact that the change in precipitation in autumn is relatively large for G_L compared to the other scenarios. The change in the amount of precipitation for G_L in 2050 is +11%, compared to +3% for e.g. W_H. This probably has its effects on the wetness of the basin at the start of the wet season and therefore on the extreme high discharges.
- The relatively wet summer in the G_L scenario, compared to the other scenarios, especially the W-scenarios (see Appendix C). The less dry summer, in combination with the very wet autumn results in a relatively large increase in discharge peaks in autumn and winter, because there is less storage in the basin.
-

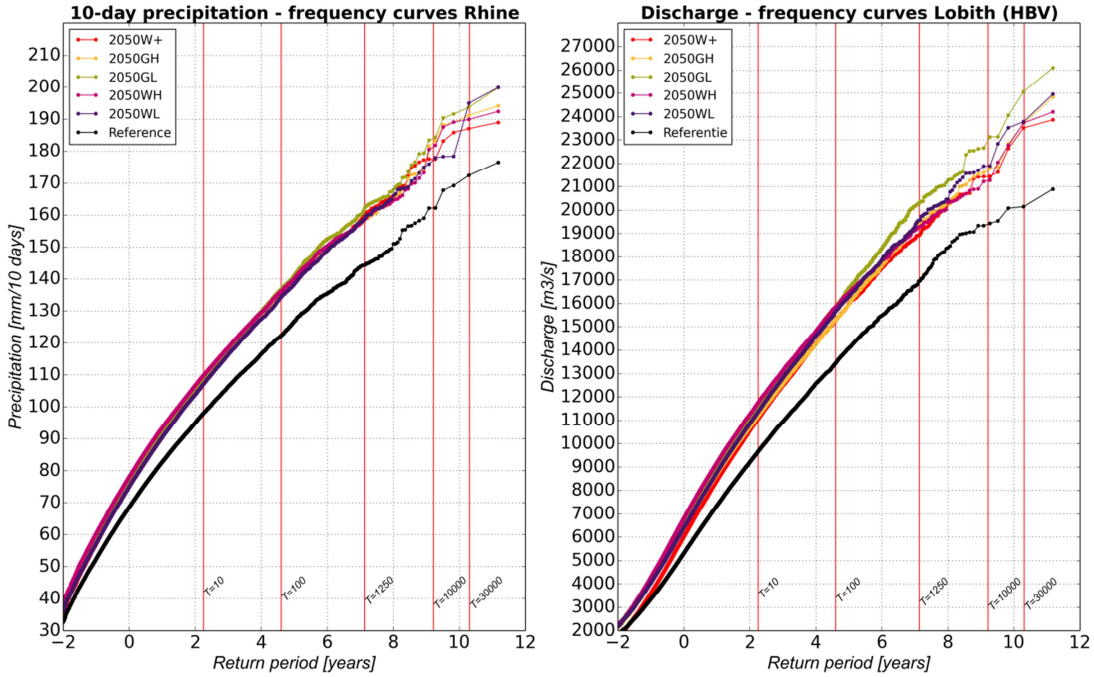

Figure 4.9 Cumulative (probability) distributions of the maximum precipitation in the Rhine basin in the winter half year (left) and of the annual discharge maxima at Lobith (right) for the KNMI'14 scenarios for 2050 based on the hydrological model results (HBV), without the effect of upstream flooding. The black curve represents the reference situation (i.e. the current climate)

In Figure 4.10 the distributions of annual discharge maxima for the KNMI14 'scenarios for 2085 based on the hydrological model (HBV) are presented in the right panel. The difference between the scenarios is larger than for 2050. For 2085, the most extreme scenario is W_H and the least extreme scenario is G_H. For the W_H scenario the change in 10-day precipitation for higher return periods is in the order of 15%. The increase in discharge is considerably larger (in the order of 25%). The difference between the relative increase in precipitation and discharge might be caused by the non-linear behaviour of the soil. Apparently the soil gets fully saturated at some point during the winter, caused by the large increase in precipitation in the W-scenarios (on average +17% for W_L and +28% for W_H). This results in more direct runoff and higher peaks.

For the Rhine, due to the larger temperature increase in 2085 an additional contribution is possible from snowmelt in the Alps (e.g. more snowmelt, earlier melting of the snow, glacier melt). This could affect the discharge peaks, although the contribution of snow melt to discharge peaks normally is small compared to the contribution of (direct) precipitation.

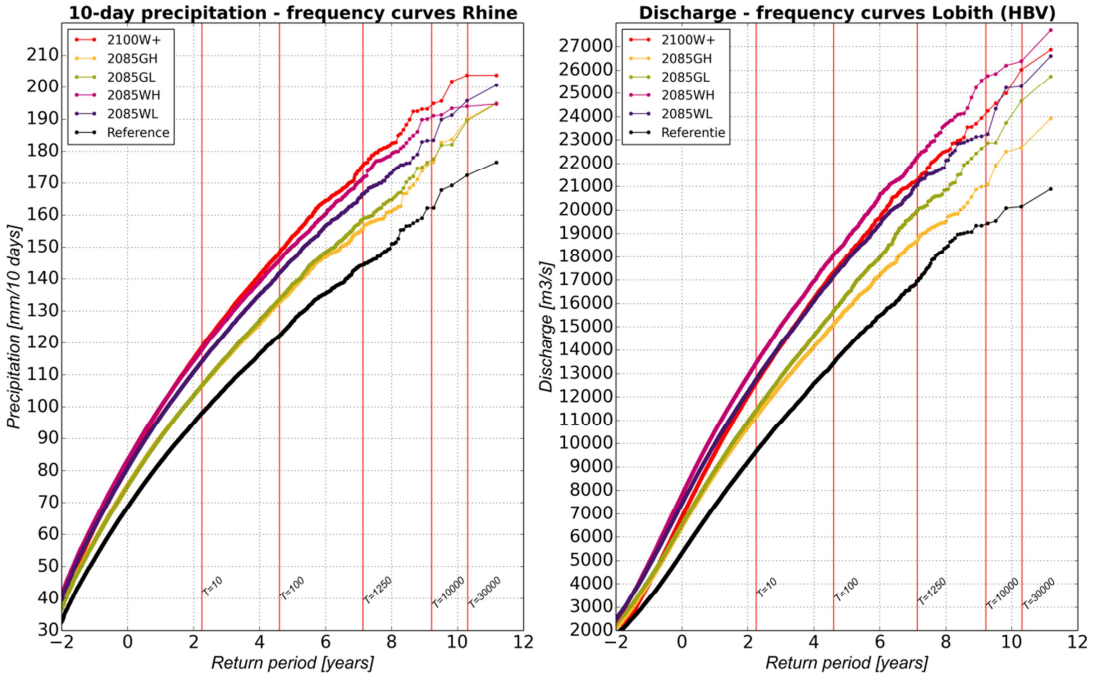

Figure 4.10 Cumulative (probability) distributions of the maximum precipitation in the Rhine basin in the winter half year (left) and of the annual discharge maxima at Lobith (right) for the KNMI'14 scenarios for 2085 based on the hydrological model results (HBV), without the effect of upstream flooding. The black curve represents the reference situation (i.e. the current climate)

The difference between the 2050 situation and the 2085 situation is presented in Figure 4.11 for all scenarios, and shows the same behaviour as the Meuse (Section 4.1.1).

The reason for this "unexpected" behaviour could be found in the change in precipitation in the different seasons (autumn and winter) as presented in Table 4.8.

Table 4.8Relative change in average precipitation autumn (September, October, November) and in winter (December, January, February) for the Rhine basin

	Autumn		Winter	
	2050	**2085**	**2050**	**2085**
G_L	+11%	+7%	+3%	+7%
G_H	+8%	+5%	+5%	+9%
W_L	+3%	+6%	+8%	+17%
W_H	+3%	+5%	+14%	+28%

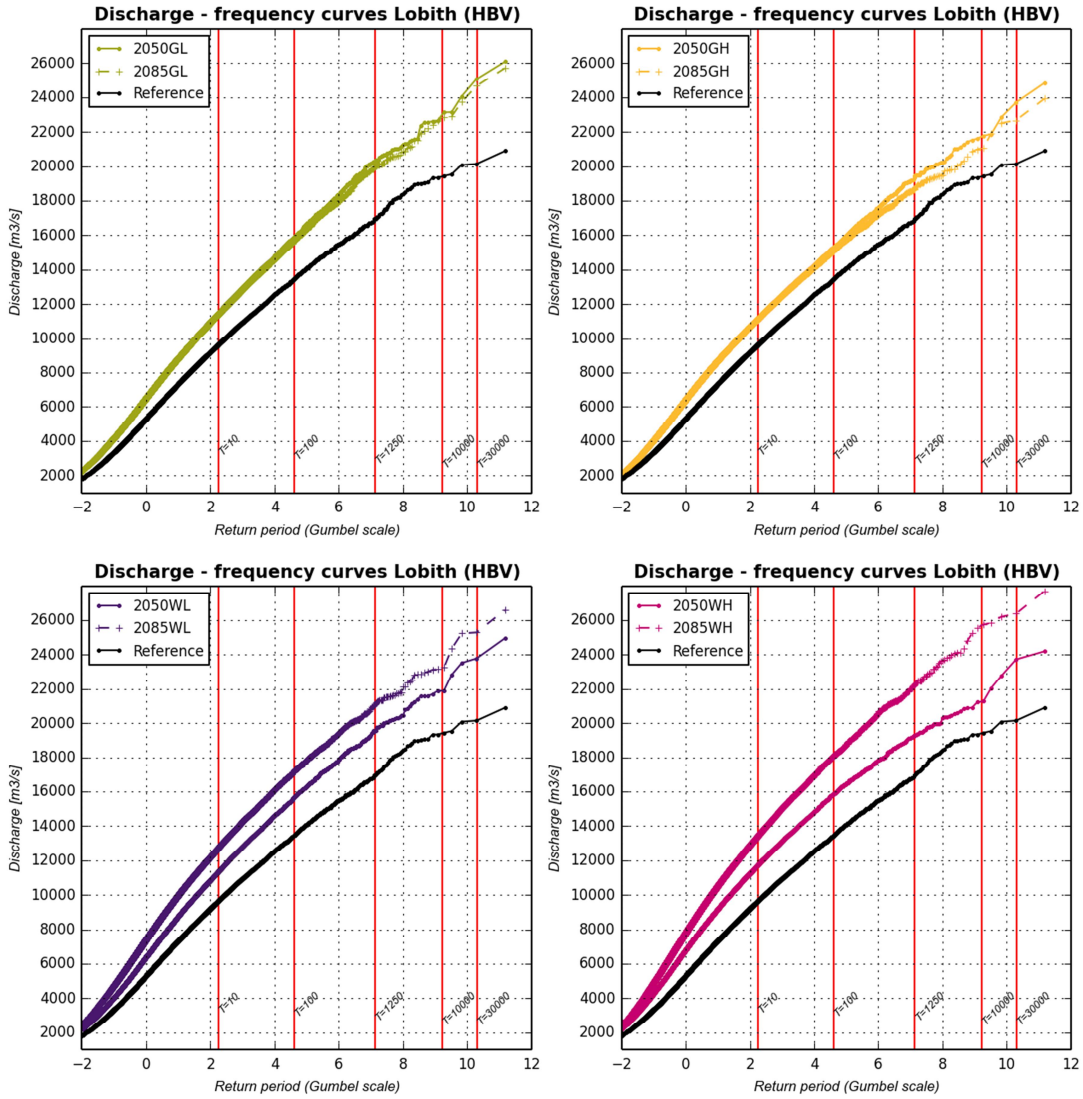

Figure 4.11 Discharge – frequency curves for the Rhine at Lobith for all scenarios and years, based on the hydrological model results (HBV), without the effect of upstream flooding

4.1.3 Upstream flooding in the Rhine

For the Rhine, the effect of upstream flooding is also taken into account. To do so, Sobek calculations were made for all flood waves for which the calculated discharge with HBV was above 10,000 m^3/s. The upstream flooding causes damping of the flood waves, resulting in lower peak discharges. In the resulting distribution of annual maximum discharges, presented in Figure 4.13, the effect is clearly visible. The slopes of the curves change when discharges are around or above 13,000 m^3/s. Beyond this discharge, upstream flooding starts. Between 13,000 m3/s and 16,000 m^3/s the slope decreases and is more or less constant again. Above 16,000 m^3/s, the slope increases again. Above 16,000 m^3/s, the behaviour of the system changes again. Beyond this discharge, most of the flood areas are completely full and no more damping could occur. This behaviour is shown in Figure 4.12.
In Figure 4.12 it is shown that the maximum discharge (red line) towards the flooded areas around Düsseldorf (i.e. the Sobek flood area D_031) is reached much earlier than the moment that the actual peak is passing (blue line). Also, the water level (green line) in the flooded area rises very quickly, meaning that the total available volume left at the time of passing of the peak in the main stem of the river is strongly reduced. Due to that, the damping of the actual peak is very limited.

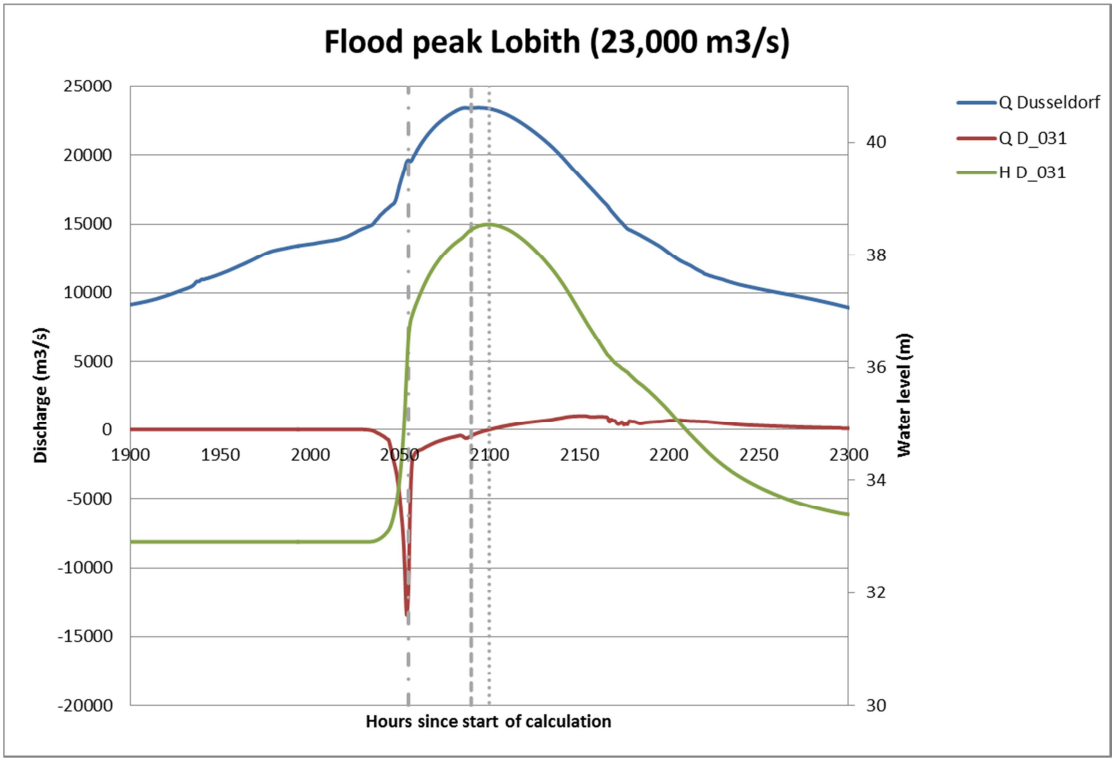

Figure 4.12 Example of limited peak damping due to full flood areas along the Rhine. The blue line represents the flood peak in the main river, the red lines shows the discharge through the dike breach at D_031 (a location near Dusseldorf) and the green line shows the corresponding water level in that particular flood area

The resulting distributions of annual maximum discharges, without any correction, are presented in Figure 4.13 (grey lines). As already mentioned in Section 3.4, the Sobek model is not equipped for such extreme discharges (e.g. the undamped discharges for these events

are above 20,000 m^3/s (!)). The flood areas behind the dikes along the trajectory Wesel-Lobith are not taken into account in the model, resulting in an overestimation of the discharge at Lobith. The discharges above 18,000 m^3/s are corrected for this using the method as described in Section 3.4.3, resulting in distributions of annual maximum discharges presented with the coloured in Figure 4.13.

The difference in the distribution of annual maximum discharges between the scenarios is large for lower return periods compared to the difference for higher return periods. For higher return periods (above 10,000 years), the results are fully dominated by the hydraulic discharge capacity of the Rhine between Wesel and Lobith.

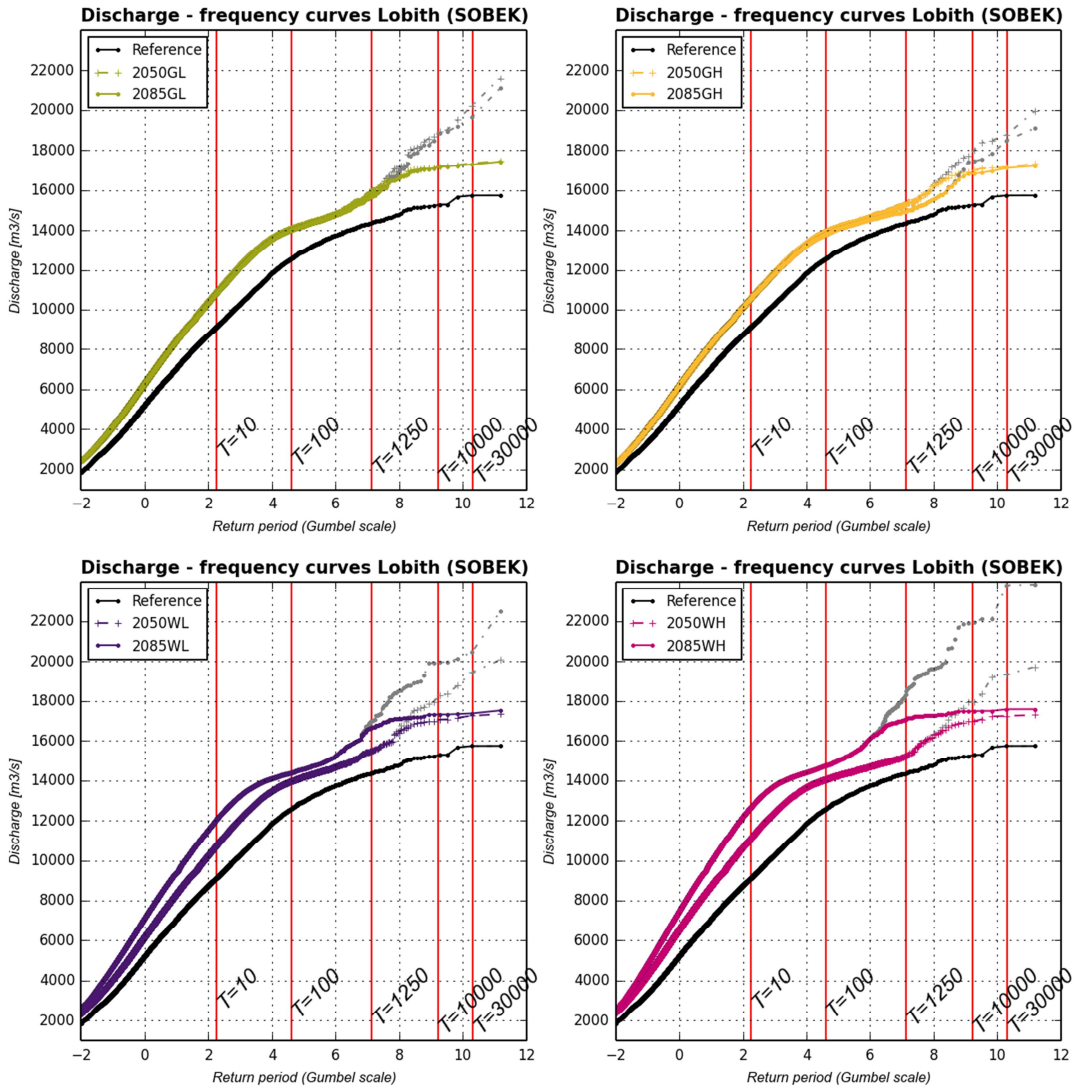

Figure 4.13 Discharge – frequency curves for the Rhine at Lobith for all scenarios and years, based on the hydraulic model results (Sobek), with the effect of upstream flooding. In grey the results without the correction for the flood areas along the stretch between Wesel and Lobith are shown

In Table 4.9 the discharges for specific return periods are given for 2050 and 2085 respectively for all KNMI'14 scenarios.

Table 4.9 Overview of discharges (Sobek) for the Rhine (at Lobith) for specific return periods for all scenarios in 2050 and 2085, including the effect of upstream flooding and including the correction for the flood areas along the stretch between Wesel and Lobith

Return period	Reference	2050G_L	2050G_H	2050W_L	2050W_H	2085G_L	2085G_H	2085W_L	2085W_H
[years]	*[m^3/s]*	*[m^3/s]*	*[m^3/s]*	*[m^3/s]*	*[m^3/s]*	*[m^3/s]*	*[m^3/s]*	*[m^3/s]*	*[m^3/s]*
10	9130	10,880	10,590	10,760	11,130	10,810	10,580	12,050	12,660
30	10,910	12,870	12,520	12,710	12,980	12,750	12,430	13,670	14,070
100	12,580	14,090	13,930	13,980	14,060	14,020	13,810	14,390	14,760
300	13,570	14,650	14,510	14,520	14,580	14,600	14,420	14,970	15,630
1000	14,290	15,680	15,170	15,370	15,100	15,490	14,860	16,420	16,980
3000	14,800	16,740	16,240	16,410	16,300	16,640	15,570	17,120	17,290
10000	15,270	17,180	16,980	17,050	16,990	17,160	16,840	17,330	17,500
30000	15,700	17,330	17,160	17,220	17,250	17,280	17,040	17,390	17,540

4.2 Comparison with other climate change assessments

4.2.1 River Meuse

As discussed in Chapter 2 several climate impact assessments have been made for the discharge of the Meuse. We here compare the implications of the KNMI'14 climate scenarios and the CMIP5 scenarios on the discharge of the Meuse with results from the AMICE project, the projections from the KNMI'06. It should be noted that over time the methods to generate future discharge projections have improved following scientific developments and using state-of-the-art techniques. This may have induced small differences in the future simulated discharge as well. In Appendix D an overview of the differences between methods is provided and the influence of some these differences is analysed. Based on this analysis a correction is applied to the CMIP5 discharge projections for the Meuse presented in this report (see Appendix D for details).

Figure 4.14 shows that overall changes in the discharge regime projected by the different scenarios sets for 2050 and 2085 correspond well with one another. Most scenario sets suggest a general tendency towards increasing discharges in winter and spring and decreasing discharges in summer, in particular in late summer. However, except for the AMICE scenarios also (relatively small) increases in (late) summer discharge are projected for the future.

The set of KNMI14 scenarios largely covers the spread in the full of CMIP5 climate model projections. Also the KNMI'06 scenarios fit within the CMIP5 ranges for 2050 and 2085. The only scenario that is not supported by the CMIP5 range is the AMICE dry scenario for 2085, which is 'too dry', in particular in winter. For 2085, the KNMI'14 $W_{H,dry}$ scenario, the KNMI'06 W+ scenario and the AMICE wet scenario resemble each other in the sense that they all have a large increase in the winter discharge and at the same time a large decrease in summer discharge.

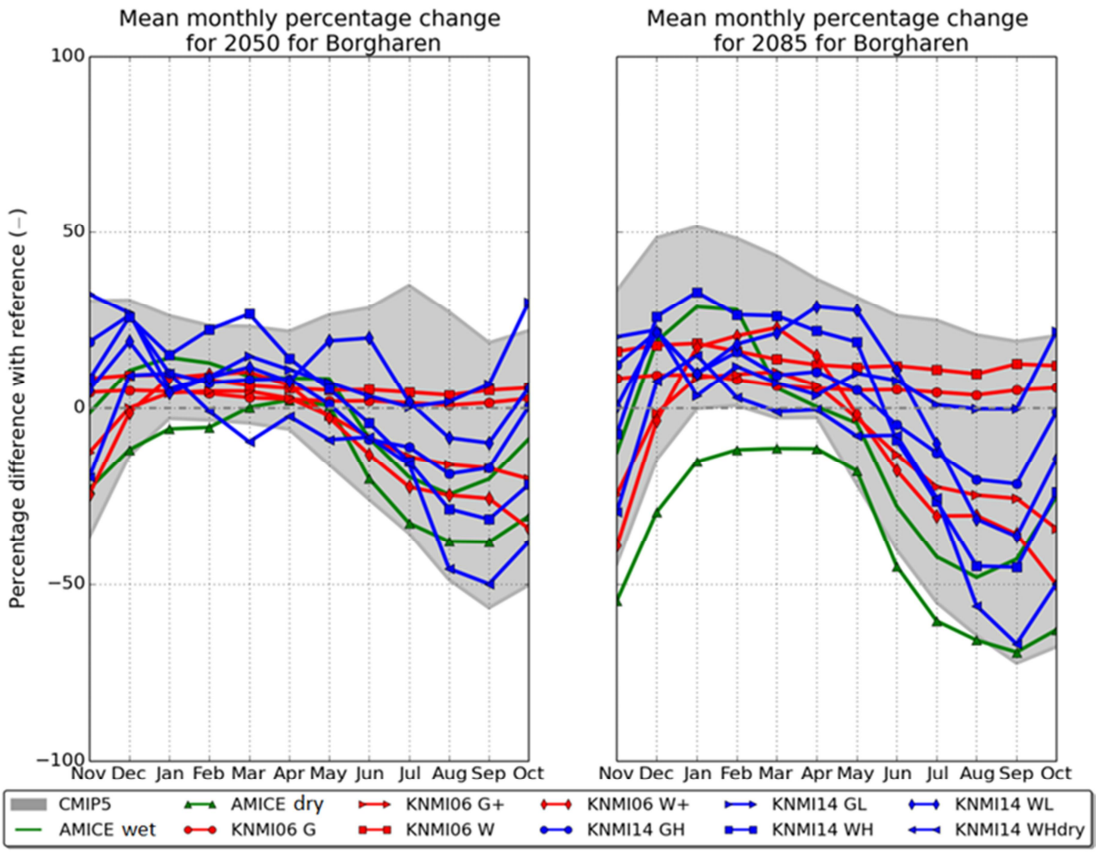

Figure 4.14 Percentage change (%) in average monthly discharge cycle for Borgharen for all climate model / scenario sets. For CMIP5 the grey band represents the 2.5 – 97.5 percentile range of projections

Change in annual mean discharge

Annual mean discharge is projected to increase for most of the KNMI'06 scenarios, the wet AMICE scenario and the KNMI'14 scenarios except for the $W_{H,dry}$ scenario. All scenarios lie within the range of the CMIP5 projections except for the AMICE dry scenario for 2085.

Change in mean annual maximum discharge

Mean annual maximum discharge (MHQ) is likely to increase according to nearly all scenario sets. The dry scenario of the AMICE project is the only scenario that projects decreases for both time horizons, but for 2085 this decrease is outside the range projected by the CMIP5 climate models. In all scenarios with increases, the increases in MHQ are larger towards the end of the century.

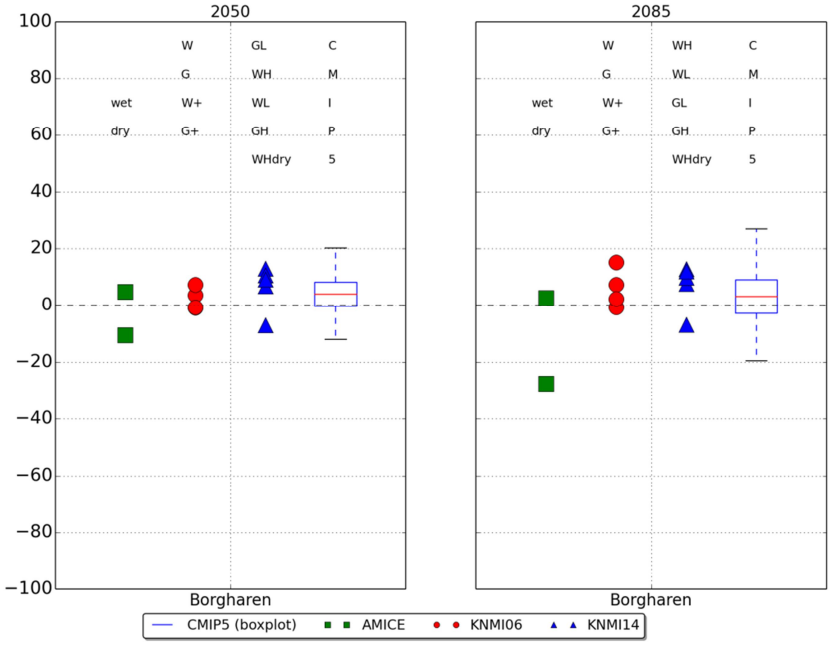

Figure 4.15 Percentage change in mean discharge (MQ) for Borgharen for all climate model / scenario sets. The colour / symbol coding and boxplots represent the scenario sets. On top of the graphs the ordering of scenarios is given

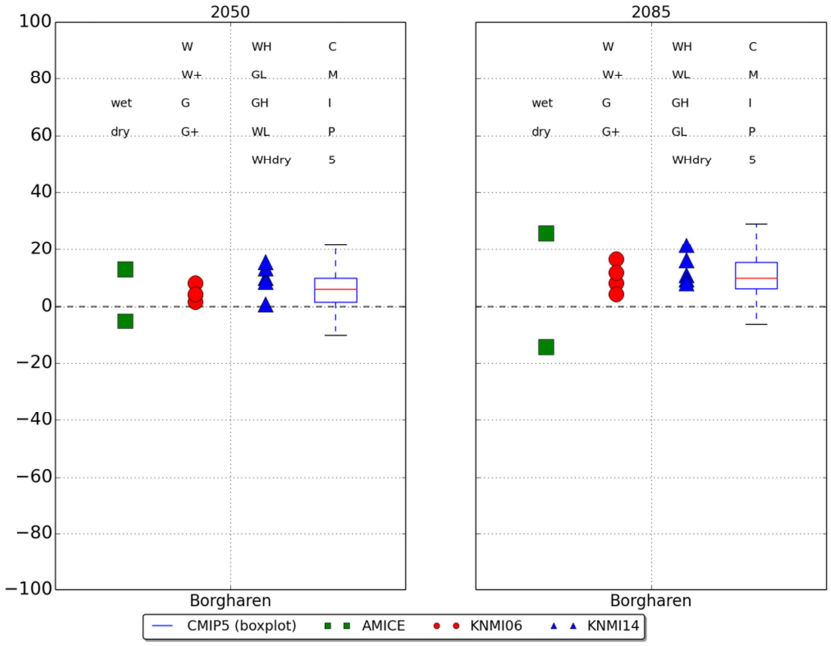

Figure 4.16 Percentage change in annual maximum discharge (MHQ) for Borgharen for all climate model / scenario sets. The colour / symbol coding and boxplots represent the scenario sets. On top of the graphs the ordering of scenarios is given

Change in mean annual7-day low flow (NM7Q)
In general the scenarios project a decreasing trend for the 7-day minimum flow sum for the Meuse. Exceptions are the KNMI'06 G and W scenarios and the KNMI'14 G_L scenario which projects small increases. All scenarios lie within the ranges provided by the CMIP5 climate model projection, and large decreases remain more likely than large increases.

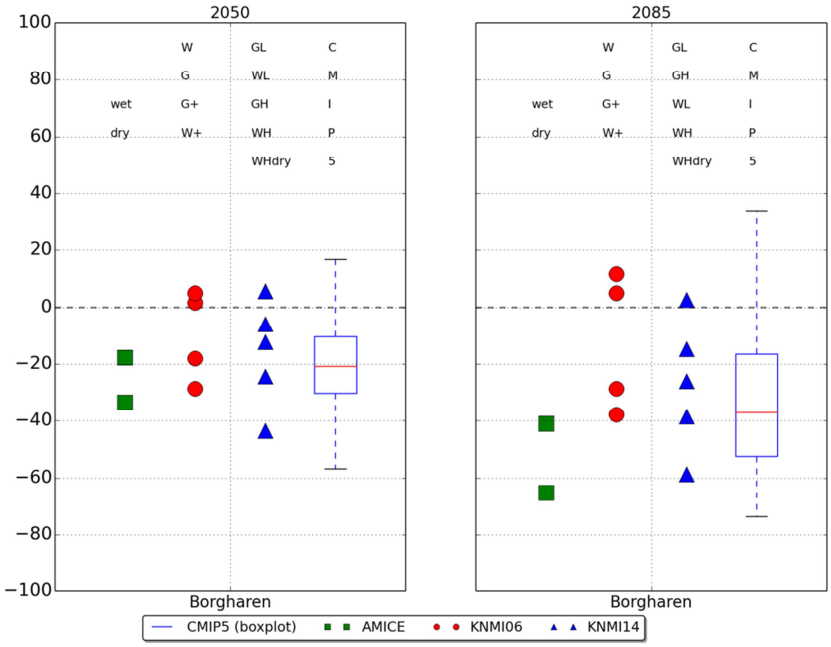

Figure 4.17 Percentage change in 7-day minimum flow (NM7Q) for Borgharen for all climate model / scenario sets. The colour / symbol coding and boxplots represent the scenario sets. On top of the graphs the ordering of scenarios is given

Changes in (the probabilities of) extreme high discharges
Compared to the KNMI'06 W+ scenario for 2050 the KNMI'14 scenarios generally result in slightly higher discharges, although the differences are small. To make a fair comparison between KNMI'06 and KNMI'14 results, the results for the 2100W+ scenario are translated to values that represent the situation 2085. This can be done, because the KNMI'06 scenarios were constructed by scaling the 2050 results to 2100.

In Table 4.3 an overview of the discharges for selected return periods is given for all scenarios and years, including the reference situation and the 2050W+ and the constructed 2085W+ results. It can be seen that the discharges for the KNMI'14 scenarios for 2050 are comparable to the 2050W+ results and that the differences are small.
For 2085, the KNMI'06 W+ scenario gives discharges that are comparable with the KNMI'14 W_L scenario, but lower discharges than the W_H scenario.

Table 4.10 Overview of discharges in m^3/s (HBV) for specific return periods for all scenarios, including the reference situation for the Meuse at Borgharen

Return period [years]	**Ref.**	**2050G_L**	**2050G_H**	**2050W_L**	**2050W_H**	***2050W+***	**2085G_L**	**2085G_H**	**2085W_L**	**2085W_H**	***2085W+***
10	2250	2550	2500	2450	2550	*2400*	2500	2450	2600	2750	2600
30	2750	3100	3000	3000	3100	*2950*	3000	2950	3150	3300	3200
100	3200	3600	3450	3500	3550	*3450*	3500	3400	3650	3850	3750
300	3550	4000	3850	3900	3900	*3850*	3900	3750	4050	4300	4200
1000	3850	4350	4200	4200	4200	*4200*	4250	4050	4400	4700	4550
1250	**3900**	**4450**	**4250**	**4250**	**4250**	***4250***	**4350**	**4100**	**4450**	**4750**	4650
3000	4100	4750	4500	4500	4550	*4450*	4600	4400	4700	4950	4850
10000	4350	5000	4700	4750	4750	*4650*	4900	4600	4900	5200	5050
30000	4600	5200	4850	4950	4900	*4850*	5050	4750	5100	5350	5200

4.2.2 River Rhine

As discussed in chapter 2 several climate impact assessments have been made for the discharge of the Rhine as well. We here compare the implications of the KNMI'14 climate scenarios and the CMIP5 datasets on the discharge of the Rhine with results from the RheinBlick2050 project, the projections from the KNMI'06 scenarios

For Lobith and also Trier most KNMI and Rheinblick scenarios envisage an increase in winter discharge and a decrease in late summer / autumn discharge – especially towards the end of the century. The moderate KNMI'06 G and W scenario project (slight) discharge increases for late summer. The summer discharge decreases projected by the new KNMI'14 scenarios are not as large as changes – ranging upto minus 80% at Trier - projected by the CMIP5 model set. Notable are the possible summer discharge increases projected by part of the CMIP5 models for 2050 and 2085.

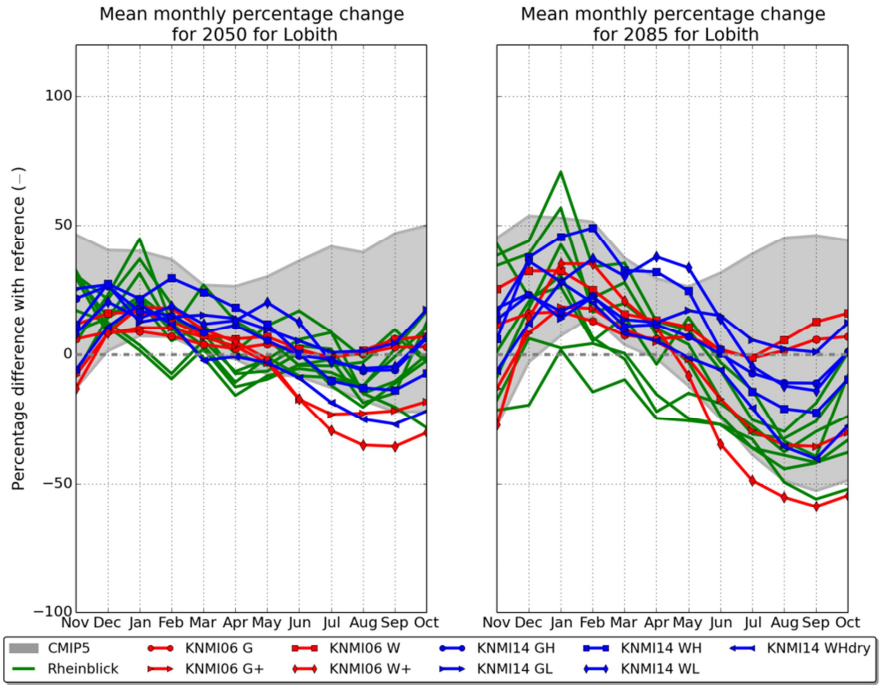

Figure 4.18 Percentage change (%) in average monthly discharge cycle for Lobith for all climate model / scenario sets

Change in annual mean discharge

Changes in annual mean flow range approximately between minus and plus 20%. Both the KNMI'14 scenarios and the majority of CMIP5 scenarios project mean discharge increases throughout the basin except for the KNMI14 W_{Hdry} scenario.Especially at the end of the century larger discharge decreases are projected by the KNMI06 and RheinBlick2050 scenarios at Lobith and Maxau than by KNMI'14.

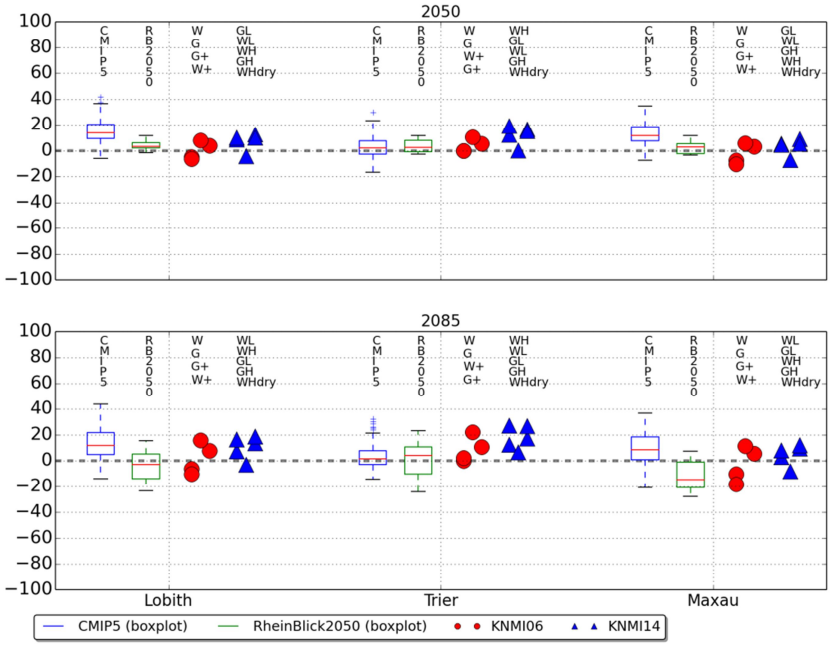

Figure 4.19 Percentage change in annual mean discharge (MQ) for the Rhine for all climate model / scenario sets. The color / symbol coding and boxplots represent the scenario sets. On top of the graphs the ordering of scenarios is given

Change in mean annual maximum flow (MHQ)

All scenario sets dominantly project increases in maximum discharge throughout the basin. Projected changes range approximately from +10 to +35% with larger increases towards the end of the century. In the CMIP5 and RheinBlick2050 datasets median changes in maximum annual discharge for Maxau are small.

Change in mean annual 7-day low flow

The RheinBlick2050 scenarios and the KNMI'06 W+, G+ and four out of five KNMI'14 scenarios project decreases in the *long term mean annual lowest seven day flow* for all locations. The CMIP5 climate model datasets only dominantly project decreases for Trier, where discharge is mainly influenced by rain over the Mosel basin. For the KNMI14 scenarios the projected decreases are small at Maxau. At Trier decreases are similar to the KNMI06 and CMIP5 scenarios and range up to minus 70%.

Figure 4.20 Percentage change in annual maximum discharge (MHQ) for the Rhine at the Lobith gauging station for all climate model / scenario sets. The colour / symbol coding and boxplots represent the scenario sets. On top of the graphs the ordering of scenarios is given

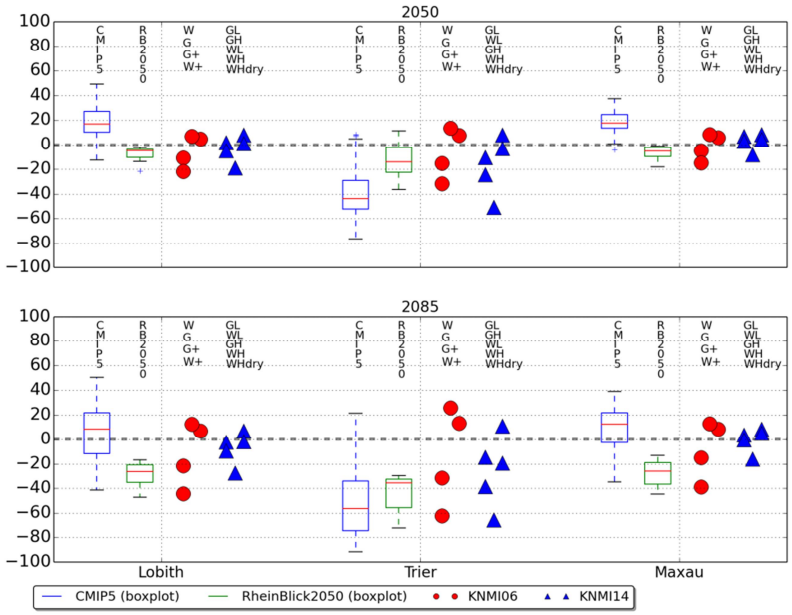

Figure 4.21 Percentage change in given7-day minimum flow (NMQ7) for the Rhine for all climate model / scenario sets. The color / symbol coding and boxplots represent the scenario sets. On top of the graphs the ordering of scenarios is given

Change in (the probability of) extremely high discharges

For 2050, the resulting statistics of extreme high discharges are comparable, or slightly higher than the KNMI'06 W+ scenario. For 2085, the KNMI'06 scenario peak discharges are generally higher than the G scenarios, but below the W-scenarios. The total overview for specific return periods is given in Table 4.11.

Table 4.11 Overview of discharges in m^3/s (Sobek) for specific return periods for all scenarios, including the reference situation for the Rhine at Lobith, including the effect of upstream flooding and including the correction for the flood areas along the stretch between Wesel and Lobith

Return period [years]	**Ref.**	**2050GL**	**2050GH**	**2050WL**	**2050WH**	***2050W+***	**2085GL**	**2085GH**	**2085WL**	**2085WH**	***2085W+***
10	9100	10900	10600	10800	11100	11000	10800	10600	12000	12700	11700
30	10900	12900	12500	12700	13000	12400	12800	12400	13700	14100	13400
100	12600	14100	13900	14000	14100	13900	14000	13800	14400	14800	14300
300	13600	14700	14500	14500	14600	14500	14600	14400	15000	15600	15000
1000	14300	15700	15200	15400	15100	15100	15500	14900	16400	17000	16300
1250	**14400**	**15900**	**15300**	**15500**	**15200**	**15300**	**15700**	**14900**	**16700**	**17100**	**16500**
3000	14800	16700	16200	16400	16300	16400	16600	15600	17100	17300	17000
10000	15300	17200	17000	17000	17000	16900	17200	16800	17300	17500	17500
30000	15700	17300	17200	17200	17300	17200	17300	17000	17400	17500	17600

5 Conclusions

In this assessment we investigated the implications of the KNMI'14 scenarios and the CMIP5 model projections for the discharge of the rivers Meuse and Rhine focussing on Borgharen and Lobith. The results of the discharge change analysis were compared with existing discharge change projections i.e. those based on KNMI'06, the full set of CMIP5 datasets and the results from the AMICE and RheinBlick2050 projects.

Assessment of the hydrological effects of climate change on the Rhine and Meuse rivers based on the KNMI'14 scenarios and the CMIP5 climate model projections for the river basins.

The results show the following implications of the KNMI'14 scenarios:

- The set of 5 KNMI'14 scenarios for the Rhine and Meuse basins largely overlaps with the full range (i.e. the 2.5 to 97.5% range) of discharge changes calculated from the CMIP5 climate model simulations in which all four RCPs are included. This is also true for the earlier discharge projections (KNMI'06, AMICE, RheinBlick2050) except for the 2085 AMICE dry scenario for the Meuse at Borgharen and for the KNMI'06 W+ scenario for the Rhine at Lobith (both for 2050 and 2100) which are so dry in respectively winter and summer that they are not supported by the ranges given by the (most recent) CMIP5 discharge projections.
- There is a general tendency towards increasing winter and spring discharge and decreasing (late) summer discharge.
- For both rivers there is a signal of increasing annual mean and annual maximum discharge, whereas annual 7-day low flow is projected to decrease.
- For both rivers Rhine and Meuse all scenarios envisage an increase of the extreme high discharges compared to the reference situation.
- The range of the change in (extremely) high discharges for all KNMI'14 scenarios increases considerably between 2050 and 2085. The fact that the CMIP5 range for 2050 is wider and the fact that the range in seasonal average precipitation and temperature is also wider indicates that the range of the change in extreme discharges for 2050 in the KNMI'14 scenarios may be somewhat underestimated.
- For the Meuse in 2050, for the 1250-year event this means an increase to between 4250 and 4450 m^3/s, respectively for scenarios G_H and G_L. In 2085 the spread between scenarios increases, resulting in a range of 4110 to 4760 m^3/s for respectively G_H and W_H. The reference estimate of the 1250-year event is 3920 m^3/s.
- For the Rhine in 2050, ignoring effects of upstream flooding, for the 1250-year event the scenarios result in discharges between 19,200 and 20,300 m^3/s. In 2085 the discharges for the 1250-year event range between 18,700 and 22,300 m^3/s for the G_H and W_H scenarios respectively. The reference estimate of the 1250-year event, in the case upstream flooding is ignored, is approximately 16,900 m^3/s.
- Upstream flooding in the Rhine reduces the extreme high discharges at Lobith significantly. The dampening effect of flooding between Wesel and Lobith on the peak discharges at Lobith is large. For very long return periods (above ~1250 years) the differences between the scenarios become small at the Lobith gauging station, due to the limited discharge capacity of the Rhine between Wesel and Lobith. The maximum discharge at Lobith in the case flooding is taken into account is between 17,500 and 18,000 m^3/s.
- For the Rhine, taking into account effects of upstream flooding, the estimated increase for the 1250-year event is considerably less. The estimates are between 15,210 and

15,950 m^3/s in 2050 for the G_H and G_L scenarios respectively. In 2085 the 1250-year discharge ranges between 14,950 and 17,100 m^3/s for the G_H and W_H scenarios. The reference estimate of the 1250-year discharge when upstream flooding is taken into account is 14,380 m^3/s.

Comparison of the resulting hydrological changes with those from the KNMI'06 based hydrological projections, the RheinBlick2050 project (for the Rhine) and the AMICE project (for the Meuse).

Comparison of the new, KNMI'14 based, projections with the existing scenario projections resulted in the following conclusions:

- Generally the trends in discharge envisaged by the KNMI'14 scenarios for the Rhine and Meuse are comparable with those envisaged in most of the existing scenarios (AMICE WET, KNMI'06 and RheinBlick2050). These are (a) larger differences between the dry and wet seasons and (b) more water in the wet (winter and spring) period and less in the dry (late) summer, autumn period.
- Specifically, the KNMI'14 scenarios for the Rhine result in higher extreme discharges compared to the KNMI'06 scenarios. For both 2050 and 2085 the KNMI'14 scenarios give for the 1250-year event at most 600 m^3/s larger discharges (respectively for G_L and for W_H) than the earlier KNMI'06 W+ scenario. For the Rhine the W+ scenario roughly lies between the KNMI'14 G_H and W_L scenarios.
- For the Meuse the KNMI'14 W_H scenario gives comparable results to the KNMI'06 W+ scenario. For 2050 KNMI'14 scenarios give for the 1250-year event at most 200 m^3/s larger discharges (G_L) than the earlier KNMI'06 W+ scenario. For 2085 the difference becomes smaller, the 1250-year discharge for W_H is 130 m^3/s higher than the KNMI'06 W+ scenario.

6 Literature

Bakker, A. & J. Bessembinder, 2012. *Time series transformation tool: description of the program to generate time series consistent with the KNMI'06 climate scenarios*. KNMI TR-326, KNMI, De Bilt, The Netherlands, 75 pp.

Bouaziz, L., F. Sperna Weiland, J. Beersma, & H. Buiteveld, 2014. *New insights for the hydrology of the Rhine based on the new generation climate models.* Geophysical Research Abstracts Vol. 16, EGU2014-11080.

Buishand, T.A. & R. Leander, 2011. *Rainfall generator for the Meuse basin : Extension of the base period with the years 1999-2008.* KNMI publications (196-V).

Buishand, T.A. & T. Brandsma, 2001. Multi-site simulation of daily precipitation and temperature in the Rhine basin by nearest-neighbor resampling. *Water Resources Research*, 37, 2761-2776.

De Keizer, O. & J.C.J. Kwadijk, 2009. *Belgische scenario's voor de Maas.* WL_rapporten 710_14.

Duits-Nederlandse Werkgroep Hoogwater, 2006a. *Risicoanalyse grensoverschrijdende dijkringen Niederhein; fase 2 en 3.* hoofdrapport, Aken en Lelystad.

Duits-Nederlandse Werkgroep Hoogwater, 2006b. *Risicoanalyse grensoverschrijdende dijkringen Niederhein; fase 2 en 3. deelrapport dijkring 42.*

Duits-Nederlandse Werkgroep Hoogwater, 2006c. *Risicoanalyse grensoverschrijdende dijkringen Niederhein; ; fase 2 en 3. deelrapport dijkring 48*.

Drogue, G., M. Fournier, A. Bauwens, F. Commeaux, O. De Keizer, D. François, E. Guilmin, A. Degré, S. Detrembleur, B. Dewals, M. Pirotton, D. Pontegnie, C. Sohier & W. Vaneuville, 2010. *Analysis of climate change, high-flows and low-flows scenarios on the Meuse basin.* WP1 report – Action 3, available at: http://orbi.ulg.ac.be/ bitstream/2268/66197/1/WP1-1%20Report.pdf.

Görgen, K., H. Buiteveld, M. Carambia, P. Krahe, E. Nilson, J. Beersma, G. Brahmer, O. de Keizer, R. Lammersen, C. Perrin & D. Volken, 2010. *Assessment of Climate Change Impacts on Discharge in the Rhine River Basin: Results of the RheinBlick2050 project.* CHR, pp.210.

Haylock, M.R., N. Hofstra, A.M.G. Klein Tank, E.J. Klok, P.D. Jones & M. New, 2008. A European daily high-resolution gridded dataset of surface temperature and precipitation for 1950-2006. *Journal of Geophysical Research*, Vol. 113, D20119, doi:10.1029/2008JD010201.

Hegnauer, M., 2013. *Technical documentation GRADE part III: Models Meuse*. Deltares report 1207771-003-ZWS-0015, Deltares, Delft, The Netherlands.

Hegnauer, M. & A. Becker, 2013. *Technical Documentation GRADE part II - Models Rhine.* Deltares, Delft, The Netherlands

Hegnauer, M., J.J. Beersma, H.F.P. van den Boogaard, T.A. Buishand & R.H. Passchier, 2014. *Generator of Rainfall and Discharge Extremes (GRADE) for the Rhine and Meuse basins: Final report of GRADE 2.0.* Deltares report 1209424-004-ZWS-0018, Delft, The Netherlands.

Homan, C., J.J. Beersma & J. Bessembinder, 2011. *Meteorologische tijdreeksen voor het Deltamodel; eerste versie tijdreeksen voor Nederland en de stroomgebieden van de Maas en de Rijn.* KNMI Rapportage A1a (zaaknummer 31007187.0003), De Bilt, The Netherlands.

IPCC, 2007. *Climate Change 2007: Synthesis Report. Contribution of Working Groups I, II and III to the Fourth Assessment Report of the Intergovernmental Panel on Climate Change. [*Core Writing Team, Pachauri, R.K and Reisinger, A. (eds.)]. IPCC, Geneva, Switzerland, 104 pp.

IPCC, 2013. *Climate Change 2013: The Physical Science Basis. Contribution of Working Group I to the Fifth Assessment Report of the Intergovernmental Panel on Climate Change*. [Core Writing Team, Stocker, T.F., D. Qin, G.-K. Plattner, M. Tignor, S.K. Allen, J. Boschung, A. Nauels, Y. Xia, V. Bex and P.M. Midgley (eds.)]. Cambridge University Press, Cambridge, United Kingdom and New York, NY, USA, 1535 pp, doi:10.1017/CBO9781107415324. IIASA (2013), RCP Database [online], https:/tntcat.iiasa.ac.at:8743/RcpDb/.

Klijn, F., K. de Bruijn, C. McGahey, M. Mens & H. Wolfert, 2008. *Towards sustainable flood risk management: on methods for design and assessment of strategic alternatives exemplified on the Schelde Estuary*. FLOODsite Report T14-08-02.

Kraaijenbrink, P., 2013. *Advanced Delta Change Method: Extension of an application to CMIP5 GCMs* – Trainee report Royal Meteorological Institute.

Kramer, N.L., R. Passchier, J. Beckers, A. Weerts & R. Schroevers, 2008. *Analysing extreme discharges within the frame work of the Generator of Rainfall and Discharge Extremes (GRADE) project.* Deltares, The Netherlands.

Lall, U. & A. Sharma, 1996. *A nearest neighbour bootstrap for resampling hydrologic time series.* Water Resources Research, 32, 697-693 .

Lammersen, 2004. *Grensoverschrijdende effecten van extreem hoogwater op de Niederrhein.* ISBN 9036956390, RIZA, Arnhem.

Leander, R., T.A. Buishand, P. Aalders & M.J.M. De Wit, 2005. Estimation extreme floods of the river Meuse using a stochastic weather generator and a rain fall-run off model. *Hydrological Sciences Journal*, 50(6), pp. 1089-1103.

Leander, R. & T.A. Buishand, 2007. Resampling of regional climate model output for the simulation of extreme river flows*. Journal of Hydrology*, 332, 487-496.

Leander, R., T.A. Buishand, B.J.J.M. van den Hurk & M.J.M. de Wit, 2008. Estimated changes in flood quantiles of the river Meuse from resampling of regional climate model output. *Journal of Hydrology*, 351, 331-343.

Leander, R., 2009. *Simulation of precipitation and discharge extremes of the river Meuse basin in current and future climate.* PhD thesis, Utrecht University.

Lenderink, G. & J.J. Beersma, 2015. *The KNMI'14 $W_{H,dry}$ scenario for the Rhine and Meuse basins.* KNMI Scientific Report WR 2015-02, KNMI, De Bilt, The Netherlands.

Lenderink, G., B.J.J.M. van den Hurk, A.M.G. Klein Tank, G.J. van Oldenborgh, E. van Meijgaard, H. de Vries & J.J. Beersma, 2014. Preparing local climate change scenarios for the Netherlands using resampling of climate model output*. Environ. Res. Lett*., 9, 115008. doi:10.1088/1748-9326/9/11/115008.

Lindström, G., B. Johansson, M. Persson, M. Gardelin & S. Bergström, 1997. Development and test of the distributed HBV-96 hydrological model*. Journal of Hydrology*, 201, 272-288.

Moss, R.H. et al., 2008. *Towards New Scenarios for Analysis of Emissions, Climate Change, Impacts, and Response Strategies*. Intergovernmental Panel on Climate Change, Geneva, 132 pp.

Paarlberg, A., 2014. *GRADE Niederrhein: Dijkoverstroming versus dijkdoorbraak.* HKV report PR2942.10, Lelystad, September 2014.

Rajagopalan, B. & U. Lall, 1999. A k-nearest-neighbor simulator for daily precipitation and other variables*. Water Resources Research*, 35, 3089-3101.

Rauthe, M., H. Steiner, U. Riediger, A. Mazurkiewicz & A. Gratzki, 2013. A Central European precipitation climatology – Part I: Generation and validation of a high-resolution gridded daily dataset (HYRAS)*. Meteorologische Zeitschrift*, Vol. 22, No. 3, 235-256.

Ruiter, A., 2012. *Delta-change approach for CMIP5 GCMs.* Trainee Report, KNMI, pp 30.

RWS WVL, Deltares & projectbureau VNK2, 2013. *Achtergrondrapport Ontwerpinstrumentarium 2014.* RWS WVL Report, version 23 december 2013.

Schmeits, M.J., J.J. Beersma & T.A. Buishand, 2014a. *Rainfall generator for the Meuse basin: Description of simulations with and without a memory term and uncertainty analysis.* KNMI Publication 196-VI, KNMI, De Bilt.

Schmeits, M.J., E.L.A. Wolters, J.J. Beersma & T.A. Buishand, 2014b. *Rainfall generator for the Rhine basin; Description of simulations using gridded precipitation datasets and uncertainty analysis.* KNMI Publication 186-VII, 29 pp.

Silva, W., 2003. *Hoeveel (hoog)water kan ons land binnenkomen via de Rijn bij Lobith, nu en in de toekomst.* Riza rapport, Rijkswaterstaat, Ministerie Verkeer en Waterstaat, Arnhem.

Taylor, K.E., R.J. Stouffer & G.A. Meehl, 2012. An overview of CMIP5 and the experiment design*. Bull. Amer. Meteor. Soc.,* 93, 485–498. doi:.

Van den Hurk, B., A. Klein Tank, G. Lenderink, A. Van Ulden, G.J. Oldenborgh, C. Katsman, H. Van den Brink, F. Keller, J. Bessembinder, G. Burgers, G. Komen, W. Hazelegger, & S. Drijfhout, 2006. *KNMI Climate Change Scenarios 2006 for the Netherlands*. KNMI Scientific Report WR 2006-01, De Bilt, The Netherlands.

Van Deursen, W., 2004. *Afregelen HBV model Maasstroomgebied.* Rapportage aan RIZA. Carthoga Consultancy. Rotterdam, The Netherlands.

Van Pelt, S.C., J.J. Beersma, T.A. Buishand, B.J.J.M. Van den Hurk & P. Kabat, 2012. Future changes in extreme precipitation in the Rhine basin based on global and regional climate model simulations. *Hydrol. Earth Syst. Sci*., 16, 4517–4530, doi:10.5194/hess-16-4517-2012.

Van Vuuren, D.P., J. Edmonds, M. Kainuma, K. Riahi, A. Thomson, K. Hibbard, G.C. Hurtt, T. Kram, V. Krey, J.-F. Lamarque, S.J. Smith & S.K. Rose, 2010. The representative concentration pathways: an overview. *Climatic Change*, 109(5-31), doi:10.1007/s10584-011-0148-z.

Vecchi, G.A., 2012. *Precipitation Response in Climate Models:What's new in CMIP5? (thus far).* NOAA / GFDL presentation - vecchi_cmip5_princeton.pdf.

Werner, M., J. Schellekens, P. Gijsbers, M. Van Dijk, O. Van den Akker & K. Heynert, 2013. The Delft-FEWS flow forecasting system. *Environmental Modelling and Software*, 40 (65-77), doi: 10.1016/j.envsoft.2012.07.010.

Winsemius, H.C.W., M. Hegnauer, W. Van Verseveld and A. Weerts, 2013. *Generalised likelihood uncertainty estimation for the daily HBV model in the Rhine Basin Part A: Germany.* Deltares report 1207771-003-ZWS-0018, Deltares, Delft, The Netherlands.

Woelders, L., 2011. *Verdamping FEWS-GRADE, Memo aan geinteresseerden FEWS-GRADE*. Deltares, Delft, the Netherlands.

Young, K.C., 1994*. A multivariate chain model for simulating climatic parameters from daily data. Journal of Applied Meteorology*, 33, 661-671.

A Potential evaporation for HBV

Here we provide an overview of the methods applied to estimate HBV sub-catchment specific potential evaporation from the different climate datasets for the Rhine and Meuse. The HBV model can either calculate daily potential evaporation from daily temperature time-series or the model can be forced with external potential evaporation. Within the HBV model potential evaporation is reduced to actual evapotranspiration depending on water availability in soil and open water.

In principle HBV uses its build-in method to derive potential evaporation from daily temperatures and long-term average climatology of temperature and evaporation. We here refer to this method as the etf-method[4]. Within this method the following formula is used to estimate daily potential evaporation at time *t* from climatological mean potential evaporation:

$$E_{p,t} = E_{p,mean} * (1 + etf\ (T_t - T_{mean}) \qquad \text{Eq. 1}$$

Where:

$E_{p,t}$ potential evaporation on day t (mm/day)
$E_{p,mean}$ long term mean monthly potential evaporation from a historical time series (mm/day)
etf correction factor of potential evaporation for long term means for actual temperature (1/°C)
T_t temperature on day *t* (°C)
T_{mean} long term mean daily temperature from historical time series on the calendar day corresponding with day *t* (°C)

In a sensitivity analysis the value of the e*tf*-parameter is varied to explore the effect on modelled discharges. In addition, T_{mean}, which is a 'parameter' in HBV for all years and which is based on the historical period 1961-1995, is compared with the mean temperature in the currently used historical temperature series being 1951-2006, and the effect this has on de simulated discharge is analyzed.

The etf-method was never intended to account for the systematic effect of climate change on the potential evaporation (due to the systematic temperature change). Within the etf-method the term $T_t - T_{mean}$ is originally used to calculate the day-to-day variations in the potential evaporation from the day-to-day variations in temperature and the long-term (monthly) mean potential evaporation (this also explains the name 'temperature anomaly correction method'). Therefore the etf-method (Eq. 1) is adapted in such a way that the systematic effect of climate change on the potential evaporation can be determined (using a scenario for the systematic change in potential evaporation) rather than (mis)using the *etf*-parameter for this.

In the sub-sections below it is described how the adaptation of the etf-method works, and how, first for the Rhine and then for the Meuse, for each type/set of climate scenarios the systematic effect of climate change on the potential evaporation is taken into account within HBV.

[4] *The etf-method is also known as the temperature anomaly correction method (see Görgen et al., 2010).*

A.1 Rhine

CMIP5, KNMI'06 and RheinBlick2050 (Deltares contribution)
For the discharge projections for the Rhine based on the CMIP5, KNMI'06 and RheinBlick2050 'scenarios' the original (i.e. unadapted) etf-method is used. For the Rhine by default, the *etf*-para*meter* has a value of 0.05 (which is used for all sub-basins and calendar months). For each HBV sub-basin the mean potential evaporation for each calendar month ($E_{p,mean}$) and the mean temperature for each calendar day (T_{mean}) were derived by Eberle et al. (2005) from the so-called CHR-Obs dataset covering the period 1961-1995).

Specifically for the extreme discharge projections for the Rhine based on the KNMI'06 W+ scenario the method described under *KNMI'14* (see below) was used, with the difference that in the KNMI'06 scenarios the scenarios for the change in potential evaporation were solely based on the change in the temperature in the scenarios.

KNMI'14
For the KNMI'14 scenarios for the Rhine (and the Meuse), corresponding climate scenarios for the change in potential evaporation were constructed based on the change in global radiation and on the change in temperature in the scenarios (see Eq. 2) that considers the influence of temperature variation caused by both natural variability and climate change on potential evaporation.

$$\Delta Ep = \Delta R + \Delta T(\frac{dEp}{dT}) \qquad \text{Eq. 2}$$

Where ΔR is the change in global radiation (%) and ΔT is the change in temperature (°C) from the scenario. dEp/dT is the relative change in Ep per °C temperature increase obtained with the Makkink equation. ΔEp is the resulting change in potential evaporation (%) corresponding to the global radiation and temperature change in the scenario.

These scenarios for the change in potential evaporation are then combined with the original etf-method to give the adapted etf-method[5]:

$$Ep' = Ep_{mean}(1 + \frac{\Delta Ep}{100})(1 + etf(T' - T'_{mean})) \qquad \text{Eq. 3}$$

Where T', Ep' and T'_{mean} refer to respectively daily temperature, daily Ep' and monthly mean temperature in the future climate. Note that when there is no climate change (i.e. when $\Delta Ep = 0$, $T' = T$ and $T'_{mean} = T_{mean}$) Eq. 3 reduces to Eq. 1, and that when there is no specific scenario for the potential evaporation (i.e. $\Delta Ep = 0$) and at the same time $T'_{mean} = T_{mean}$ but T' still represents the temperature in the future climate Eq. 3 corresponds to the etf-method where the *etf*-parameter accounts for the systematic effect of climate change on the potential evaporation, i.e. the method used for CMIP5, KNMI'06 and RheinBlick2050.

[5] *For the discharge projections for the Rhine the adapted etf-method was implemented in Delft-FEWS by Deltares.*

A.2 Meuse

KNMI'06
For the discharge projections for the Meuse based on the KNMI'06 scenarios the original (i.e. unadapted) etf-method is used. At that time a HBV-Meuse *etf*-parameter value of 0.17, derived by van der Wal (2002) was used (for all sub-basins and calendar months).
Specifically for the extreme discharge projections for the Meuse based on the KNMI'06 W+ scenario the same method as for the extreme discharge projections for the Rhine based on KNMI'06 W+ (described in A.1) was used

AMICE
The external daily potential evaporation time-series used within the AMICE project are based on historical sub-catchment specific daily potential evaporation time-series (Leander, 2009) which are adjusted with 4% per °C air temperature increase.

KNMI'14
For the KNMI'14 scenarios for the Meuse, the procedure described under Rhine – *KNMI'14* was applied, with this difference that the monthly *etf*-parameter values and monthly mean evaporation for each HBV sub-basin as derived by Leander and Buishand (2007) specifically for HBV-Meuse were used[6].

CMIP5
For the CMIP5 based discharge projections for the Meuse the original (i.e. unadapted) etf-method was applied using the monthly *etf*-parameter values as derived by Leander and Buishand (2007). Appendix D gives a motivation for and describes the corrections that are applied afterwards to the CMIP5 discharge projections for the Meuse.

[6] *For the discharge projections for the Meuse this adapted etf-method was implemented by KNMI and the resulting potential evaporation time series for the HBV-Meuse sub-basins were provided to Deltares by KNMI together with the corresponding time series for precipitation and temperature.*

B Discharge projections Meuse for additional gauges

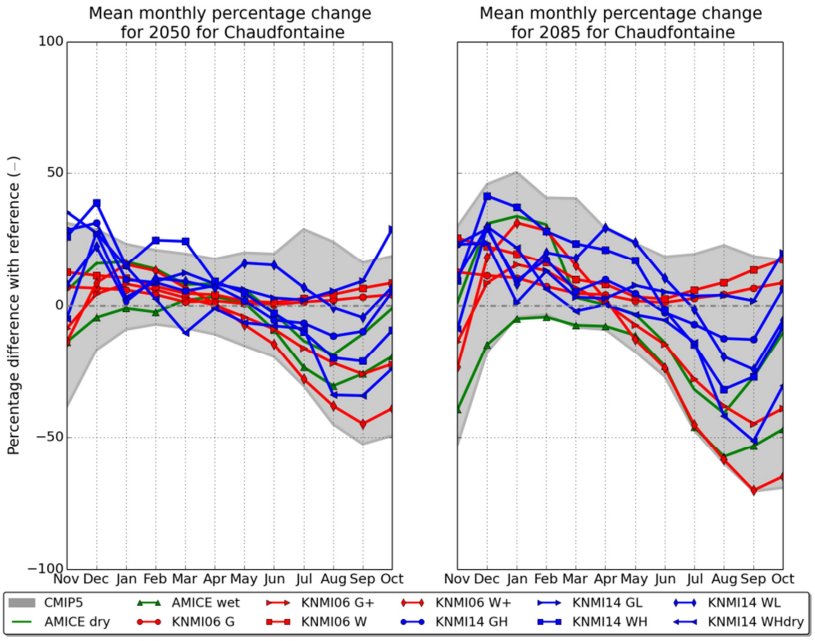

Figure D.1 Percentage change (%) in average monthly discharge cycle for Chaudfontaine for all climate model / scenario sets

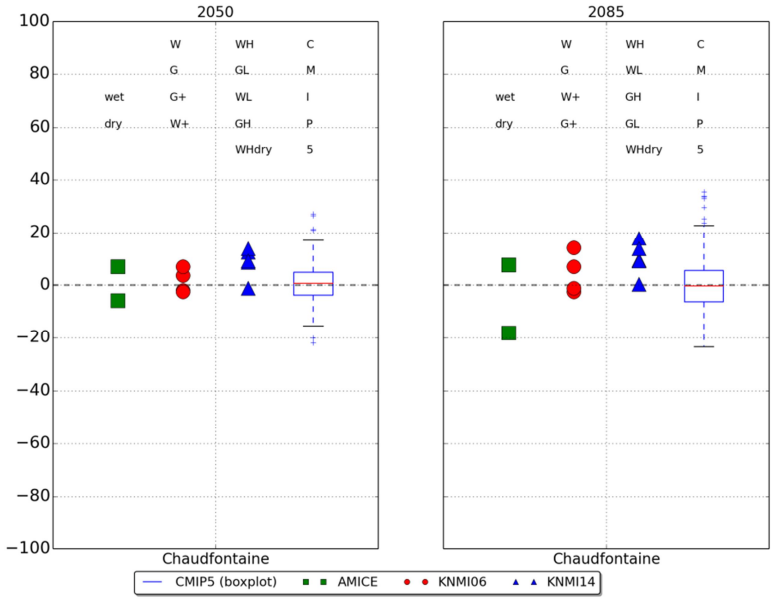

Figure D.2 Percentage change in annual mean discharge (MQ) for Chaudfontaine for all climate model / scenario sets. The color / symbol coding and boxplots represent the scenario sets. On top of the graphs the ordering of scenarios is given

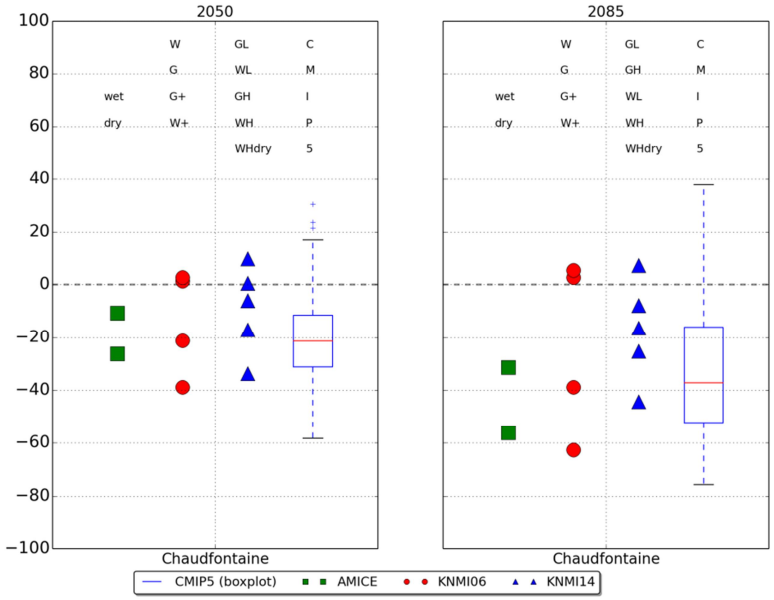

Figure D.3 Percentage change in 7-day low flow (NMQ7) for Chaudfontaine for all climate model / scenario sets. The color / symbol coding and boxplots represent the scenario sets. On top of the graphs the ordering of scenarios is given

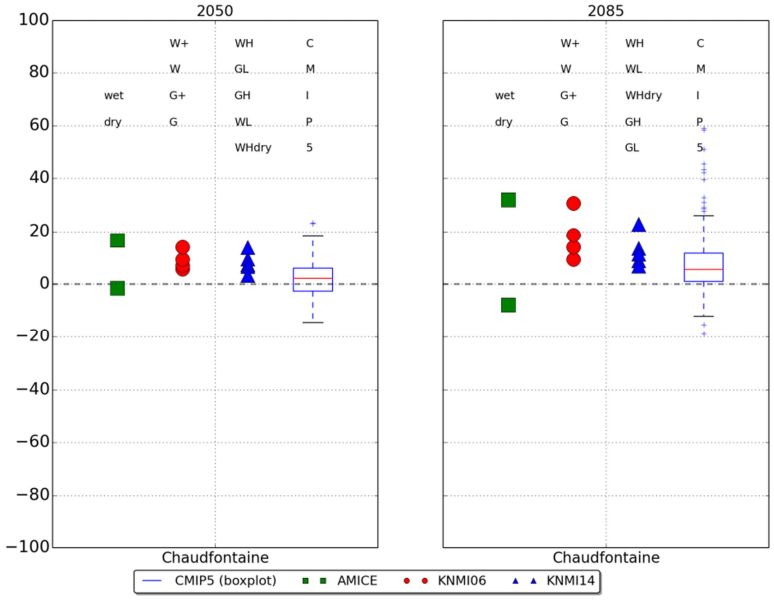

Figure D.4 Percentage change in Annual Maximum Flow (MHQ) for Chaudfontaine for all climate model / scenario sets. The color / symbol coding and boxplots represent the scenario sets. On top of the graphs the ordering of scenarios is given

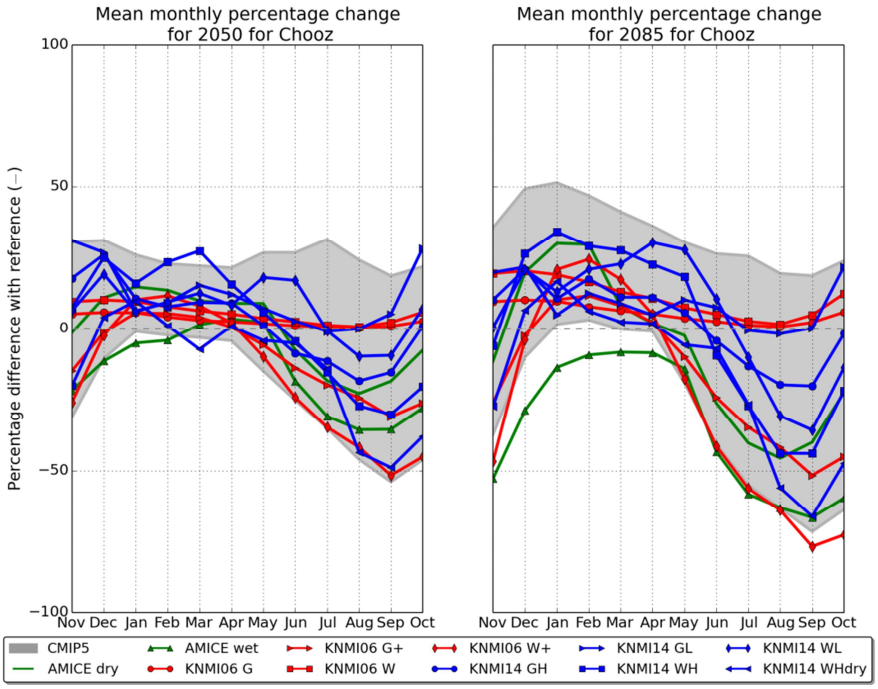

Figure D.5 Percentage change (%) in average monthly discharge cycle for Chooz for all climate model / scenario sets

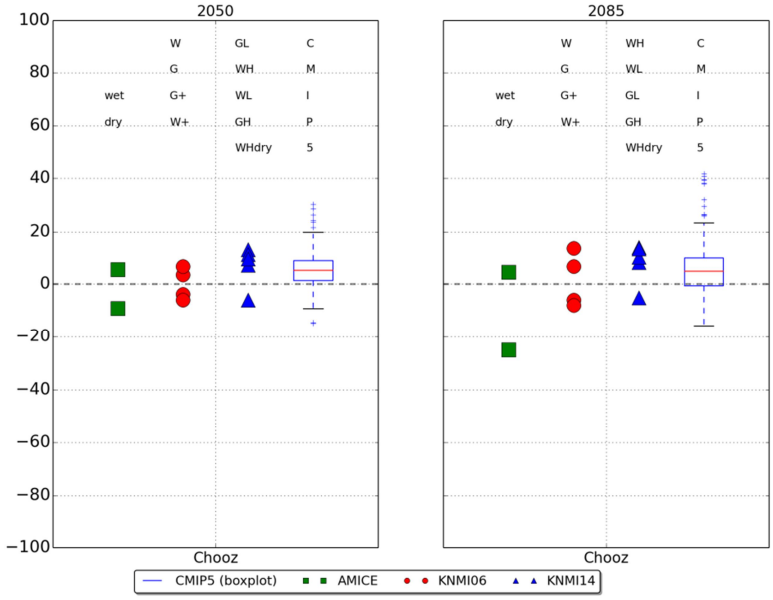

Figure D.6 Percentage change in annual mean discharge (MQ) for Chooz for all climate model / scenario sets. The color / symbol coding and boxplots represent the scenario sets. On top of the graphs the ordering of scenarios is given

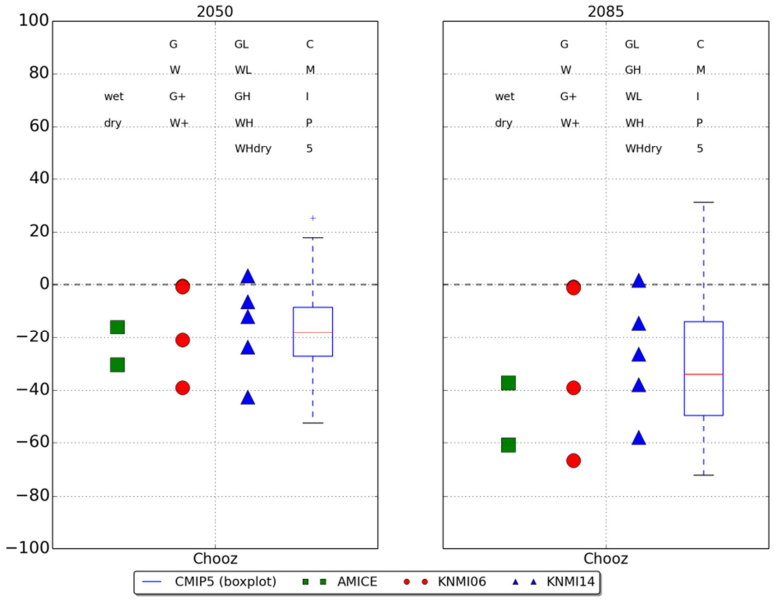

Figure D.7 Percentage change in 7-day low flow (NM7Q) for Chooz for all climate model / scenario sets. The color / symbol coding and boxplots represent the scenario sets. On top of the graphs the ordering of scenarios is given

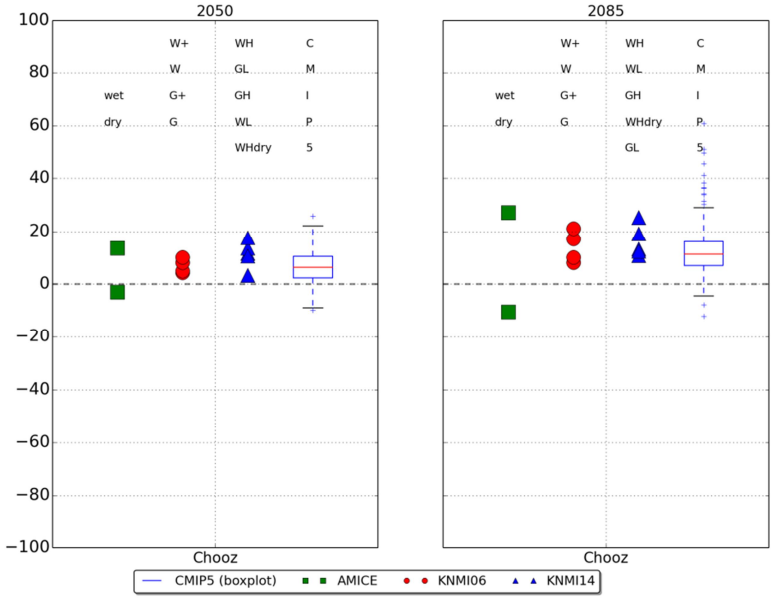

Figure D.8 Percentage change in Annual Maximum Discharge (MHQ) for Chooz for all climate model / scenario sets. The color / symbol coding and boxplots represent the scenario sets. On top of the graphs the ordering of scenarios is given

C Change in season averaged precipitation

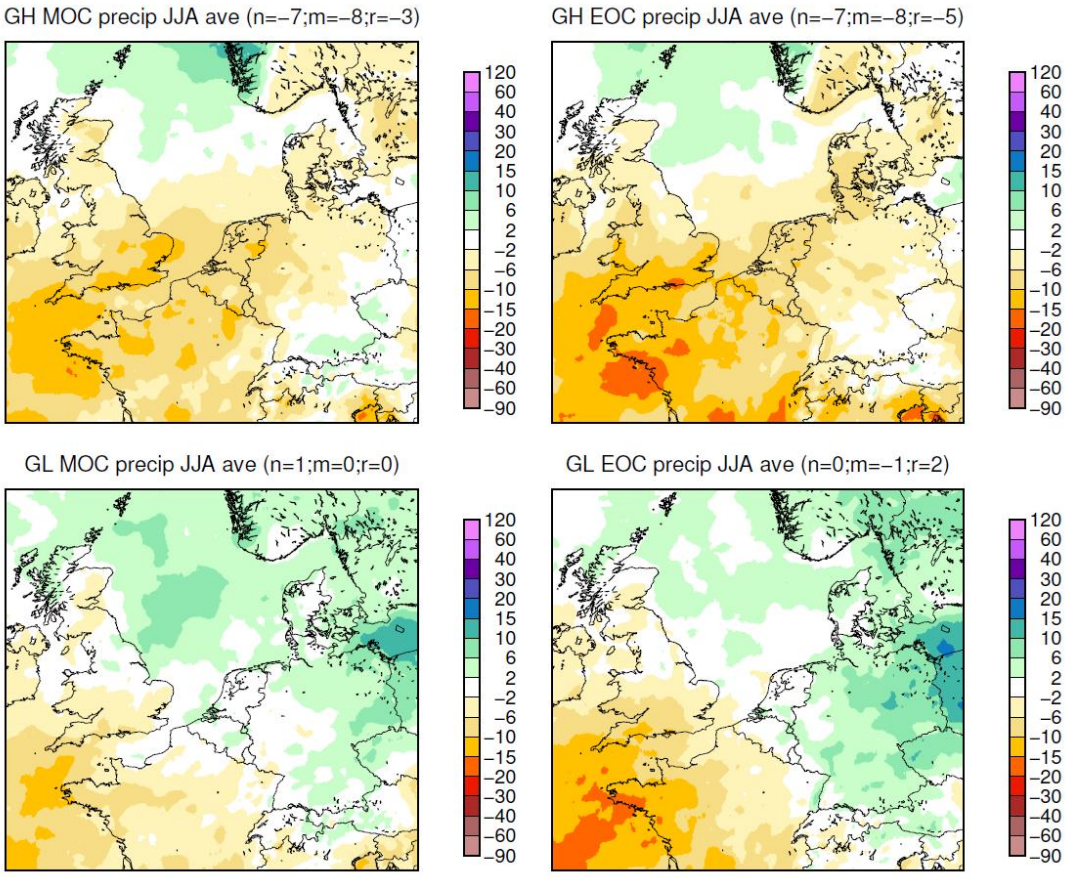

Figure C.1 Graphical overview of the relative change in season averaged precipitation for the Meuse and Rhine basins for summer (June, July and August) for the G_L and G_H scenarios. "MOC" refers to the 30-yr Middle Of Century period and is equivalent to 2050 and "EOC" refers to the 30-yr End Of Century period and is equivalent to 2085

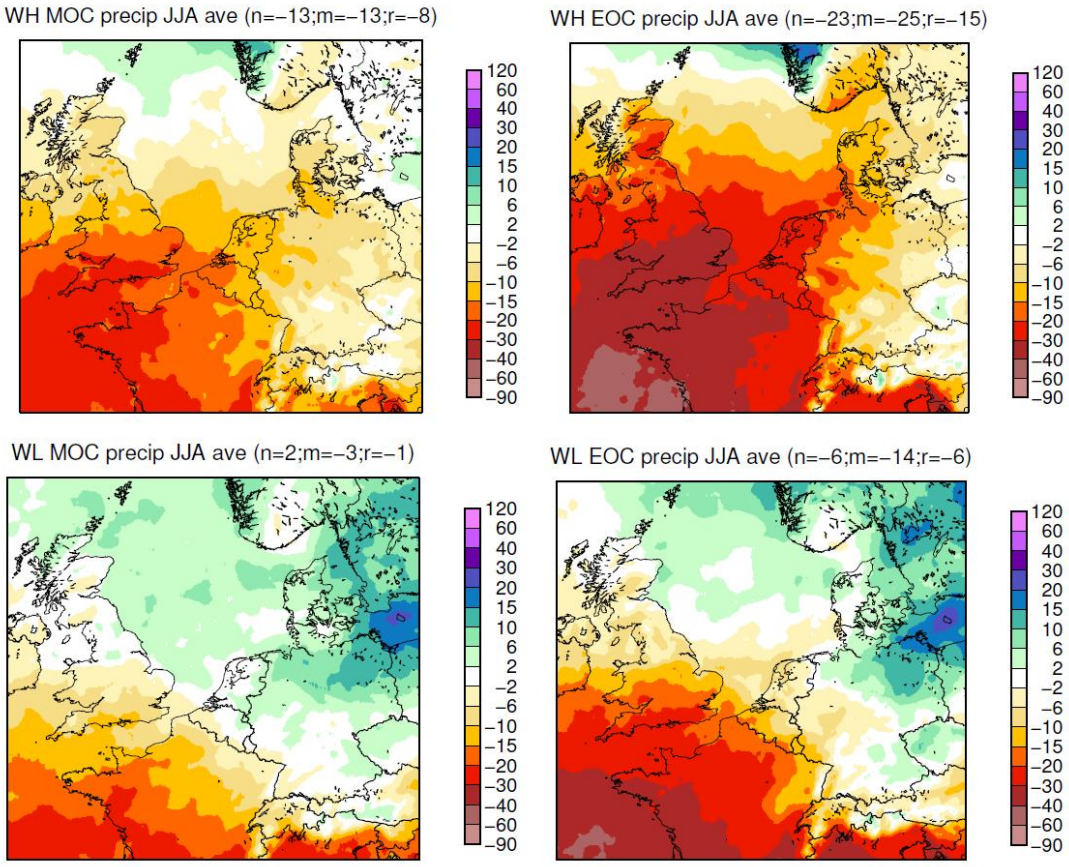

Figure C.2 Graphical overview of the relative change in season averaged precipitation for the Meuse and Rhine basins for summer (June, July and August) for the W_L and W_H scenarios. "MOC" refers to the 30-yr Middle Of Century period and is equivalent to 2050 and "EOC" refers to the 30-yr End Of Century period and is equivalent to 2085

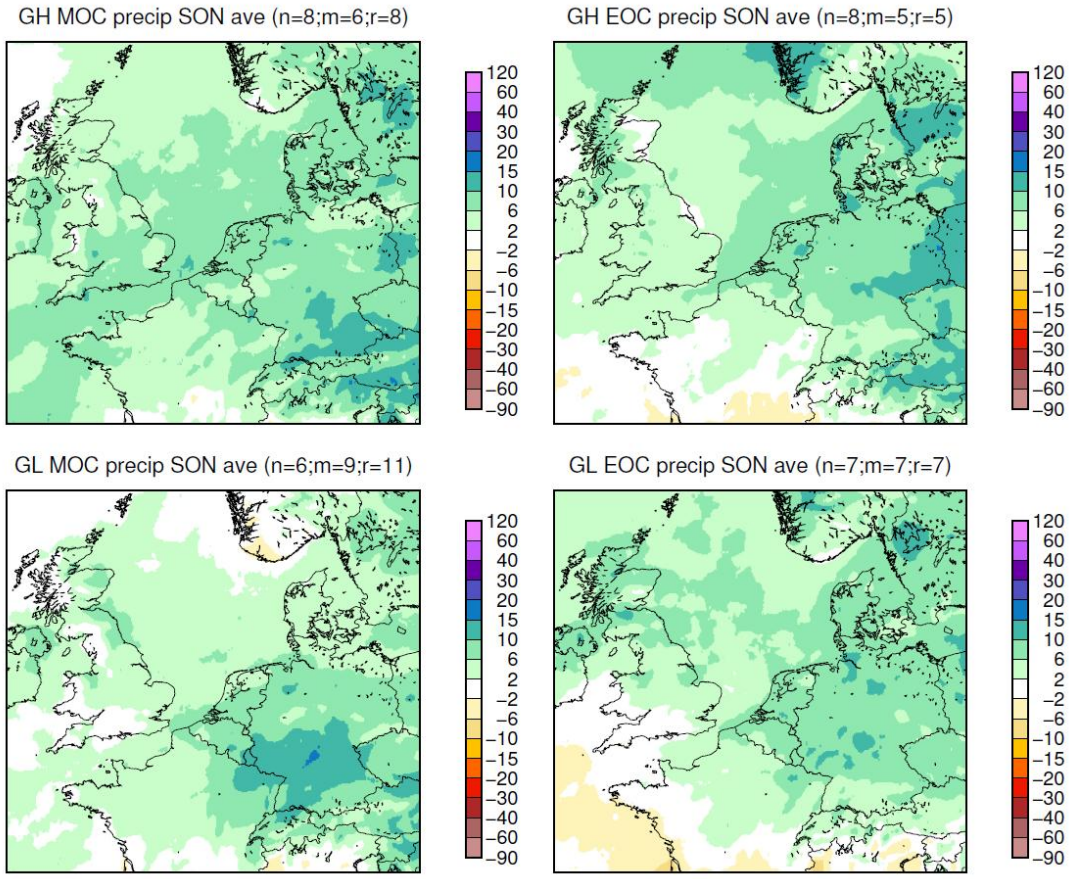

Figure C.3 Graphical overview of the relative change in season averaged precipitation for the Meuse and Rhine basins for autumn (September, October and November) for the G_L and G_H scenarios. "MOC" refers to the 30-yr Middle Of Century period and is equivalent to 2050 and "EOC" refers to the 30-yr End Of Century period and is equivalent to 2085

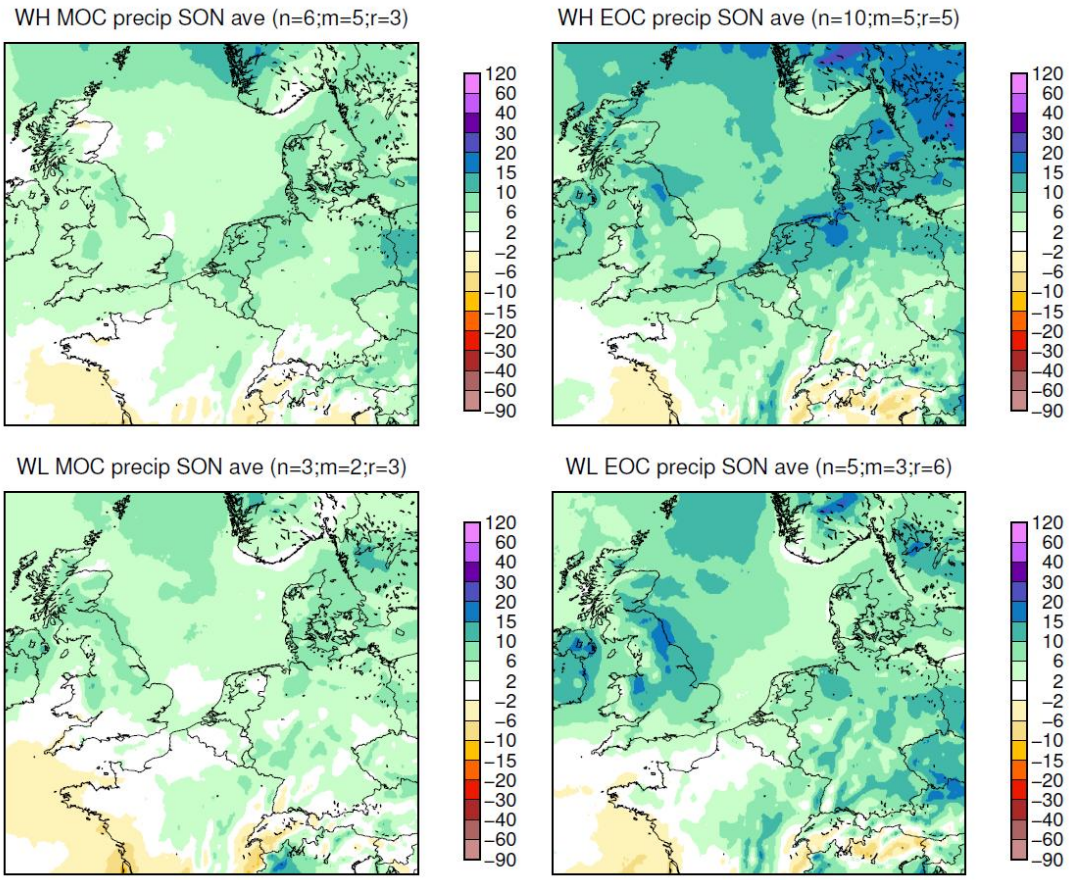

Figure C.4 Graphical overview of the relative change in season averaged precipitation for the Meuse and Rhine basins for autumn (September, October and November) for the W_L and W_H scenarios. "MOC" refers to the 30-yr Middle Of Century period and is equivalent to 2050 and "EOC" refers to the 30-yr End Of Century period and is equivalent to 2085

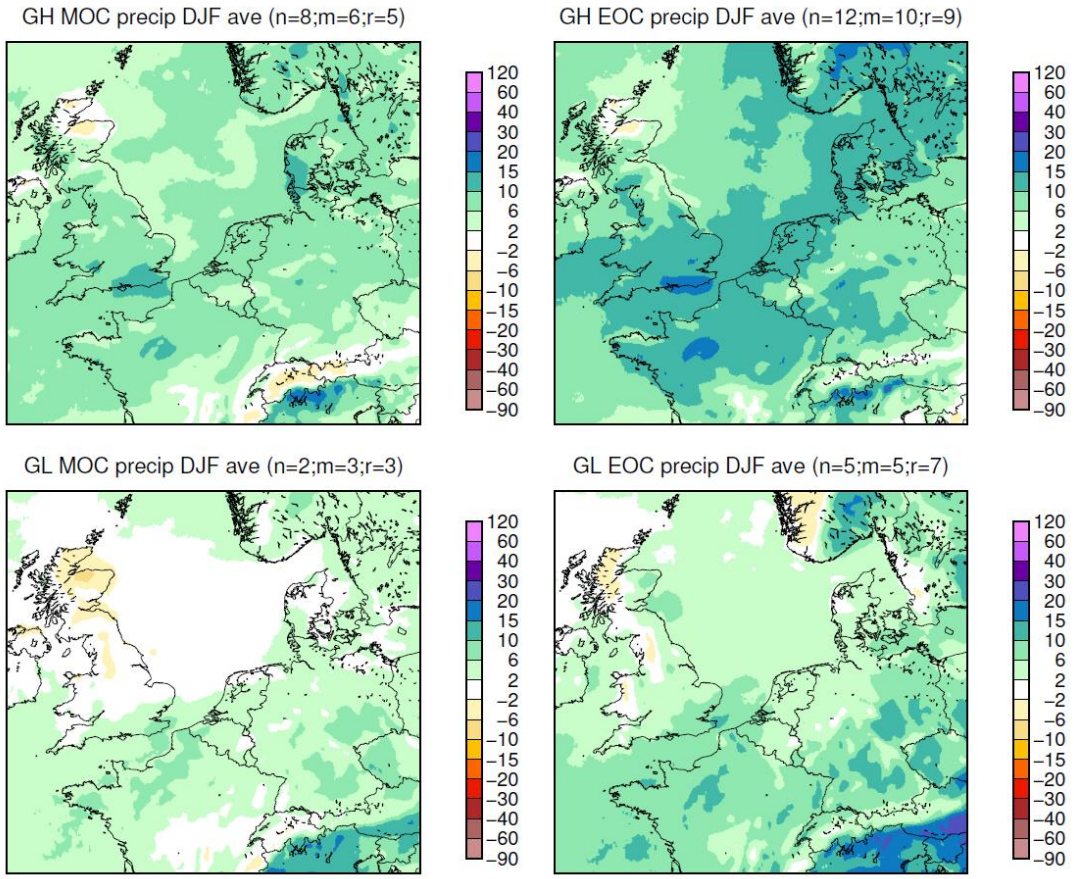

Figure C.5 Graphical overview of the relative change in season averaged precipitation for the Meuse and Rhine basins for winter (December, January and February) for the G_L and G_H scenarios. "MOC" refers to the 30-yr Middle Of Century period and is equivalent to 2050 and "EOC" refers to the 30-yr End Of Century period and is equivalent to 2085

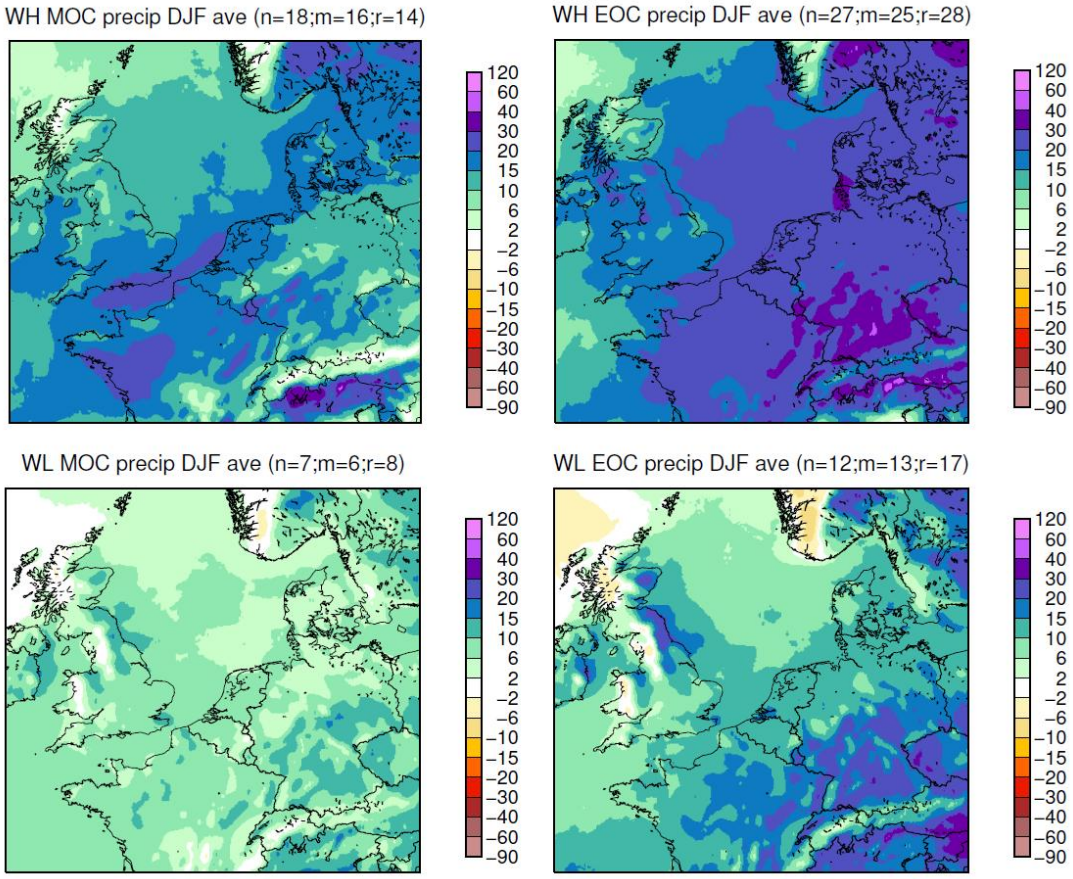

Figure C.6 Graphical overview of the relative change in season averaged precipitation for the Meuse and Rhine basins for winter (December, January and February) for the W_L and W_H scenarios. "MOC" refers to the 30-yr Middle Of Century period and is equivalent to 2050 and "EOC" refers to the 30-yr End Of Century period and is equivalent to 2085

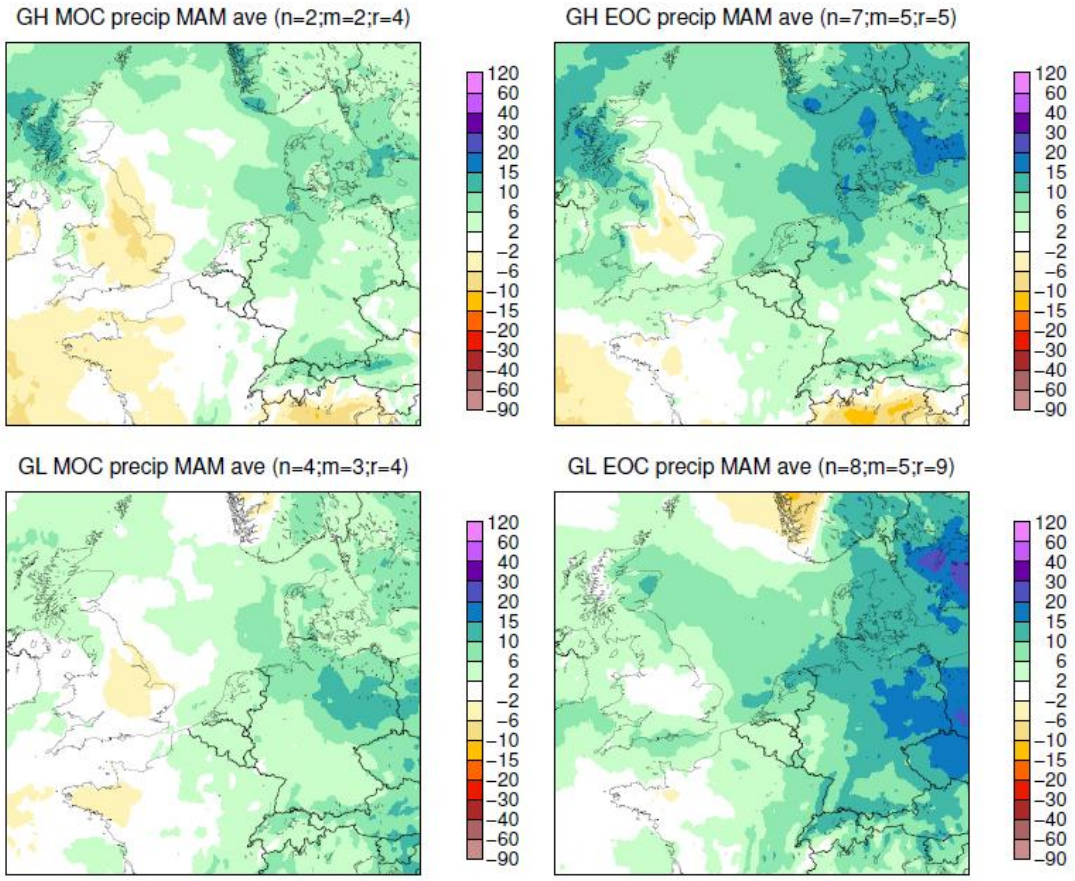

Figure C.7 Graphical overview of the relative change in season averaged precipitation for the Meuse and Rhine basins for spring (March, April and May) for the G_L and G_L scenarios. "MOC" refers to the 30-yr Middle Of Century period and is equivalent to 2050 and "EOC" refers to the 30-yr End Of Century period and is equivalent to 2085

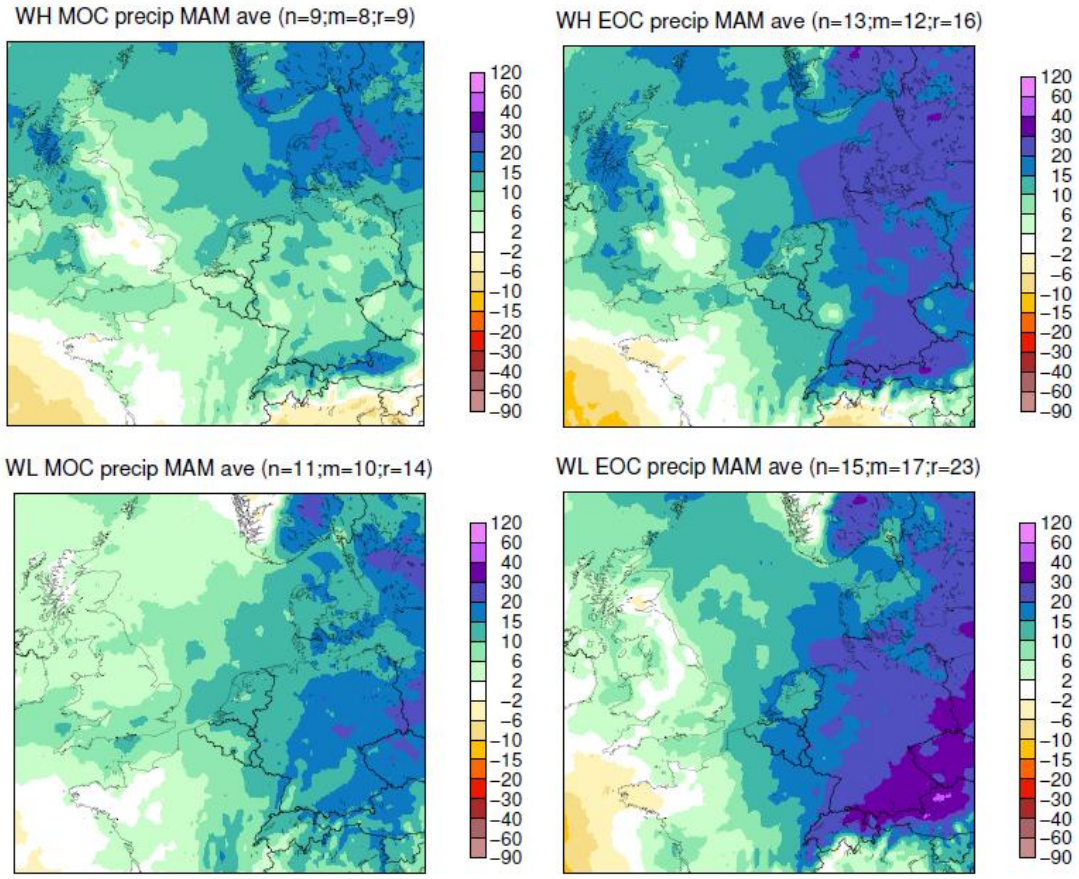

Figure C.8 Graphical overview of the relative change in season averaged precipitation for the Meuse and Rhine basins for winter (March, April and May) for the W_L and W_H scenarios. "MOC" refers to the 30-yr Middle Of Century period and is equivalent to 2050 and "EOC" refers to the 30-yr End Of Century period and is equivalent to 2085

D The effects of changes in models and methods on the results

Over time methods and techniques to estimate the impacts of climate change on river discharges for the Rhine and Meuse have evolved following the international scientific developments and using state-of-the-art techniques. These changes may have introduced differences in flows calculated for the different scenarios sets which do not results from climate change. Yet, these are generally small compared to the actual change values. One should realize that for the projections relative changes are calculated, in each case the same methods have been applied for both the historical and future time period and relative changes are likely comparable.

Because of the variety of differences and the fact that several improvements have been introduced at the same time, a transparent evaluation of all individual influences is not feasible. Based on expert judgement we assume the following changes have the largest influence on modelled discharges:

- Re-calibration and improvement of the HBV models
- Use of different methods to account for the climate induced change in potential evaporation in HBV

These changes are discussed in this Appendix. Table D.1 and Table D.2 summarize all differences that exist in the generation of discharge projections for the Rhine and the Meuse for the different scenario sets.

Table D.1 Most relevant differences in the discharge projections for the Rhine

Rhine						
Climate scenario	***Historical time-slice***	***Historical data source***	***Future time-slice / horizon***	***Future precipitation and temperature series***	***HBV model version***	***Future potential evaporation (E_p) series***
KNMI'06[7]	1961-1995	CHR-OBS	2050 2100	KNMI'06 transformation programme (Homan et al., 2011)	Eberle et al. 2005	Using HBV etf-parameter For extreme discharge calculations: using KNMI'06 scenarios for change in E_p
CMIP5	1951-2006	HYRAS / E-OBS	2021-2050 2071-2100	ADC-method (van Pelt et al., 2012)_	Winsemius et al., 2013[8]	Using HBV etf-parameter
RheinBlick2050	1961-1990	CHR-OBS	2021-2050 2071-2100	Bias-Corrected RCM (Görgen et al., 2010)	Eberle et al. 2005	Using HBV etf-parameter
KNMI'14[9]	1951-2006	HYRAS / E-OBS	2050 2085	ADC-method (van Pelt et al., 2012)	Winsemius et al., 2013	Using KNMI'14 scenarios for change in E_p

[7] *Based on IPCC (2007)*

[8] *This version of the HBV-Rhine model includes the extended schematization of the lakes in Switzerland.*

[9] *Based on IPCC (2013)*

Table D.2 Most relevant differences in the discharge projections for the Meuse

Meuse						
Climate scenario	***Historical time-slice***	***Historical data source***	***Future (time-slice)***	***Future precipitation and temperature series***	***HBV model version***	***Future potential evaporation series***
KNMI'06[10]	1961-1995	Leander (2005)	2050 2100	KNMI'06 transformation programme	Van Deursen (2004)	For extreme discharge calculations: using KNMI'06 scenarios for change in E_p
KNMI'14[11]	1967-2007	Leander (2005)	2050 2085	ADC-method (van Pelt et al., 2012)	Kramer et al. (2008); Hegnauer et al. (2013)	Using KNMI'14 scenarios for change in E_p
CMIP5	1967-2007	Leander (2005)	2021-2050 2071-2100	ADC-method (van Pelt et al., 2012)	Kramer et al. (2008); Hegnauer et al. (2013)	Using HBV etf-parameter (Leander et al., 2009)
AMICE	1961-1990	Leander (2005)	2021-2050 2071-2100	Seasonal Delta Change	Van Deursen (2004)	Seasonal Delta Change

D.1.1 Improvement of the hydrological models for the Rhine and the Meuse

Between the production of the KNMI'06 and the KNMI'14 discharge scenarios the HBV models have been re-calibrated and for the Rhine the representation of four large lakes in Switzerland has been improved. Herewith the discharge simulations have been improved.

The annual average discharge, long-term average February and long-term average September discharge calculated from HBV simulations for Lobith and Borgharen for the KNMI'06 and KNMI'14 scenarios are listed in Table D.3 .

Table D.3 Mean annual, February and September discharge obtained with the different HBV versions

Scenario	Station	Mean ref Q (m^3/s)	Mean ref Q feb (m^3/s)	Mean ref Q sept (m^3/s)
KNMI'06	Lobith	2286	2928	1632
KNMI'14	Lobith	2163	2585	1710
KNMI'06	Borgharen	229	465	56
KNMI'14	Borgharen	292	514	103

[10] *Based on IPCC (2007)*

[11] *Based on IPCC (2013)*

From the table is can be seen that for annual average discharge the differences are small. Yet, especially the September discharge at Borgharen has increased and the February discharge at Lobith has decreased after calibration. Consequently, some of the results are only presented as relative changes and when historical discharges are shown the reference simulations for the KNMI'14 scenarios are used.

D.1.2 Correction of the CMIP5 discharge projections for the Meuse.

Ideally for any discharge projection using the HBV model not only specific 'scenarios' for the changes in precipitation (*P*) and temperature (*T*) are needed but also the corresponding scenarios for the changes in potential evaporation (E_p), which is a relevant (input) variable in HBV. For the KNMI'14 (and the earlier KNMI'06) scenarios the changes in E_p are part of the scenarios[12]. However for the CMIP5 climate models the ADC-method only provides the scenario changes for *P* and *T* but not the accompanying ones for E_p. Without the scenarios for E_p, the HBV *etf*-parameter together with the scenario change in *T* can be used to determine the systematic (i.e. scenario) change in E_p within HBV. However, this will likely lead to a systematic error in the discharge response to the climate scenario. Note that, although this *etf*-parameter was never intended for this purpose it was used in earlier studies for this purpose. And its use was motivated by the fact that for the Rhine the HBV *etf*-parameter, which has a values of 0.05 (i.e. 5% per ºC) is relatively close to the value of 4% increase in E_p per ºC temperature increase which is quite often used in climate studies (and which is based on the empirical E_p - temperature relation, which is e.g. also used in the KNMI'06 climate scenarios). However for the Meuse the HBV *etf*-parameter derived by Leander et al. (2009) is two to three times as large[13] as for the Rhine and thus much more at variance with the 4%/ºC used in climate scenarios. It can therefore be expected that the use of the *etf*-parameter to determine the change on E_p within HBV has a noticeable effect on the discharge response. In fact, it is expected that using the *etf*-parameter for this purpose the increase of the potential evaporation in the scenarios is overestimated. And as a result discharges will be underestimated. Consequently, when the discharge according to the scenario tends to increase, this increase will be underestimated and when the discharge tends to decrease, this decrease will be overestimated. To estimate this effect, for the KNMI'14 scenario $W_{H,dry}$ (both for 2050 and 2085) the discharge response for the Meuse was determined in both ways. For MHQ, MQ and NM7Q the results for three gauging stations (including Borgharen) are presented in Table 4.19.

The results in this table are presented as the difference between the HBV simulation in which the change in E_p is directly taken form the $W_{H,dry}$ scenario and the simulation in which the change in E_p is determined by HBV using the *etf*-parameter and the $W_{H,dry}$ change in temperature. The Table shows that, as expected, using the *etf*-parameter leads to a smaller increase/larger decrease of the discharge. Looking in more detail at the table shows that the effect is: for 2085 about 2% larger than for 2050, about equal for MQ and NM7Q but somewhat lower for MHQ, and about equal for Borgharen and Chooz but smaller for Chaudfontaine. Altogether this led to the simplified correction table, Table D.5 , that was used to correct all the CMIP5 discharge projections for the Meuse presented in this

[12] *In the KNMI'14 scenarios for the Rhine and the Meuse the change in potential evaporation is based on the change in the global radiation (as projected by the EC-Earth-RACMO2 model) and the change in the temperature in the scenarios.*

[13] *Note that in the HBV-Meuse model the etf-parameter varies over the calendar months (in contrast to the HBV-Rhine model).*

report[14]. Note that in this table all corrections are positive meaning that e.g. for a correction of 5%, an uncorrected CMIP5 response of 6% gives a corrected CMIP5 response of 11% and a uncorrected CMIP5 response of -6% gives a corrected CMIP5 response of -1%. All CMIP5 responses for the Meuse presented in this report have thus been shifted 'upwards' given by the numbers in Table D.5 . For responses in monthly mean discharges the same corrections as for the response in the annual mean discharge (MQ) are used.

Table D.4 Difference in discharge response (in %) between the HBV etf-parameter method (systematically used for the CMIP5 discharge projections) and the preferable scenario method for E_p for MHQ, MQ and NM7Q for the KNMI'14 $W_{H,dry}$ scenario

Gauge	2050			2085		
	MHQ	MQ	NM7Q	MHQ	MQ	NM7Q
Borgharen	-5.8	-9.9	-10.0	-7.8	-12.3	-10.0
Chooz	-5.0	-9.2	-9.1	-6.9	-11.4	-9.8
Chaudfontaine	-3.2	-5.1	-5.3	-5.0	-7.6	-6.8

Table D.5 Applied correction (%) of the percentage discharge change for CMIP5 Meuse projections (see text for the motivation for this correction)

Gauge	2050			2085		
	MHQ	MQ/Monthly	NM7Q	MHQ	MQ/Monthly	NM7Q
Borgharen	5	10	10	7	12	12
Chooz	5	10	10	7	12	12
Chaudfontaine	3	5	5	5	7	7

[14] *The authors are aware that this is not a perfect correction but are of the opinion that with this correction the "true" range of the CMIP5 discharge projections for the Meuse is much better represented than without this correction.*

Deltares

PO Box 177
2600 MH Delft, The Netherlands
T +31 (0)88 335 82 73
info@deltares.nl
www.deltares.nl